

Ministry of Water Resources



Bangladesh Water Development Board

Coastal Embankment Improvement Project, Phase-I (CEIP-I)

Long Term Monitoring, Research and Analysis of Bangladesh Coastal Zone (Sustainable Polders Adapted to Coastal Dynamics)

Sibsa River: Meso scale bank erosion modelling - current situation & future projections



Joint Venture of



The expert in **WATER ENVIRONMENTS**

&



in association with IWM, Bangladesh and University of Colorado, Boulder and Columbia University

May 2022

Ministry of Water Resources



Bangladesh Water Development Board

Coastal Embankment Improvement Project, Phase-I (CEIP-I)

Long Term Monitoring, Research and Analysis of Bangladesh Coastal Zone (Sustainable Polders Adapted to Coastal Dynamics)

Sibsa River: Meso scale bank erosion modelling - current situation & future projections

May 2022

Joint Venture of



The expert in **WATER ENVIRONMENTS**

&



in association with



University of Colorado, Boulder, USA
Columbia University, USA

Long Term Monitoring, Research and Analysis of Bangladesh Coastal Zone

Office: Flat #3/B, House #4, Road #23/A, Banani, Dhaka 1213, BANGLADESH

Phone +880 1307 693299

Memo No: CEIP/LTMRA/0622/171

5 June 2022

Project Management Unit
Coastal Embankment Improvement Project, Phase-I (CEIP-I)
Pani Bhaban, Level-10
72, Green Road, Dhaka-1205

Attn: Mr. Syed Hasan Imam, Project Director

Dear Mr Imam,

Subject: Submission of the Sibsa River: Meso Scale Bank Erosion Modelling – current situation and future projections (D-4A-2:1,2&3)

It is our pleasure to submit herewith five copies of the Report Titled “**Sibsa River: Meso Scale Bank Erosion Modelling – Current situation & future projections**”. According to the World Bank Tracker, this report falls under component **D-4A-2:1,2&3**.

This report includes both model development and applications. The model development report titled “Meso scale bank erosion modelling – current situation – interim report” was submitted earlier and was reviewed by the World Bank. DHI revised the interim report to address the review and extended to include future projections.

There are five chapters in this report. Chapter 1 is the introduction chapter describing the background, objective and approach. Chapter 2 gives an overview on the availability of measurement data and how the data was processed. The development and calibration/validation of the model are described in Chapter 3. Model applications are documented in chapter 4, while the report finalizes with conclusions in Chapter 5.

Thanking you,

Yours sincerely,



Dr Ranjit Galappatti
Team Leader

Copies: Engineer Fazlur Rashid, Director General, BWDB
Dr. Zia Uddin Baig, ADG (Planning), BWDB
Dr Kim Wium Olesen, Project Manager, DHI
Ms. Sonja Pans, Deltares Project Manager
Mr Zahirul Haque Khan, Deputy Team Leader
Mr AKM Bodruddoza, Procurement Specialist
Swarna Kazi, Sr. Disaster Risk Management Specialist, World Bank

CONTENTS

1	Introduction.....	1
1.1	Background	1
1.2	Objective and Approach	3
1.3	This report	4
1.4	General definitions	5
1.5	Important note regarding MIKE 21C version.....	5
2	Data.....	7
2.1	Bathymetry	7
2.2	Hydrometric time-series	9
2.3	Sediment bed samples.....	11
2.4	Suspended sediment data	15
2.5	Suspended sediment particle size distribution data.....	17
2.6	Historical bank lines from satellite imagery	18
2.7	Subsidence.....	22
3	Model development	25
3.1	Grid and bathymetry.....	25
3.1.1	2011 model grid and bathymetry.....	25
3.1.2	2019 model grid and bathymetry.....	28
3.2	Hydrodynamic boundary conditions	30
3.3	Hydrodynamic boundary conditions for scenario simulations	31
3.4	Hydrodynamic calibration and validation	33
3.4.1	Hydrodynamic model calibration 2011	33
3.4.2	Hydrodynamic model validation for 2015 and 2016.....	35
3.4.3	Summary of the hydrodynamic calibration and validation	36
3.5	Sediment model	36
3.5.1	Alternative 2-fraction sediment model including sand and silt	37
3.6	Sediment transport boundary conditions	37
3.7	Calibration against observed bed level changes 2011-2019	38
3.8	Longitudinal validations.....	40
3.9	Bank erosion model	41
3.10	Comparison of observed and simulated bank lines 2011-2019.....	42
4	Model applications	45
4.1	Bank erosion forecast 30 years into the future	45
4.2	Impact of climate change on future bank erosion	49
4.3	Protection of the long eroding western bank.....	50
5	Conclusions	55
5.1	Recommended future data collection	56
5.2	Recommended model improvements	57
5.3	Conclusions from the scenario simulations.....	57
6	References	59

FIGURES

Figure 1-1	Revetment along Baleswar River (photo 11 February 2019).....	2
Figure 1-2	The five MIKE 21C models developed for the project.	3
Figure 2-1	Bathymetry and bed level changes 2011-2019, from left: 1) 2011 bathymetry, 2) 2019 bathymetry, 3) bed level changes 2011-2019.....	8
Figure 2-2	Field data collection map for 2011, 2015, 2016 and 2019.....	10
Figure 2-3	Bed samples d_{50} with locations during 2011 for the GRRP project.....	12
Figure 2-4	Bed samples d_{50} with locations during 2016 for the CEIP-1 project.....	13
Figure 2-5	Measured sediment fraction of bed sample for Sibsa River. The colours indicate the cohesive sediment content.	14
Figure 2-6	Sibsa River bed samples from 2011 to 2019 (February) collected by IWM.	15
Figure 2-7	Correlation between discharge and sediment concentration for the Nalian station in Sibsa River. It is noted that the suspended sediment samples taken at the left and right banks on 6 July 2019 show distinctly lower concentrations due to the proximity to the banks. These are only shown for the sake of completeness but are clearly outliers (with almost identical concentrations).....	16
Figure 2-8	Suspended sediment particle size distribution at Nalian (IWM, 2001) compared to 2019 bed samples at the same location. Top: As a function of grain size, bottom: As a function of fall velocity calculated from Stokes' Law.	17
Figure 2-9	Locations of the 25 characteristic eroding banks along the Sibsa River based on digitized bank lines in 1988, 1995, 2001, 2011, 2019. The bathymetry is based on the 2011 survey.	19
Figure 2-10	Observed bank erosion in 2011-2019 along the west bank of Sibsa River as a function of the BTM northing coordinate along the bank. The 2011 bathymetry is shown for reference to illustrate the correlation between bed level and bank erosion.	20
Figure 2-11	Observed bank erosion in 2011-2019 along the east bank of Sibsa River as a function of the BTM northing coordinate along the bank. The 2011 bathymetry is shown for reference to illustrate the correlation between bed level and bank erosion.	20
Figure 2-12	Accumulated area curves associated with bank erosion and accretion along each bank and total for the period 2011-2019.	21
Figure 2-13	Estimated bank erosion accumulated bulk volume curves for the Sibsa River 2011-2019 compared to the observed accumulated bathymetry changes bulk volume curve.	21
Figure 2-14	Subsidence spatial map in the area where the four models are located.	22
Figure 2-15	Subsidence interpolated to the Sibsa 2019 model grid.	23
Figure 3-1	Sibsa River curvilinear 500x20 grid 2011 with boundary locations shown to avoid too many figures.....	26
Figure 3-2	Sibsa River curvilinear bathymetry 2011 shown with the 2011 Landsat image as background.	27
Figure 3-3	Illustration of the differences between the 2011 and 2019 grids, which cannot be identified without looking at the details. This is the large bend in the downstream end with consistent erosion since 1988 along the western bank. The 2019 grid conforms to the 2019 bank line, as seen in the figure. Even at this scale it is necessary to look carefully to see the differences between the grids (hint: western bank in the downstream end).	28
Figure 3-4	2019 bathymetry on 2019 grid with the 2019 Landsat image as background.	29
Figure 3-5	Daily minimum, maximum and mean flows 2011-2019 upstream boundary in the Sibsa River model.....	31
Figure 3-6	Daily minimum, maximum and mean flows 2018-2019 upstream boundary in the Sibsa River model for the two cases Base and Sub+CC.	32
Figure 3-7	Daily minimum, maximum and mean water levels 2018-2019 downstream boundary in the Sibsa River model for the two cases Base and Sub+CC.....	32
Figure 3-8	Discharge calibration at Akram Point in Sibsa River during the 2011 monsoon (October).	34
Figure 3-9	Discharge calibration at Akram Point in Sibsa River during the dry season (February).....	34
Figure 3-10	Discharge calibration at Akram Point in Sibsa River during the dry season (March).	34
Figure 3-11	Water level validation at Nalian in Sibsa River during 2015. The results include the Sibsa River model and the SWRM, and both validate convincingly against the Nalian water level observations.	35
Figure 3-12	Discharge validation at Nalian in Sibsa River during 2016.	35

Figure 3-13	Comparison of observed and simulated bathymetry development 2011-2019. From left: Observed bathymetry 2011, Observed bathymetry 2019, Simulated bathymetry 2019, Observed bed level changes 2011-2019, Simulated bed level changes 2011-2019.....	39
Figure 3-14	Comparison of observed and simulated width-integrated bed level changes 2011-2019.	40
Figure 3-15	Comparison of observed and simulated bulk volume curves for 2011-2019.	40
Figure 3-16	Observed and simulated west bank erosion for the Sibsa River model 2011-2019.	42
Figure 3-17	Observed and simulated east bank erosion for the Sibsa River model 2011-2019.	42
Figure 3-18	Comparison of observed and simulated bank lines in a local area in the upstream end.	43
Figure 3-19	Comparison of observed and simulated bank lines in a local area in the downstream end.	44
Figure 4-1	Bathymetries from various years. From left: 2011 (observed), 2019 (observed), 2034 (simulated), 2049 (simulated).....	46
Figure 4-2	Width-integrated bed levels as a function of northing in the Sibsa River for 2011 (observed), 2019 (observed), 2034 (simulated) and 2049 (simulated).	46
Figure 4-3	Bank lines 2019 (observed), 2034 (simulated), 2049 (simulated).	47
Figure 4-4	Bank erosion along the Sibsa River west bank for 2011-2019, 2019-2034 and 2019-2049.	48
Figure 4-5	Bank erosion along the Sibsa River east bank for 2011-2019, 2019-2034 and 2019-2049.	48
Figure 4-6	Simulated effect of climate change in 2049 in the shape of width-integrated bed levels along the Sibsa River.	49
Figure 4-7	Simulated bank erosion along the east bank 2034-2049 with and without climate change.	49
Figure 4-8	Simulated bank erosion along the west bank 2034-2049 with and without climate change.	50
Figure 4-9	Bank protection was considered along this bank to quantify the impact on local bed levels from bank protection. It is noted that there is no polder along the western bank in this area, so the case is purely hypothetical.	51
Figure 4-10	Induced bed level changes 2019-2034 associated with protecting one bank from erosion.	52
Figure 4-11	Simulated bed levels for existing conditions along the east bank along with differences induced by protecting the bank.	53
Figure 4-12	Simulated bed levels for existing conditions along the west bank along with differences induced by protecting the bank.	53

TABLES

Table 2-1	Bathymetry data for the Sibsa River. The two recent datasets have similar spatial resolution with cross-sections typically spaced 1 km longitudinally and with 3 m spacing across the river. The older bathymetry datasets were available in cross-section databases but were not used in the 2D model due to too low resolution for 2D contouring.	7
Table 2-2	Measured water level data from Sibsa River.	9
Table 2-3	Measured discharges data from Sibsa River.	9
Table 2-4	Bed samples data from the Sibsa River collected in 2011, 2016 and 2019. The Krumbein (1934) scale for size classes has been used, i.e. VFS = very fine sand, FS = fine sand, MS = medium sand.	11
Table 2-5	Suspended sediment concentration data for Sibsa River.	16
Table 3-1	Boundary conditions for the Sibsa River model.	30

ACRONYMS AND ABBREVIATIONS

ADCP	Acoustic Doppler Current Profiler
BDP2100	Bangladesh Delta Plan 2100
BIWTA	Bangladesh Inland Water Transport Authority
BMD	Bangladesh Meteorological Department
BoB	Bay of Bengal
BWDB	Bangladesh Water Development Board
CBA	Coast Benefit Analysis
CCP	Chittagong Coastal Plain
CDMP	Comprehensive Disaster Management Program
CDSP	Char Development Settlement Project
CEA	Cost Effectiveness Analysis
CEGIS	Centre for Environmental and Geographic Information Services
CEIP	Coastal Embankment Improvement Project
CEP	Coastal Embankment Project
CERP	Coastal Embankment Rehabilitation Project
CPA	Chittagong Port Authority
CPP	Cyclone Protection Project
CSPS	Cyclone Shelter Preparatory Study
DDM	Department of Disaster Management
DEM	Digital Elevation Model
DOE	Department of Environment
EDP	Estuary Development Program
EHRM	Eastern Hilly Regional Model
FAP	Flood Action Plan
FM	Flexible Mesh
FFWC	Flood Forecasting and Warning Centre
GBM	Ganges Brahmaputra Meghna
GCM	General Circulation Model

Joint Venture of



The expert in **WATER ENVIRONMENTS**

&



in association with



University of Colorado, Boulder, USA
Columbia University, USA

GIS	Geographical Information System
GRRP	Gorai River Restoration Project
GTPE	Ganges Tidal Plain East
GTPW	Ganges Tidal Plain West
HD	Hydrodynamic
InSAR	Interferometric Synthetic Aperture Radar
IPCC	Intergovernmental Panel for Climate Change
IPSWAM	Integrated Planning for Sustainable Water Management
IWM	Institute of Water Modelling
LCC	Life Cycle Costs
LGED	Local Government Engineering Department
LGI	local Government Institute
LRP	Land Reclamation Project
MCA	Multi Criteria Analysis
MES	Meghna Estuary Study
MIKE 11	DHI's 1-dimensional hydraulic model
MIKE 21C	DHI's 2-dimensional model made specifically for river morphology
MIKE FM	DHI's 2-dimensional flexible mesh flow model
MoWR	Ministry of Water Resources
MPA	Mongla Port Authority
MSL	Mean Sea Level
NAM	Nedbor Afstromnings Model
PPMM	Participatory Polder Management Model
PSD	Particle Size Distribution
PWD	Public Works Datum
RCP	Representative Concentration Pathways
RTK	Real-Time Kinematic
SET-MH	Surface Elevation Tables – Marker Horizons
SLR	Sea Level Rise
SOB	Survey of Bangladesh
SSC	Suspended Sediment Concentration
SWMC	Surface Water Modelling Centre

SWRM	South West Region Model
TBM	Temporary Bench Mark
TRM	Tidal River Management
ToR	Terms of Reference
UTM	Universal Transverse Mercator
WARPO	Water Resources Planning Organization
WL	Water Level

Joint Venture of



The expert in **WATER ENVIRONMENTS**



in association with



University of Colorado, Boulder, USA
Columbia University, USA

EXECUTIVE SUMMARY

DHI and IWM studied five rivers in the coastal zone of Bangladesh as part of the project “Long Term Monitoring, Research and Analysis of Bangladesh Coastal Zone (Sustainable Polders Adapted to Coastal Dynamics)”.

This Executive Summary applies to all meso-scale bank erosion models and reports developed during the study. The same Executive Summary can be found in all five model reports.

The main objectives of the modelling study were to develop predictive bank erosion tools for selected rivers and to estimate future bank line changes under different scenarios.

The five rivers were studied with emphasis on meso-scale bank erosion, and the rivers listed from west to east are: Sibsa, Pussur, Baleswar, Bishkhali and Sangu. The four rivers in the SW region of Bangladesh are all tidally dominated, while the Sangu in morphological terms is dominated by the monsoon hydrograph.

One report was issued for each of the studied rivers. The same overall modelling approach was used for all five rivers, and therefore all the reports followed the same template.

The overall approach can be summarized into:

- Preliminary study of historical bank erosion in the larger tidal rivers by using satellite imagery
- Digitization of historical bank lines (Landsat) for the selected rivers
- Review of publications related to bank erosion with the emphasis on identifying the most suited bank erosion description for the tidal rivers in Bangladesh
- Setup, calibration, and validation of the model with field measurements and remote sensing data
- Morphological hindcast – reproduce historical bathymetric and bank line shifting
- Scenario runs - study future changes in the morphological processes based on possible scenarios, e.g. climate change, upstream development and subsidence
- Output - geospatial datasets of present erosion and sedimentation in the river system for various seasons and for possible scenarios

The following data were required for each model:

- Bathymetries
- Hydrometric data (water levels and discharges)
- Sediment bed samples
- Sediment bank material samples
- Suspended sediment concentrations
- Suspended sediment particle size distributions
- Historical bank lines from satellite imagery

All meso-scale bank erosion reports follow this template:

- Introduction
- Data
- Model development
- Model application
- Conclusions

Bank erosion

Bank erosion patterns in Bangladesh vary significantly from the monsoon dominated fluvial rivers to the tidally dominated muddy rivers. Two main reasons were identified in the study:

Firstly, tidal flow: The monsoon dominated rivers exhibit large imbalances between the dry season and monsoon, while the tidally dominated rivers do not show this imbalance, but instead exhibit similar discharge amplitudes during the dry season and monsoon. Due to this, the monsoon dominated rivers will experience very high morphological activity during the monsoon, which will be followed by high bank erosion rates, while the tidal rivers are better adjusted morphologically to the hydraulic conditions all year. In practice, monsoon dominated rivers are morphologically inactive during the dry season.

Secondly, cohesion: The tidally dominated rivers have cohesive banks, which are erosion resistant, while the sandy banks in most inland fluvial rivers have much higher erodibility.

The difference between fluvial and tidal rivers is significant and can also be followed along the coastal zone with strong tidal dominance in the west and monsoon dominance in the east. The increase in erosion from west to east can even be followed gradually from the Baleswar to the Bishkhali and increases further in the Sangu River.

Bank erosion rates in the tidally dominated muddy rivers are typically 5-10 m/year, while the rivers are kilometres wide, hence annual erosion is less than 1% of the width. Further to the east, bank erosion increased markedly in the Bishkhali and increases dramatically in the Lower Meghna and Sangu when measured relatively to the width (the absolute erosion rates in Lower Meghna are measured in hundreds of meters per year, while Sangu is narrow).

The value of Landsat data in Bangladesh

In most countries, Landsat data (30 m satellite imagery) is of little use for determining bank line movements due to the lack of resolution in the images compared to bank erosion rates. However, in Bangladesh, Landsat imagery is extremely useful because bank erosion rates are high. Although annual bank erosion cannot be followed in the tidal rivers from Landsat images, bank erosion over 5-10 years can be tracked accurately in the Landsat imagery. The Landsat data hence became a prism through which bank erosion in the past could be identified accurately.

The relatively slow bank erosion in the tidally dominated rivers was also found through data analysis to be systematic, such that a bank eroding in 1988 is extremely likely also to be eroding in 2019, and more or less with the same rate.

Model development template

The model development followed this template:

- Select model extent
- Develop curvilinear grid
- Interpolate bathymetry data to the curvilinear grid
- Extract hydrometric boundary conditions from e.g. the South West Regional Model (SWRM)
- Develop sediment transport boundary conditions
- Calibrate hydrodynamic model to observed water levels
- Calibrate sediment transport and morphological model to observed bed level changes
- Calibrate bank erosion model to observed bank line changes

The models were developed as hydro-morphological models with bank erosion included and physically moving the curvilinear grids to account for bank line changes. Model calibration was performed in depth by using the period 2011-2019 as hindcast, which was found ideal due to the two bathymetry datasets typically collected in 2011 and 2019 by IWM with almost identical resolution and accuracy. The value of such data cannot be overstated, and by combining with bank erosion obtained from Landsat data in the same period, the models could be calibrated in depth. There are exceptions to this, namely that no 2011 bathymetry was available for Bishkhali River, while Sangu River was calibrated to 2018-2020 for which good data was available.

The calibration of the tidally dominated rivers resulted in very similar calibration parameters, especially the silt transport models and bank erosion formulas were almost identical in the rivers.

Bank erosion mechanics and formula

The bank erosion formula is central to the simulated behaviour of the rivers. Several bank erosion descriptions were investigated in detail in the models, and the optimal choice was found to be a formula derived from Hasegawa (1989). The Hasegawa model is based on a near-bank excess velocity approach, which means that bank erosion occurs when the near-bank flow speed is higher than the cross-section average flow speed. This could in principle have been adopted in the model engine, but it was found to give some practical problems because the Hasegawa formula was developed for meandering rivers with an outer bend and associated bend scour, which is not always the layout for the tidal rivers. Hence, the formula was modified by estimating the excess flow speed from the near-bank flow speed and an estimated average flow depth using the Manning formula. This resulted in bank erosion derived from the near-bank flow speed and water depth, notably bank erosion is proportional to the near-bank flow speed and a function of the water depth, such that the water depth must exceed a characteristic average depth for bank erosion to occur and then it will increase with depth beyond this limit.

Several bank erosion expressions were found calibratable to observed bank erosion, even with significant variations in the described mechanics. The best calibration was obtained by simply using a critical bank height (Mosselman, 1995) beyond which bank erosion increases with the exceedance of the bank height beyond the critical height. However, this was found mechanistically problematic because it does not state anything about erosive fluid forces along the bank, and hence bank erosion would continue along any bank independent of the flow along the bank, if the bank height exceeded the critical limit.

Bank erosion calibration using the Hasegawa derived formula is only slightly less accurate than for the critical height formulation, and Hasegawa has a solid theoretical foundation in addition to its inclusion of the flow speed along the bank. Hence, all taken into consideration, there was no doubt that Hasegawa was the correct choice.

Several traditional bank erosion descriptions were tested without success. For instance, a simple bank erosion description is to derive bank erosion from near-bank scouring; however, this does not work in the tidal rivers because the description is only valid for sandy banks. Surprisingly, relating the bank erosion rate to the shear stress was initially found to give a bad description of bank erosion. This was also the case when relating bank erosion rate to the flow speed without considering water depth.

It is important to understand that in addition to being able to describe the bank line changes over time, the bank erosion formula also needs to describe the physical processes in a lumped manner. The adopted Hasegawa derived formula derives bank erosion from flow speed and water depth, which proved to be the two most important variables.

Limitations in the models and data

In general, the models developed suffer from similar limitations, which are also related to the lack of specific types of data. The limitations are listed in the order of importance.

In particular, all models show that simulated bar formation is sensitive to flow resistance used in the models and that the flow resistance calibrations adopted in the models are only one variant in a calibration space. Detailed investigations were conducted to show that different resistance models can be developed to yield the same simulated water levels but resulting in different velocity distributions between bars and channels as well as different sediment transport patterns and hence different bar sizes. Essentially the models have calibration spaces where the true calibration cannot be identified solely by matching water levels. Consequently, the bathymetry and bank erosion behaviours can vary significantly. The best approach for reducing calibration uncertainties is to collect ADCP velocity profiles, but this was not done as part of the present project.

The sensitivity of bar development to the flow resistance model used is very pronounced. For instance, a constant resistance number applied in a model can cause bars to erode in a manner where the deep channel will be located where the bar should be located and vice versa. In turn, this will lead to a simulated bank erosion where the erosion pattern essentially becomes the opposite of the observed. Due to feedback in the river morphology, this can also cause other bars to behave incorrectly. The implication of this sensitivity is that when the model simulates the right morphological development, this is a strong indication that the right resistance model has been applied.

The models also suffer from uncertainties in the calibration of sediment concentrations. This comes back to the traditional way of collecting data in Bangladesh, namely the standard collection of total sediment concentrations (i.e. the combined concentration of clay, silt and (fine) sand). The tidal rivers contain significant clay concentrations, which do not contribute morphologically. In the tidal rivers only the silt transport contributes to the morphological development since the sand concentration is negligible. Hence, it is not possible to calibrate silt transport models to the observed concentrations, as the observations generally only show the total concentration. However, observed particle size distribution data was available only in a few cases.

Only a handful of bank sediment samples were available. The erosion resistance of banks depends on the sediment composition of the banks. Bank erosion plays an important role in the river morphology, in some of the rivers contributing significantly to sedimentation, but the particle size distributions in the banks is largely unknown.

Rivers with mixed sediments require many bed samples to identify the particle size distribution in the riverbed. All the tidally dominated rivers are probably characterized by a mixture of sand and silt (while clay is morphologically inactive), but it was only possible for some of the rivers to identify this mixture, and none of the rivers had enough bed samples to determine the spatial distribution of the bed sediment composition.

The limitations of the available dataset have probably impacted the quality of the calibration of the models. However, the fact that the models all predict the overall morphology of the rivers quite well, including bank line migration and erosion/deposition pattern of the riverbeds, gives some confidence that also flow distribution, sediment transport etc. are well represented in the final model calibrations. Further model improvements can be made at a later stage if/when additional data collection is carried out. IWM has the capacity to conduct the necessary data collection.

Model applications

Model applications included the following:

- Projection of bank lines 30 years into the future
- Impact of climate change
- Impacts of bank protection on bank erosion and bed levels
- Dredging of shoals to mitigate or eliminate bank erosion
- Access to Mongla Port

Projection of bank lines 30 years into the future

The most important deliverable of the project was projected bank lines 30 years into the future for the four tidally dominated rivers in the west (Sibsa, Pussur, Baleswar and Bishkhali). The future projections showed that most of the banks currently eroding will continue eroding in the future with more or less the same rates. Hence, the future development was essentially projected to be similar to the 1988-2019 development. This is a very important finding that can be utilized for planning and managing polders and embankments. There are deviations from the overall systematic behaviour, but these are few in numbers. The projected future bank lines were also submitted to the CEIP-2 feasibility study in digital format (line themes) in order to maximize the value to planners and decision makers. Projection of bank erosion 30 years into the future is not meaningful for the Sangu River because the erosion rates are too high compared to the river width for projections on such timescale and was therefore not conducted.

Impact of climate change

In most of the models, climate change increases the tidal flow amplitude slightly, leading to a small increase in bank erosion. However, the impact of climate change is small compared to the absolute future bank line changes. Hence, the impact of climate change on future bank lines is modest.

Impacts of bank protection on bank erosion and bed levels

Bank protection was also shown to induce scouring due to the removal of sediment sources associated with bank erosion. The effect on bed levels is not insignificant, while bank erosion impacts are small. The models do not suggest that local bank protection will cause significant changes to the erosion of other banks, which is an important conclusion to keep in mind for management purposes, i.e. eroding banks do not seem to significantly influence each other in the tidal rivers.

Dredging of shoals to mitigate or eliminate bank erosion

The use of dredging of shoals located opposite of eroding banks was tested in the Baleswar River. The model results suggest that shoal dredging is potentially very effective at reducing bank erosion, especially if combined with backfilling of dredged spoils in the deep channel along the eroding bank. Unfortunately, this cannot be conducted simply by dumping the spoils in the deep channel due to the settling length for the silt exceeding the length of the eroding bank. However, the impact of shoals dredging combined with filling the deep channel essentially eliminates bank erosion over a long timescale and should be studied further, assuming that the filling problem can be addressed. A simple approach using geotextile (e.g. jute) bags to secure sedimentation in the deep channels was proposed, but needs to be investigated further and tested.

Access to Mongla Port

A separate investigation was also carried out for Mongla Port. Several scenarios were tested using the model, including quantification of the impact of Ganges Barrage, bank protection, closing and/or regulating upstream connections to Sibsa, guide bunds at Mongla, and TRM applied to Pussur or Sibsa. The investigation confirmed that the fundamental problem with Mongla Port is that the Sibsa incoming flood tide occupies (captures) most of the tidal prism located upstream of Mongla Port, preventing the incoming slower tide in the shallower Pussur River from occupying the tidal prism. The Pussur flood tide hence stagnates at Mongla Port, making the port susceptible to sedimentation, and model results show that Mongla Port indeed has the highest sedimentation rate in the Pussur River. The only way to really fix the sedimentation problem is to prevent the Sibsa from capturing tidal prism from the Pussur, while other schemes do not really solve the underlying problem, although they can act to mitigate. Schemes involving attempts to add tidal prism to the Pussur are remarkably ineffective due to the always faster flood tide in Sibsa, which will occupy tidal storage before Pussur. In effect adding tidal basins to Pussur downstream of Mongla Port just causes the Sibsa to capture more of the upstream tidal prism.

Conclusions

The conclusions from the study can be summarized into the following.

Bank erosion in the tidally dominated rivers of Bangladesh is slow and systematic, and therefore the predictability is very good, even over decades. This is a very important finding that can be utilized for planning and managing polders and embankments, for instance, designing embankments in safe distance from the eroding rivers, planning future retirement of embankments or when to implement bank erosion measures. On the contrary, fluvial systems in Bangladesh are known to have good predictability only over relatively short timescale, if even that.

The five developed models reflect the bank erosion predictability. For the four tidally dominated rivers, the bank erosion model was applied for projections 30 years into the future, while this is not meaningful for the Sangu River.

Although one should never take morphological predictions as accurate, the project team is confident that the future bank lines projected 30 years into the future are reliable enough for decision-making purposes. The predictable planform development should be exploited when managing polders and banks.

Dredging of shoals located opposite of eroding banks shows promising results, although only tested conceptually. The best outcome is achieved by combining dredging with dumping of the spoils into the deep channel flowing along the eroding bank, which will give two synergizing effects, namely attracting flow to the dredged flow path through the shoal and attracting less flow to the deep outer channel. There is a major practical issue with the approach, namely that it is not easy to dump the spoils into the outer channel. One proposal for handling this is to fill the spoils into geotextile bags and dump them in the outer channel, which is similar to the approach followed in some meandering rivers for navigation purposes (by preventing deep bend scour), but here done to prevent bank erosion (by also preventing deep bend scour).

For the Sangu and other fluvial systems, managing polders via predictable future bank lines is not meaningful. However, a river like the Sangu has a meander belt, which has good predictability, even if the bank lines themselves are difficult to predict. However, this may require allowing the Sangu River to move within its meander belt, which means accepting a loss of land area behind polders.

The model shows that Mongla Port has the highest sedimentation rate in the Pussur River model. In other words, Mongla Port happens to be located at the worst possible location for a port.

The Pussur River model was also applied to scenario testing at Mongla Port. The fundamental problem with Mongla Port is that it is located just south of the tidal meeting point between the Pussur and Sibsa tides, which has been understood for decades, and indeed some of the scenarios addressing this problem have been tested before. Several mitigation schemes were tested, and it was found that the most effective solution is to increase the Pussur tidal prism located upstream of Mongla Port. Getting the Pussur flood tide to flow north from Mongla can only be done by preventing the faster Sibsa flood tide from occupying the prism. Closing the three upstream connections to the Sibsa River was proposed and tested almost 30 years ago by DHI (1993), and the present study reverified the validity of this scheme. However, the scheme can be further developed by using regulators on the connection rivers to enhance the outgoing tide (ebb) at Mongla Port, which is the driver for keeping the Mongla Port water depths sufficiently large. It was shown that closing the connections appears neutral in the Mongla Port bed levels, while significant scouring can be achieved with regulators, opening up for managing the Mongla Port bathymetry by using the regulators to adjust the hydraulic dredging driven by the ebb flows.

The use of guide bunds at Mongla Port, proposed before, was investigated by using the MIKE 21C model. It was found that this scheme can sustain deep channels at Mongla Port, but it will also induce sedimentation further downstream due to the slightly reduced tidal discharges associated with the added flow resistance from the guide bunds. This suggests that the guide bund scheme cannot stand alone in solving the Mongla Port problem.

Various other schemes were also investigated, in particular increasing the tidal prism of the Pussur downstream of the tidal meeting point located upstream of Mongla Port. Schemes involving an increase in the Pussur tidal prism downstream of the tidal meeting point are problematic because they ultimately leave more tidal prism for the Sibsa flood tide to occupy from the Pussur upstream of Mongla Port.

A real solution to the Mongla Port problem must address the ability of the faster Sibsa flood tide to capture (from the Pussur) tidal prism upstream of Mongla Port, which is the fundamental problem. Mitigation schemes that do not address the fundamental problem do not seem to be able to stand alone.

1 Introduction

1.1 Background

Bangladesh is situated at the confluence of three great trans-Himalayan rivers, the Ganges, the Brahmaputra or Jamuna, and the Meghna, which form the Bengal (or GBM) Delta. While over 90 percent of the catchment of the GBM system lies outside of Bangladesh, more than 200 rivers and tributaries and distributaries of the GBM system drain through the country via a constantly changing network of channels, tidal inlets and creeks, forming the most active large delta on the planet. The coastal land mass is shaped by the interaction of large volumes of sediment laden water with the moderate to high tides of the Bay of Bengal.

Land in the coastal zone is built up by the deposition of river sediments in the tidal delta, including the mangroves of the Sundarbans, the largest mangrove forest in the world. The deposits of sand, silt, clay, and organic material form the land mass which, despite subsidence due to continuous consolidation of layers many kilometres deep, is kept around the level of the highest tides by the continuing deposition of sediments.

The coastal zone of Bangladesh spans over 710 km of coastline and is subject to multiple threats. Sixty-two percent of the coastal land has an elevation less than 3 meters above mean sea level. With a sediment supply of 1 billion tons per year, this is the delta with the largest sediment supply in the world. This leads to continuing accretion of the land area in the coastal zone (5-10 km²/year), mainly in the Meghna Estuary, but also erosion of the coast farther west. It has been observed that the land subsidence rate may vary from place to place due to anthropogenic factors such as drainage and ground water extraction as well as the properties and depth of underlying strata. On top of this there are tectonic plate movements, particularly in the eastern delta, that give rise to other changes in ground level.

The coastal lands, particularly in SW Bangladesh, being subject to regular flooding by saline water during high tides, could not be used for normal agricultural production in a country with a very high demand for land. The Coastal Embankment Project (CEP) was initiated in the 1950s and 1960s to build polders surrounded by embankments preventing the spilling of saline water onto the land at high tides. These embankments were built along the larger rivers and across the smaller rivers and creeks which then formed the drainage system within each polder and connected to the peripheral rivers via appropriately sized flap gate regulators, that open at low tide to let the drainage water out.

The Coastal Embankment Project enabled the reclamation of large tracts of land for agriculture from 1960 onwards. Polder building proceeded continuously until today. Up till now, 1.2 million hectares have been reclaimed in 139 active polders in the coastal zone of Bangladesh.

In over half a century of its existence, a number of challenges have surfaced that threaten the long-term safety and even the very existence of the polder system as a viable and sustainable resource. These are:

- Sea level rise and changes in precipitation and water discharge due to climate change
- Threats of damming and diversion to the delivery of river sediments from upstream
- Subsidence of lands (except where it has been allowed to be rebuilt by tidal flooding) and structures founded on existing land
- Drainage congestion due to accumulation of silt in some peripheral waterways around polders
- Changes in tidal hydrodynamics and related river erosion and siltation in the peripheral rivers of polders
- Increasing vulnerability to cyclones and storm surges

The main objective of the “Long-term monitoring, research and analysis of Bangladesh coastal zone” project is to create a framework for polder design, based on understanding of the long-term and large-scale dynamics of the delta and sustainable polder concepts. The field and modelling work within the project is carried out to improve understanding of the long-term and large-scale dynamics of the Ganges-Brahmaputra-Meghna (GBM) delta. There is insufficient knowledge about sediment budget in the delta involving sediment transport within the estuaries, sediment sources and sediment distribution into the river system. Sediment and tidal dynamics are important for river and coastal erosion, land reclamation, and delta development. Subsidence of the land alters the topography and hydrodynamics and increases flooding, coastal erosion and salinization. The knowledge of sediment dynamics, distribution, subsidence, erosion-deposition processes, sediment management at present and in the future under climate change, land use changes and proposed interventions in the upstream reaches of the Ganges Brahmaputra River systems is essential for the framework of polder design.

In the coastal zone of Bangladesh – both in the major estuaries and in the peripheral rivers of the polders – bank erosion is a significant problem even though the erosion rates are normally smaller than those encountered further upstream in the non-tidal main rivers (e.g. Padma, Brahmaputra). Failure of embankments in the coastal zone during storms has not always been as the result of overtopping. There have been many failures as a result of undermining of the toes of the embankment due to riverbank erosion. In fact, unexpectedly high levels of bank erosion have already been encountered in the execution of CEIP-1. This matter was highlighted in the Inception Workshop of this project leading to the recommendation that a special meso-scale study of “Bank Erosion Hindcasting” should be undertaken to analyse the bank erosion processes that have taken place in the large tidal estuaries in the last 20 or more years in areas where large and often intensive data collection programmes have been mounted for various projects. Improved guidelines for predicting medium term bank erosion are supposed to emerge from this study.



Figure 1-1 Revetment along Baleswar River (photo 11 February 2019).

1.2 Objective and Approach

The main objective of the modelling presented in this report is to develop a predictive bank erosion tool for the Pussur River and to estimate future bank line changes under different scenarios.

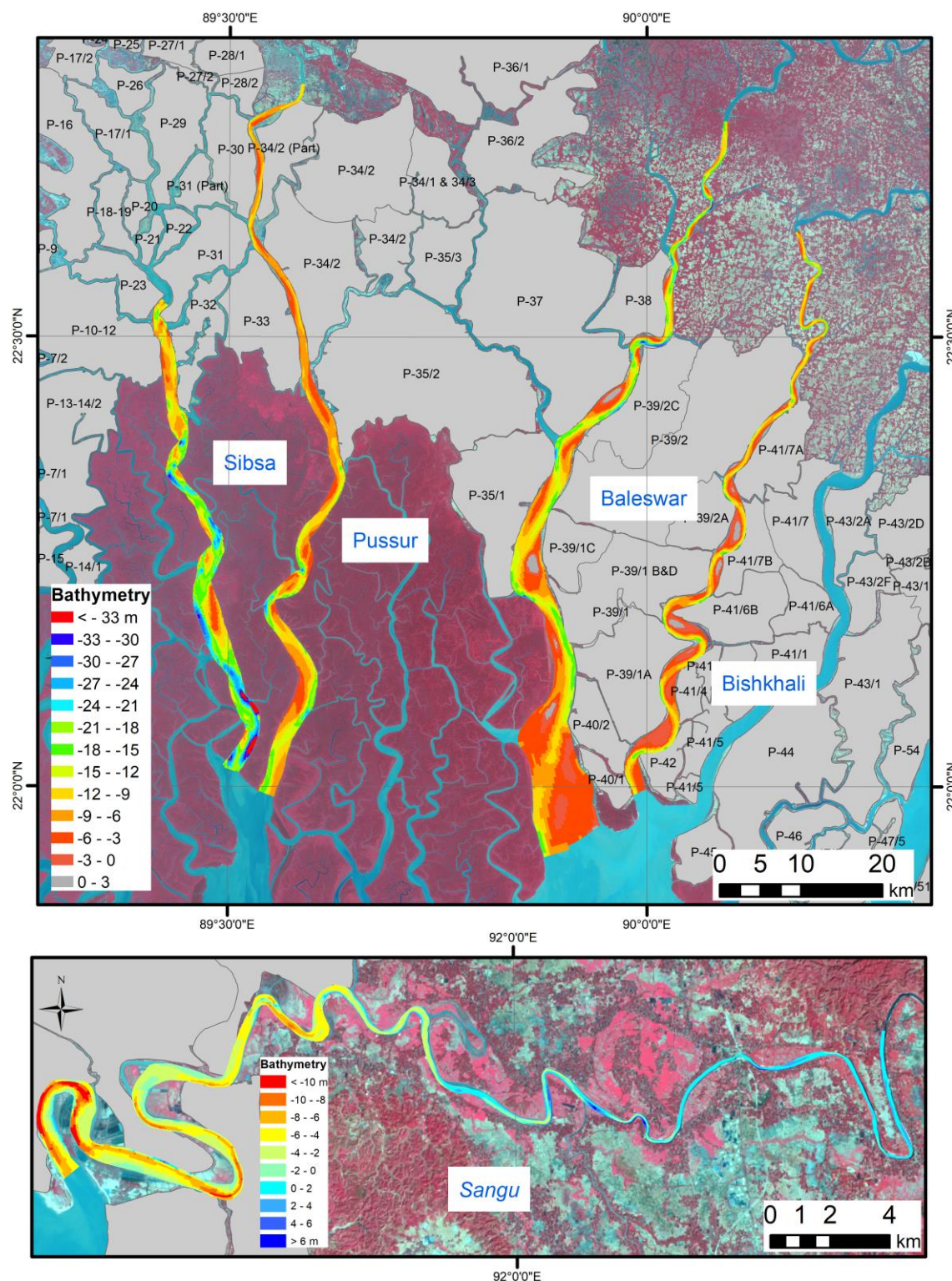


Figure 1-2 The five MIKE 21C models developed for the project.

Joint Venture of



The expert in **WATER ENVIRONMENTS**

&



in association with



University of Colorado, Boulder, USA
Columbia University, USA

The general approach for this modelling is the following:

- Preliminary study of historical bank erosion in the larger tidal rivers by using satellite imagery
- Digitization of historical bank lines (Landsat) for the selected rivers
- Review of publications related to bank erosion with the emphasis on identifying the most suited bank erosion description for the tidal rivers in Bangladesh
- Setup, calibration, and validation of the model with field measurements and remote sensing data
- Morphological hindcast – reproduce historical bathymetric and bank line shifting
- Scenario runs - study future changes in the morphological processes based on possible scenarios, e.g. climate change, upstream development and subsidence
- Output - geospatial datasets of present erosion and sedimentation in the river system for various seasons and for possible scenarios 25, 50 and 100 years from now, for various seasons and circumstances

The modelling is carried out using MIKE 21C. The key features of this modelling system are:

- Curvilinear boundary conforming grids allowing accurate representation of the river planform with relatively few grid points
- 2D Saint-Venant equations with a parallelized and optimized solver allowing time-true simulations covering several years
- Helical flow
- Multi-fraction sediment framework covering mixtures of clay, silt, sand, gravel
- Bed-load calculated with inclusion of helical flow and bed slope
- Suspended load calculated from advection-dispersion with helical flow included
- Morphological updating of the bed levels
- N-layer substrate model
- Bank erosion with optional inclusion of eroded material in the sediment budget
- Dynamic updating of the curvilinear grid to account for bank line changes

Waves are not included in any of the MIKE 21C models. The fetch is generally small within the estuaries of the delta, and the modelled rivers are very deep, usually at least 10 m and often up to 40 m water depth along eroding banks, which means that the small surface waves will not penetrate to the lower water column, hence it may be assumed that waves have little influence on the sediment transport in the areas modelled.

1.3 This report

An interim report describing the model development for the current situation was submitted earlier in the study and reviewed by the World Bank. The interim report was titled:

“Meso scale bank erosion modelling - current situation - interim report”

DHI revised the interim report to address the review, and the report was extended to include future projections. The final report was titled:

“Meso scale bank erosion modelling – current situation & future projections”

The interim report is included already in the final report and not submitted separately.

The five modelling reports are organised in a similar manner with the following chapters: Chapter 2 gives an overview on the availability of measurement data, as well as how the data was processed. These data are used in Chapter 3, which describes the development and calibration/validation of the model used to study the river morphology and bank erosion. Model applications are documented in Chapter 4, while the report finalizes with conclusions in Chapter 5.

1.4 General definitions

It is useful to provide some general definitions and explanations for the terminology used in this report.

The projection is always BTM, and the vertical datum is always mPWD. In some cases, data was made available in UTM and MSL, but they were converted.

All MIKE 21C models were developed with the grid direction going in the direction of the river from upstream. This means that the discharge sign convention is that ebb flow is positive and flood flow is negative in all models.

The term “mud” is defined as a mixture of mainly fine-grained sediments, organic matter and water where the cohesive properties of the clay fraction, enhanced by the properties of the organic matter, dominate the overall behaviour of the sediment mixture.

Several figures present results in ways that can seem confusing if the reader is not aware:

- Some figures show Sibsa River divided into upstream and downstream
- Some figures show several Sibsa River maps side-by-side

The MIKE 21C models are very long, and to avoid narrow graphics, the 2D figures are made by splitting the river into upstream and downstream parts shown side by side, with the upstream part to the left and the downstream part to the right. Grids and bathymetries are shown in this manner.

The plots with several Sibsa River 2D maps shown next to each other are useful for showing several results together because they belong together. Examples include bathymetries that need to be compared as well as bed level changes shown together with the bathymetries. When showing these, the 2D maps are displaced 5 km in eastern direction (to the right), and the easting coordinates are hence only correct for the first 2D maps shown to the left. When showing more 2D variations together in this manner, there can be several colour scales in a figure, and the reader is notified in the caption.

For one-dimensional variations, the fact that the Sibsa River runs almost north to south makes it convenient to use the BTM northing as coordinate in the graphics. This cannot be done for all MIKE 21C models (e.g. Baleswar has a sharp bend where the northing coordinate hardly changes over some kilometres). For models where the BTM northing cannot be used as unique longitudinal coordinate, a chainage coordinate was applied, but Sibsa River is not included in that group.

1.5 Important note regarding MIKE 21C version

The developed MIKE 21C models take advantage of the most recent developments of the modelling software, hence it is important that MIKE 21C version 2022.1 or later is used. This version is installed on the project computers.

2 Data

This section documents all the data that was used for the model development.

The projection is BTM, and the vertical datum is mPWD.

2.1 Bathymetry

A very detailed bathymetry survey was conducted in 2011 for the Pussur-Sibsa river system as part of the Gorai River Restoration Project (GRRP). For the present project, a similarly detailed survey was conducted in the Pussur-Sibsa system in 2019. In addition, several older sets of cross-sectional data were available for the two rivers, which are tabulated for the sake of completeness. However, these old cross-sectional datasets do not have the required density to generate reliable 2D model bathymetries and are therefore not used in the present project.

Table 2-1 Bathymetry data for the Sibsa River. The two recent datasets have similar spatial resolution with cross-sections typically spaced 1 km longitudinally and with 3 m spacing across the river. The older bathymetry datasets were available in cross-section databases but were not used in the 2D model due to too low resolution for 2D contouring.

Bathymetry data collection year	Sources
1977-92 (dates not available)	SWMC
2001 (dates not available)	IWM
2011 (dates not available)	IWM (GRRP)
2019 (March)	Primary data (present project)

General information for the available bathymetry datasets is shown in Table 2-1.

Table 2-1 summarises the bathymetry datasets used, while the contoured bathymetries and bed level changes (difference plot) are shown in Figure 2-1. The plot of bed level changes shows that the Sibsa River experienced both erosion and deposition in the period 2011-2019.

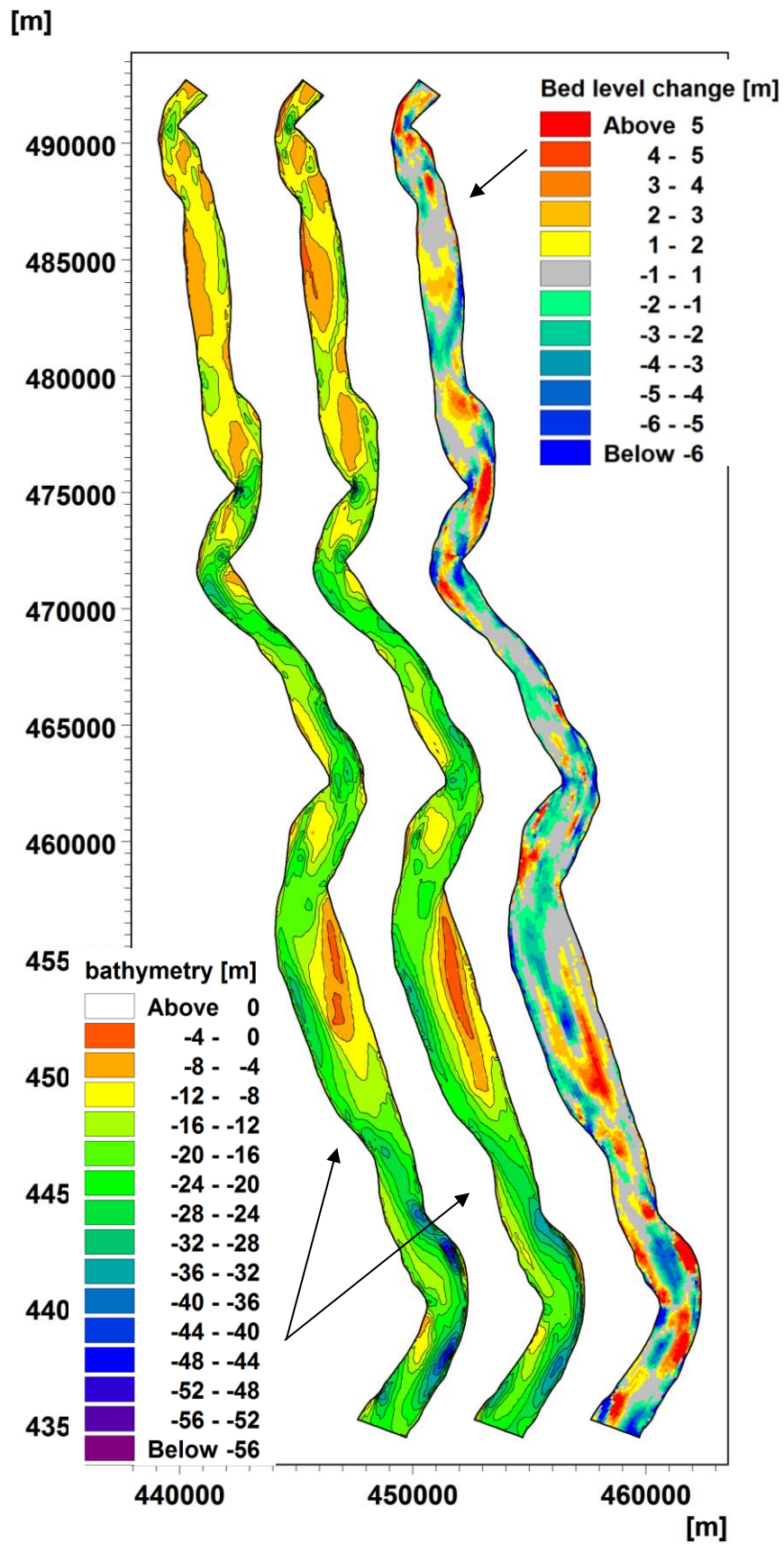


Figure 2-1 Bathymetry and bed level changes 2011-2019, from left: 1) 2011 bathymetry, 2) 2019 bathymetry, 3) bed level changes 2011-2019.

2.2 Hydrometric time-series

Hydrometric data includes water levels and discharges.

There are no water level measurements for 2011. Water level data at the Nalian station was collected for 2015 by IWM under the CEIP-1 project. In the present study, water levels were collected at Nalian in the beginning of 2019.

Water level and discharges data collected as part of the project during 2019 were not used in the model development process, as they were not available at the time when the model was developed.

Table 2-2 Measured water level data from Sibsa River.

Water level collection year	Station name	Sources
2015	Nalian	CEIP-1 project
2019	Nalian	Primary data (present project)

Table 2-3 Measured discharges data from Sibsa River.

Discharge collection year	Station name	Sources
2011	Akram Point	IWM (GRRP)
2016	Nalian	CEIP-1 project
2019	Nalian	Primary data (present project)

The stations are shown in Figure 2-2, while datasets details are provided in Table 2-2 and Table 2-3. The discharge data was collected by IWM, typically during one day using tide tables to plan for neap and spring data collection. Water level data was collected at the same time, and often IWM also collects suspended sediment concentration data with the ADCP data. Water level stations are often permanent and contain water levels data collected every 30 min.

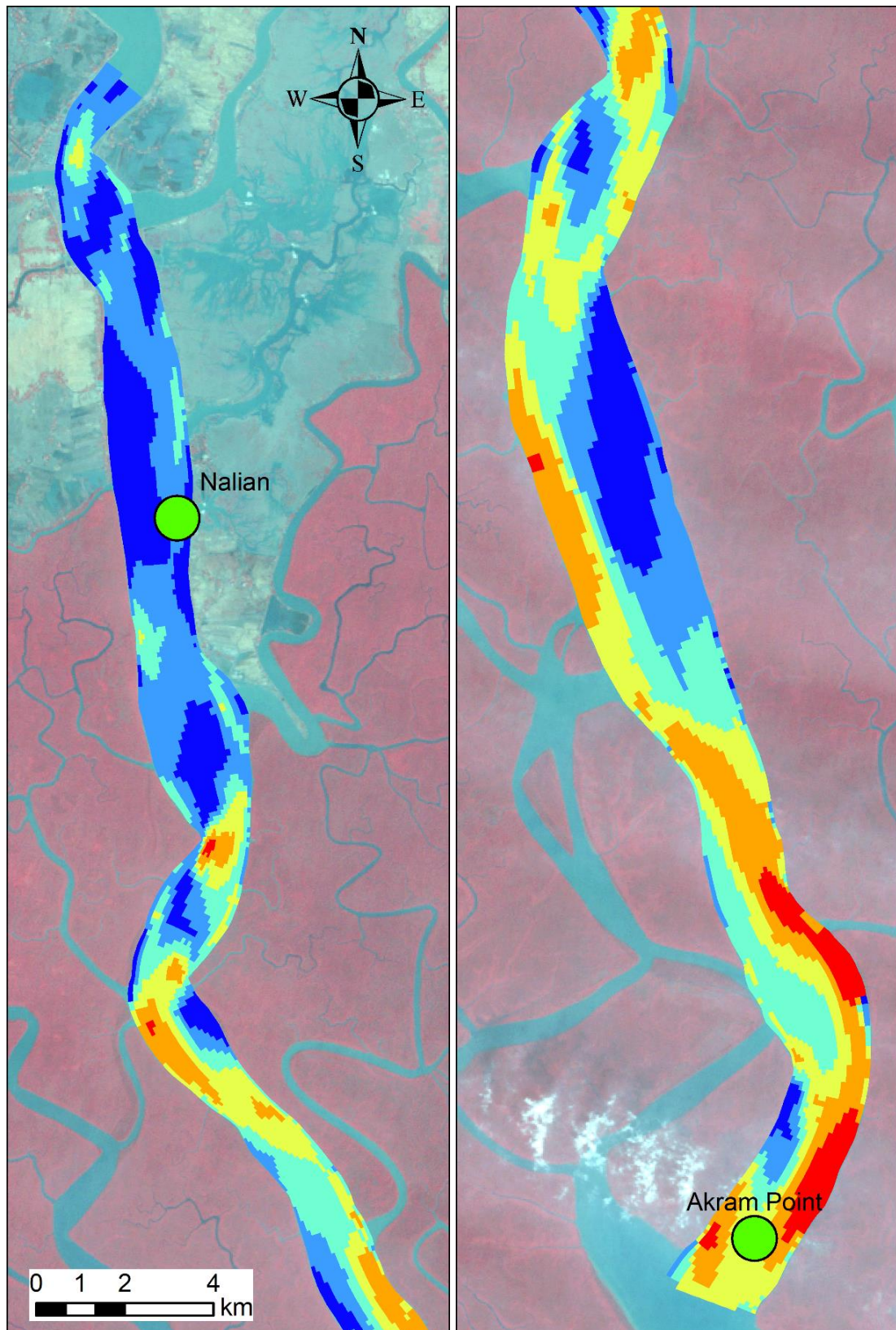


Figure 2-2 Field data collection map for 2011, 2015, 2016 and 2019.

2.3 Sediment bed samples

In this section all readily available bed samples for Sibsa River are compiled. Many samples have been collected for various projects, namely GRRP (2011), CEIP-1 (2016) and the present project (2019), but the data has not before been compiled to obtain a comprehensive picture of the sediment bed.

Table 2-4 Bed samples data from the Sibsa River collected in 2011, 2016 and 2019. The Krumbein (1934) scale for size classes has been used, i.e. VFS = very fine sand, FS = fine sand, MS = medium sand.

BTM X [m]	BTM Y [m]	Year	Name	Clay <0.005 mm [%]	Silt <0.063 mm [%]	VFS <0.125 mm [%]	FS <0.25 mm [%]	MS >0.5 mm [%]
440969	479694	2019	Shibsha_1B_RB	7.84	77.07	8.57	5.67	0.85
442300	479831	2019	Shibsha_1B_LB	7.98	72.13	12.06	6.45	1.37
440272	485419	2019	Shibsha_2B_RB	10.83	82.61	4.85	1.33	0.37
442113	484068	2016	Shibsa_LB	18.33	78.79	2.88	0	0
441201	483925	2016	Shibsa_CL	10.5	77.73	5.93	4.16	1.68
440355	483961	2016	Shibsa_RB	9.18	83.8	3.32	2.65	1.06
440559	482364	2011	Nalianala_RB	45.13	54.53	0.33	0	0
442171	483359	2011	Nalianala_LB	13.14	85.56	1.29	0	0

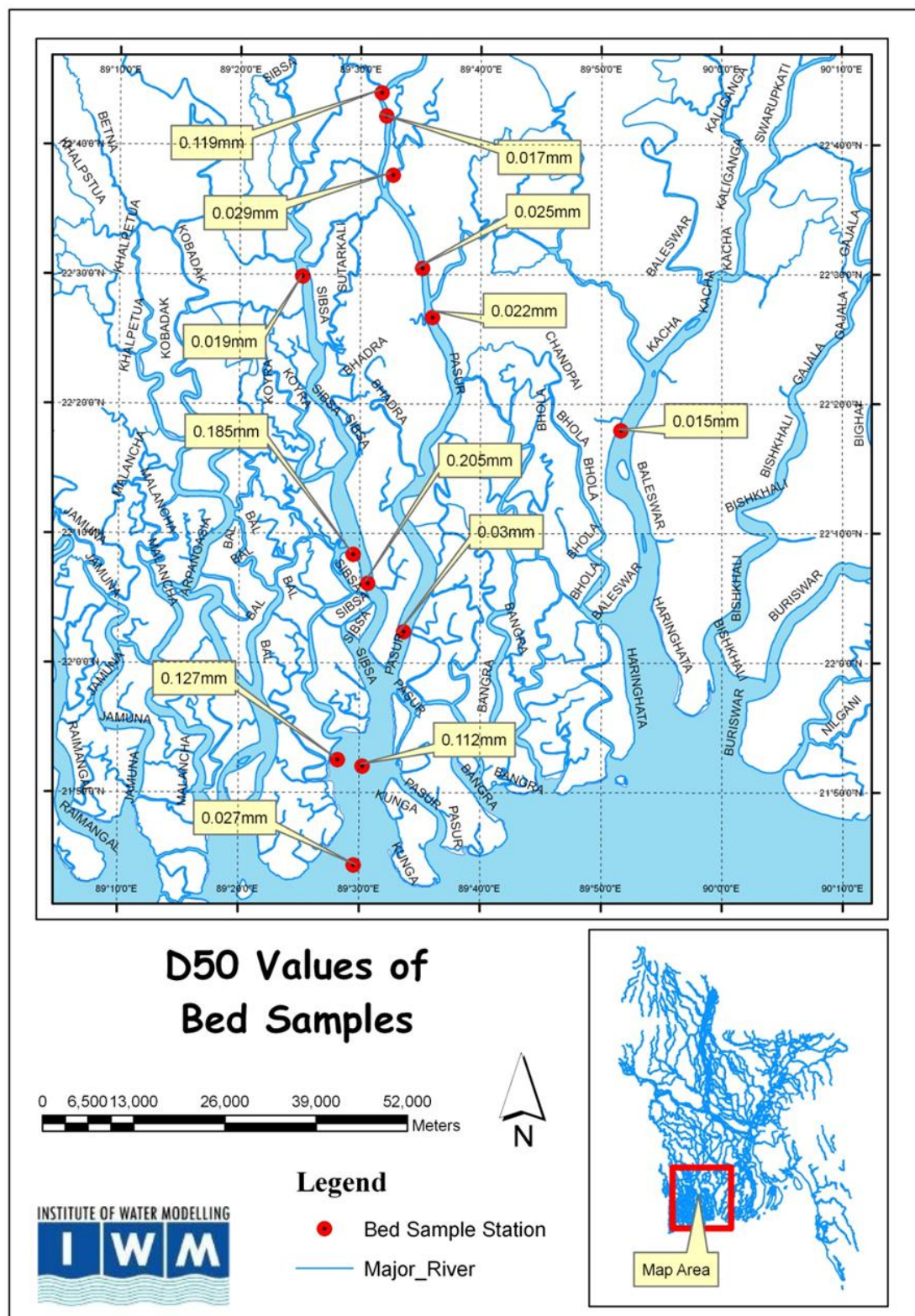


Figure 2-3 Bed samples d_{50} with locations during 2011 for the GRRP project.

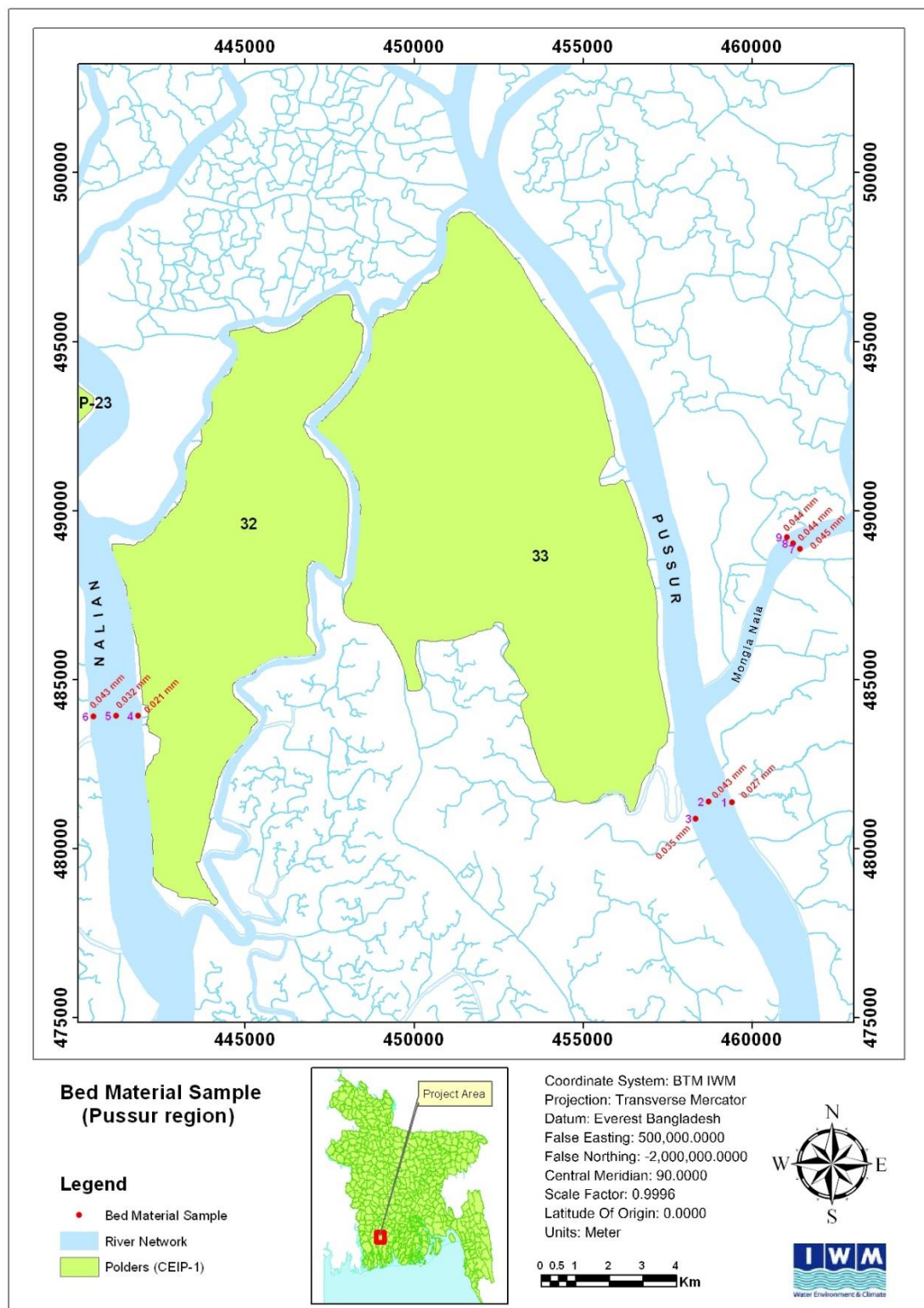


Figure 2-4 Bed samples d_{50} with locations during 2016 for the CEIP-1 project.

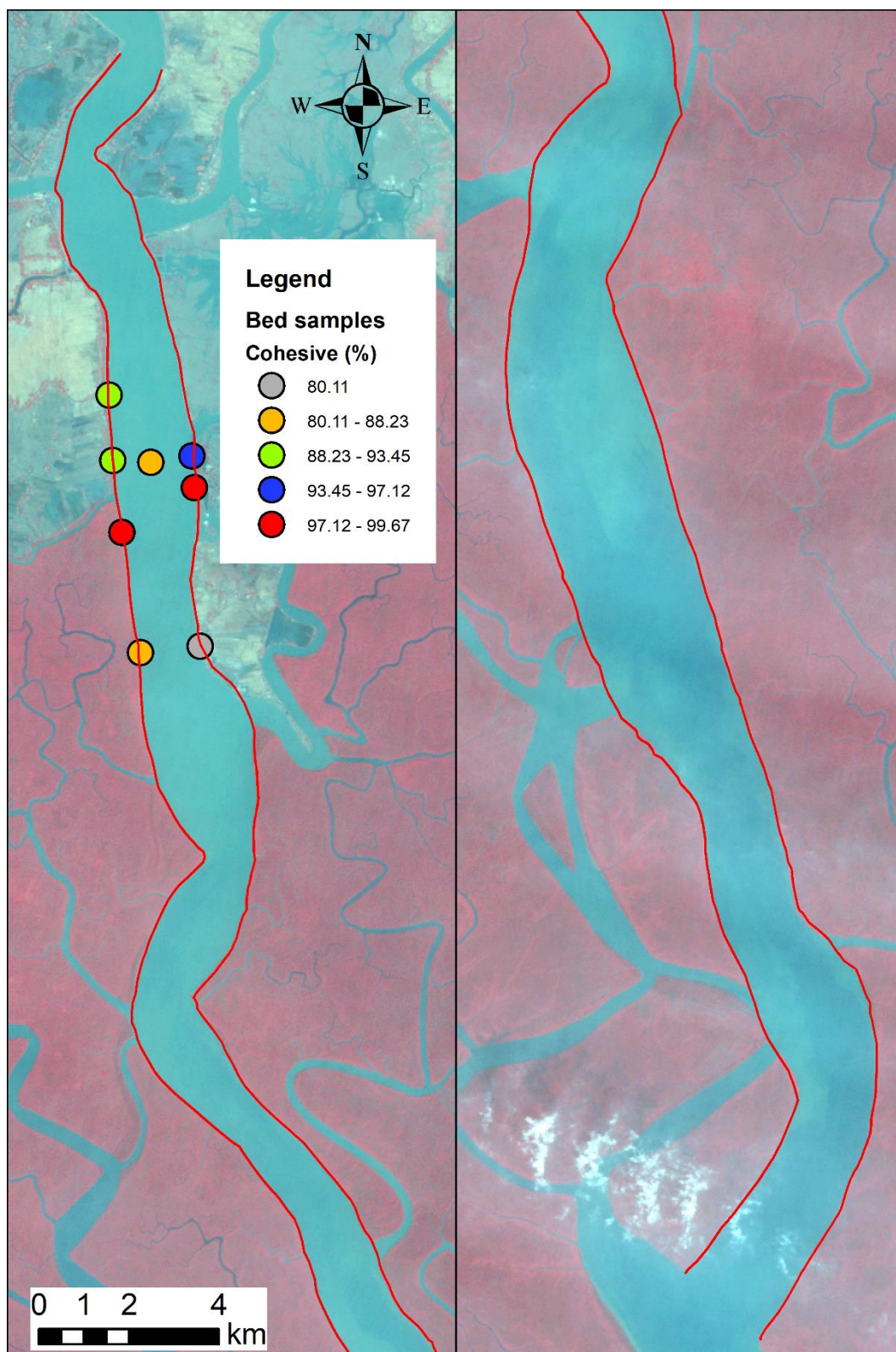


Figure 2-5 Measured sediment fraction of bed sample for Sibsa River. The colours indicate the cohesive sediment content.

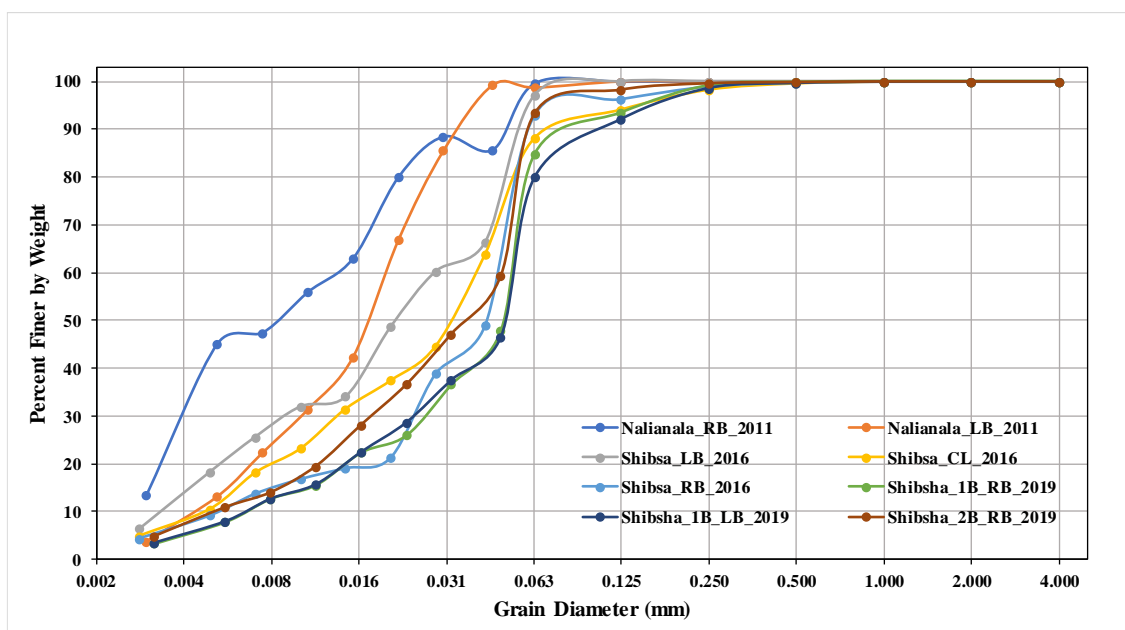


Figure 2-6 Sibsa River bed samples from 2011 to 2019 (February) collected by IWM.

Table 2-4 shows the bed samples processed into the Krumbein (1934) scale for the sand partition and clay/silt for the cohesive partition. The corresponding particle size distribution curves are shown in Figure 2-6.

The available bed samples for Sibsa River show consistently cohesive sediment dominated by silt. Many of the available bed samples for the neighbouring Pussur River show sand. It is noted that although the rivers are next to each other, they are known to be very different, with the Pussur River connecting upstream to Gorai River and Sibsa River being essentially a dead end. Some samples in the Sibsa River are sandy in the downstream end of the river (see Figure 2-3). However, particle size distributions are not available for those samples, which is an unfortunate shortcoming for the Sibsa River model development.

2.4 Suspended sediment data

Suspended sediment concentration data was collected in 2016 at Nalian station. Data was also collected during 2019 for the present project at Nalian.

Data was also available at the Sibsa River outfall in 2019, but there was no discharge data associated with these observations, and the SWRM 2019 model was not available for generating the Sibsa River outfall discharge when the data was processed. Therefore, the Sibsa River outfall data was not used in the C(Q) correlation.

Table 2-5 Suspended sediment concentration data for Sibsa River.

Suspended sediment sample data collection year	Station	Sources
2016 (4/3 and 9/3)	Nalian	CEIP-1
2019 (20/2, 28/2 and 8/5)	Nalian	Primary data (present project)
2019 (19/3)	Sibsa River outfall	Unknown

The suspended sediment samples are summarised in Table 2-5, while the locations of the two stations are shown in Figure 2-2.

In the following sections, C(Q) correlations (discharge versus sediment concentration) are processed. This is a common approach in fluvial systems where it is used to establish a sediment transport rating curve. In fluvial systems flows and sediment transport will be slowly varying, and there will generally be a relation between discharge, water level and bed shear stress, so also a unique sediment rating curve. This contrasts with a tidal system as the present, which means that a unique relation between discharge and sediment concentration cannot be expected. The plots, however, are useful for developing an understanding of the sediment dynamics and to generate continuous sediment concentration time-series to be used at the model boundaries.

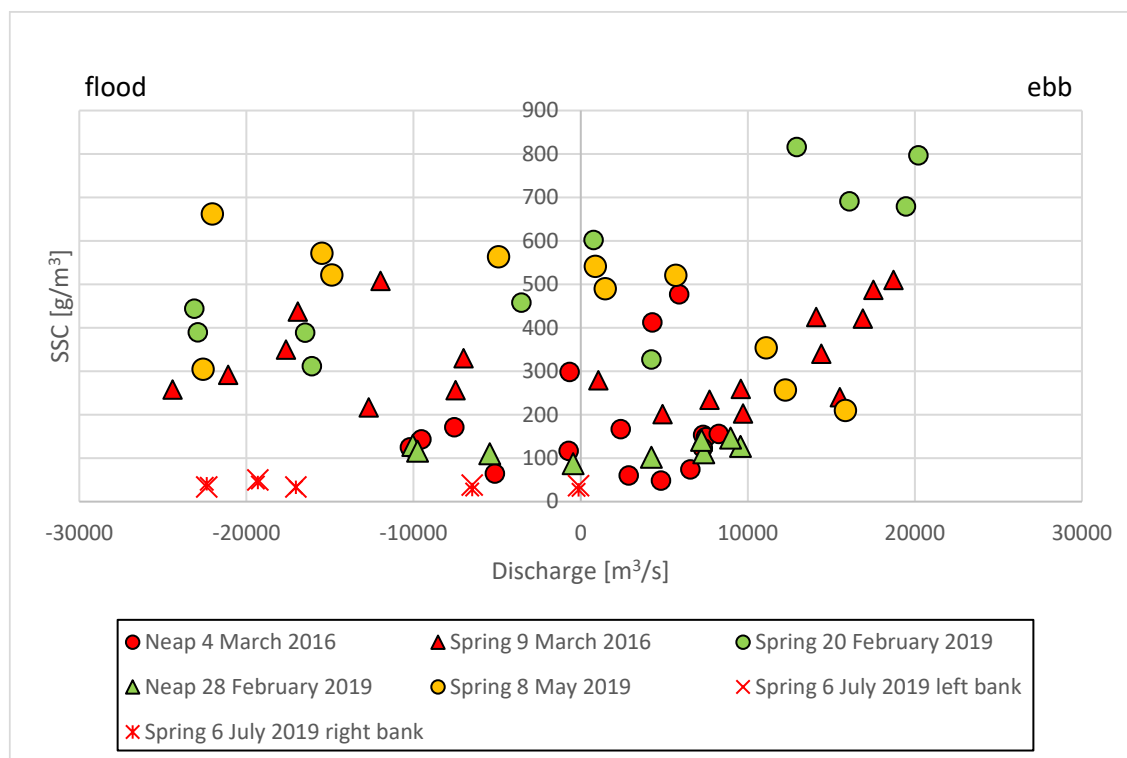


Figure 2-7 Correlation between discharge and sediment concentration for the Nalian station in Sibsa River. It is noted that the suspended sediment samples taken at the left and right banks on 6 July 2019 show distinctly lower concentrations due to the proximity to the banks. These are only shown for the sake of completeness but are clearly outliers (with almost identical concentrations).

The observations were processed into one graph showing the concentrations as a function of the discharge, see Figure 2-7. The correlation shows increasing concentration with the discharge and slightly higher concentrations for ebb flow compared to flood flow, although not significant. Nalian is not very far from the upstream model boundary in the Sibsa River model, and Sibsa is considered a dead end, so it is likely that Nalian has very low net sediment flux. That does not necessarily mean

the same concentrations for ebb and flood due to tidal asymmetry, but it would be reasonable to expect somewhat similar concentrations.

2.5 Suspended sediment particle size distribution data

Suspended sediment particle size distribution data was collected by IWM in 2001.

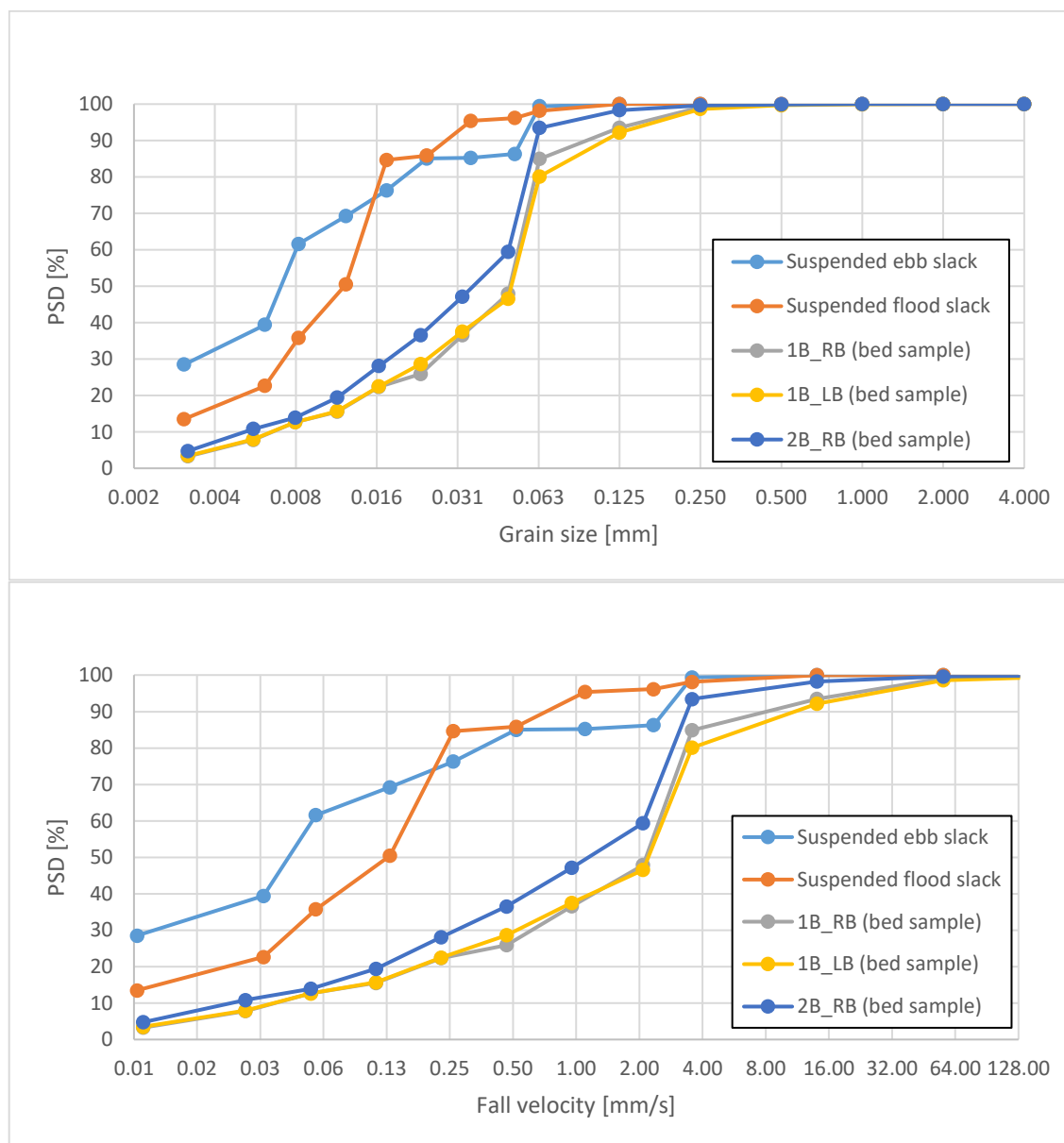


Figure 2-8 Suspended sediment particle size distribution at Nalian (IWM, 2001) compared to 2019 bed samples at the same location. Top: As a function of grain size, bottom: As a function of fall velocity calculated from Stokes' Law.

The data was processed into particle size distributions as function of the grain size and compared to the bed samples. In addition, the particle size distributions were shown as a function of the fall velocities calculated from Stokes' Law. The results are shown in Figure 2-8.

The data shows that the sediment in suspension is finer than the sediment in the bed. The suspended samples were from ebb and flood slack, suggesting that the samples contain more fine material compared to what would be observed for the more relevant ebb and flood peaks. However, there are no observations for the ebb and flood peaks, hence the analysis is conducted keeping that in mind. Even though the particle size distributions are only available for slack conditions, the observations are extremely valuable considering that they are the only available observations of suspended particle size distributions.

The bed suspended median grain sizes are very different, roughly 0.008 mm for the suspended sediment versus 0.05 mm for the bed samples. The bed samples have a median fall velocity around 1 mm/s, while the suspended samples show around 0.1 mm/s (rough numbers). This suggests that a representative fall velocity should not be 1 mm/s if wanting to correctly simulate sediment concentrations. However, 1 mm/s is representative for the bed samples. Cohesive sediment with a fall velocity of 0.1 mm/s has a settling time through 20 m water longer than the tidal cycle and will therefore have very limited morphological activity. This is also reflected in the bed samples, which show very little of the finest material abundant in the suspended samples.

Ultimately the analysis suggests that it is difficult to model the cohesive sediment with one representative fall velocity if wanting to correctly reproduce both bed levels and sediment concentrations. The single fraction model fall velocity has been selected from bed samples and the erosion function adjusted to obtain the correct bed level changes, but at the cost of not getting the best reproduction of sediment concentrations.

2.6 Historical bank lines from satellite imagery

Historical bank lines were studied based on satellite images. To this end, nine cloud-free scenes of Landsat imagery were acquired for the period of 1988-2019 from the Earth Explorer database of the U.S. Geological Survey. The acquired images cover all the rivers in the coastal zone for which meso-scale modelling was carried out in this project, thus also the Sibsá River. All the images were from the dry season from November to February as there were no cloud-free images during other seasons.

Bank lines were digitized from the images from 1988, 1995, 2001, 2011, and 2019 and are shown in Figure 2-9. In this figure, 25 locations with consistent and significantly eroding banks are indicated. It is observed that nearly all the locations with eroding banks are located along outer bends where the water depth adjacent to the bank is large (ebb channels). In addition, some eroding banks (see especially bank 18 shown in the figure) can be explained from smaller channels located between the bars and the inner bank (flood channels).

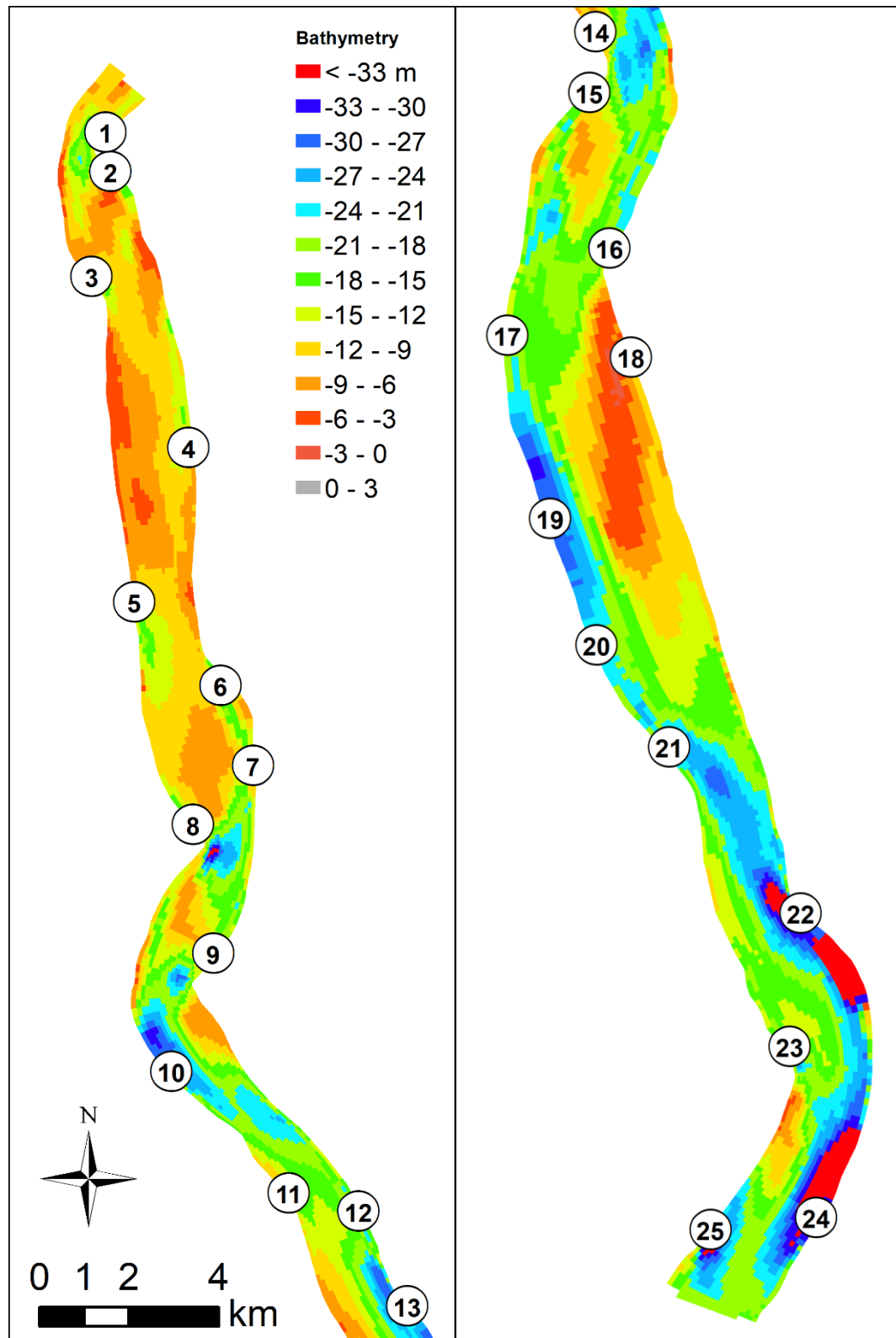


Figure 2-9 Locations of the 25 characteristic eroding banks along the Siba River based on digitized bank lines in 1988, 1995, 2001, 2011, 2019. The bathymetry is based on the 2011 survey.

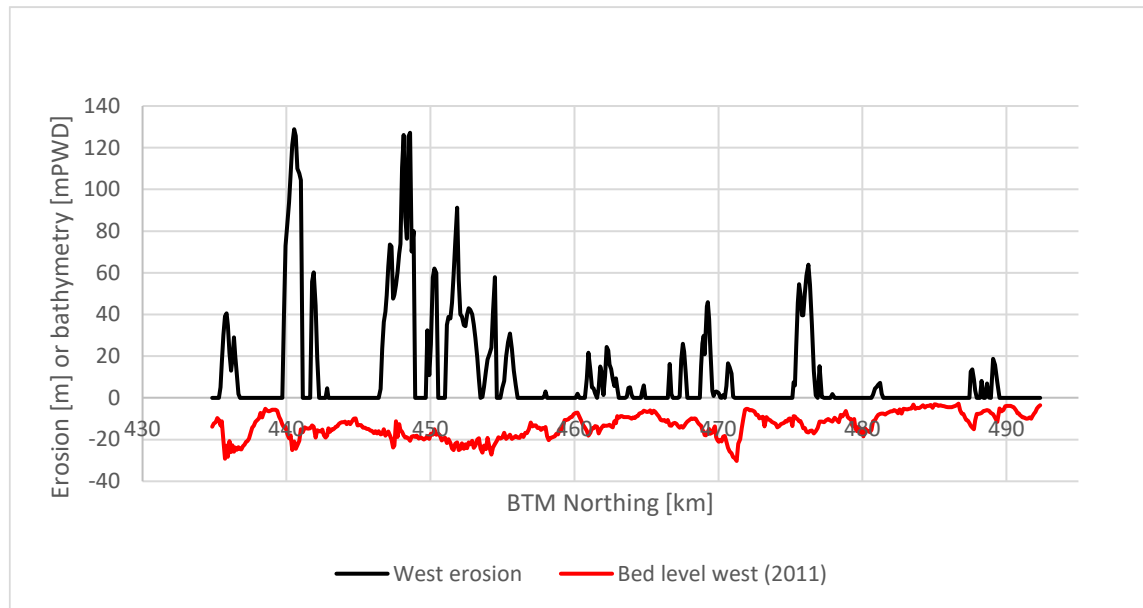


Figure 2-10 Observed bank erosion in 2011-2019 along the west bank of Sibsa River as a function of the BTM northing coordinate along the bank. The 2011 bathymetry is shown for reference to illustrate the correlation between bed level and bank erosion.

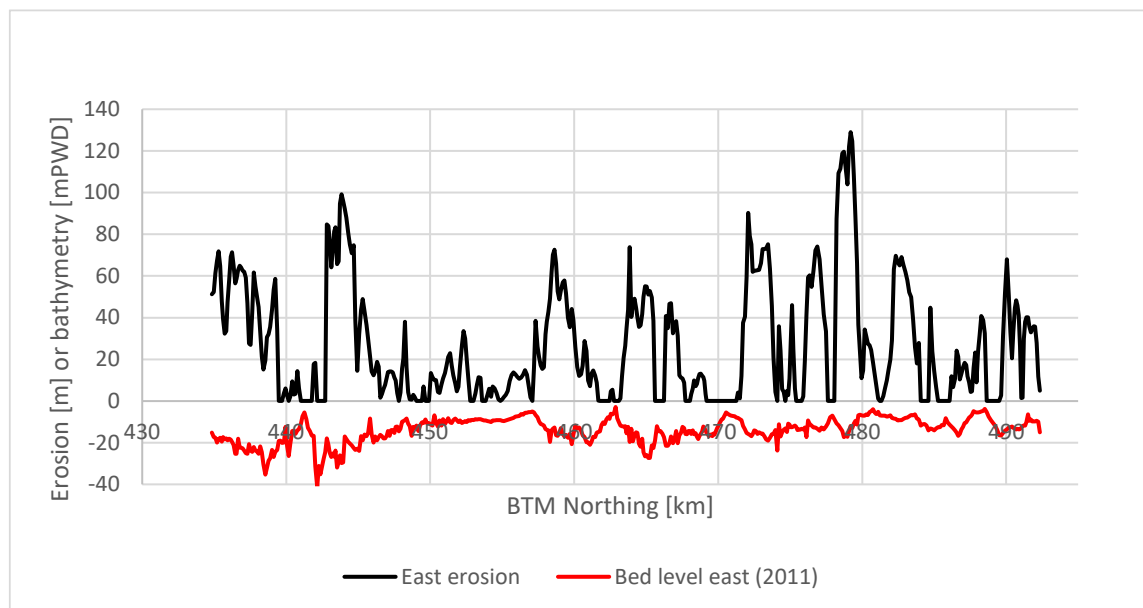


Figure 2-11 Observed bank erosion in 2011-2019 along the east bank of Sibsa River as a function of the BTM northing coordinate along the bank. The 2011 bathymetry is shown for reference to illustrate the correlation between bed level and bank erosion.

The bank erosion for the period 2011 to 2019 was processed from the digitised 2011 and 2019 bank lines by determining the distance from the 2011 to the 2019 bank line along normal vectors based on the 2011 bank lines. The results are shown in Figure 2-10 and Figure 2-11. The horizontal axis in these figures is the BTM northing coordinate since the Sibsa River largely runs north to south.

The eroded and accreted areas were calculated from the erosion and accretion curves and shown in Figure 2-12. It is interesting to note that the west bank experienced significant accretion exceeding erosion, while the east bank was dominated by erosion.

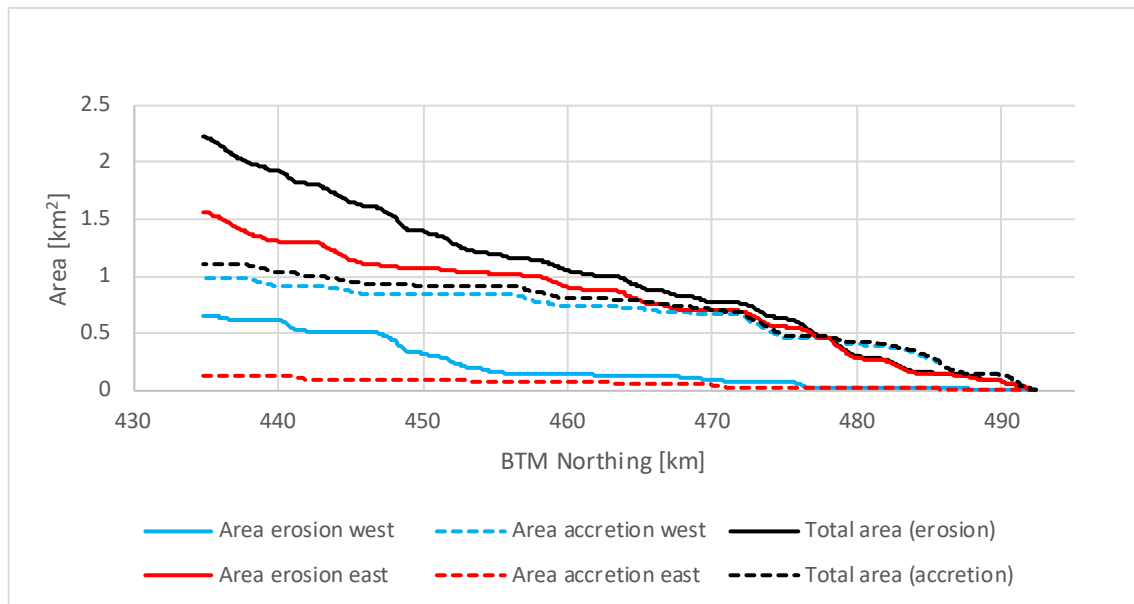


Figure 2-12 Accumulated area curves associated with bank erosion and accretion along each bank and total for the period 2011-2019.

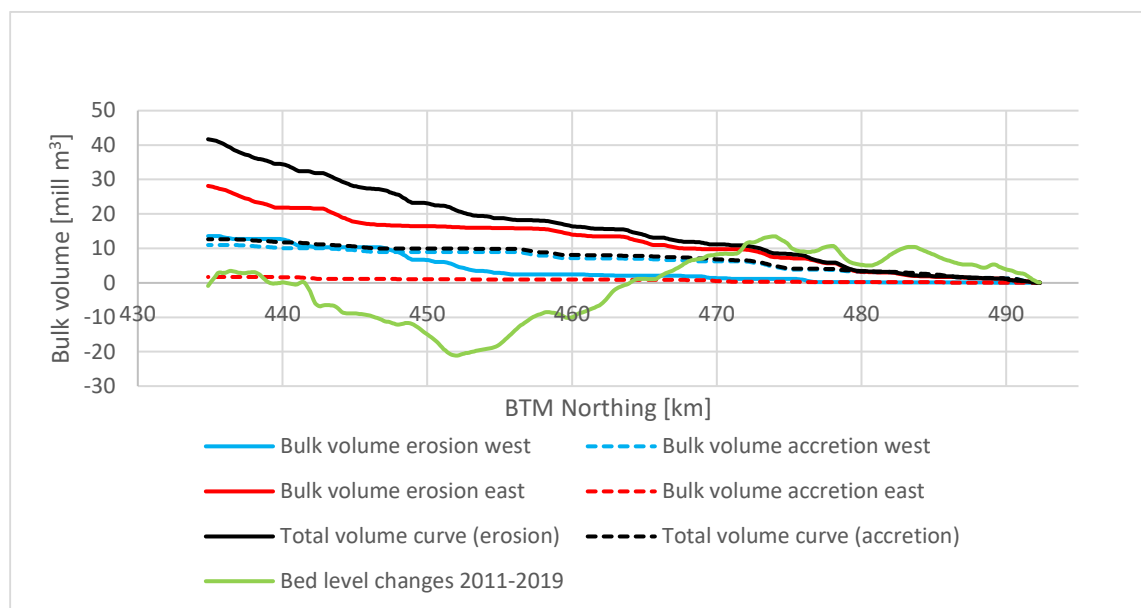


Figure 2-13 Estimated bank erosion accumulated bulk volume curves for the Sibsa River 2011-2019 compared to the observed accumulated bathymetry changes bulk volume curve.

The bank erosion bulk volume curves are interesting because they tell us how much the eroded material will contribute to the bathymetry changes. The local eroded volume was estimated from the 2011 bathymetry at the bank:

$$Vol = E (H_b - z) \Delta s$$

Where H_b is the bank level (estimated 2 mPWD in the Sibsa River model), z is the local bed level at the bank, E the erosion [m] and Δs the local grid spacing [m]. The volume curve is the integration of the eroded volumes along the bank, starting from upstream. Hence the downstream volume in the integrated bulk volume curve is the total eroded bulk volume.

Figure 2-13 shows a comparison of the bulk volume curves associated with bed level changes and bank erosion in the period 2011-2019. It is seen that the bulk volumes associated with bank erosion are higher than the volumes associated with bed level changes.

The same porosity (0.5) was used for the bank material and bed material. The bank material is more compacted than the bed material, which means that the eroded material will fill an even larger part of the sediment budget for 2011-2019.

Bank accretion was processed separately from the observations, although bank accretion is considered a passive process in the model. It can be seen from the figures that bank accretion amounts to half the eroded area in 2011-2019 but only around 25% of the volumes due to the generally much shallower water at accreting banks compared to eroding banks.

It can be concluded that the sediment bulk volumes associated with bank erosion are significant compared to the bulk volumes associated with changes to the bathymetry.

2.7 Subsidence

Subsidence was studied as part of the overall project and processed into a raster.

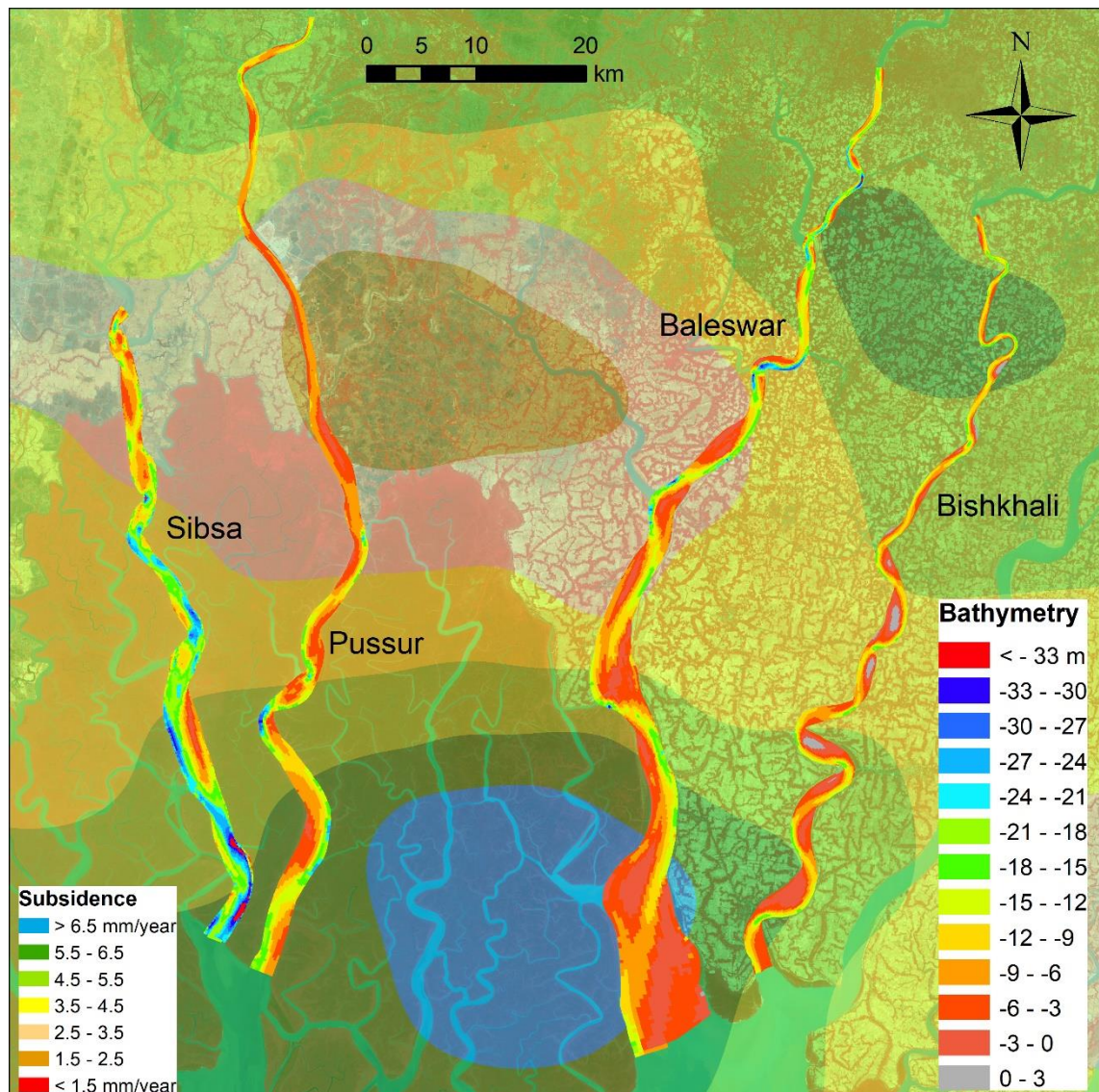


Figure 2-14 Subsidence spatial map in the area where the four models are located.

Figure 2-14 shows the subsidence based on the observations made for the project. The values were contoured to a 100 m raster for use with the MIKE 21C models, and the raster was converted to the individual curvilinear grids.

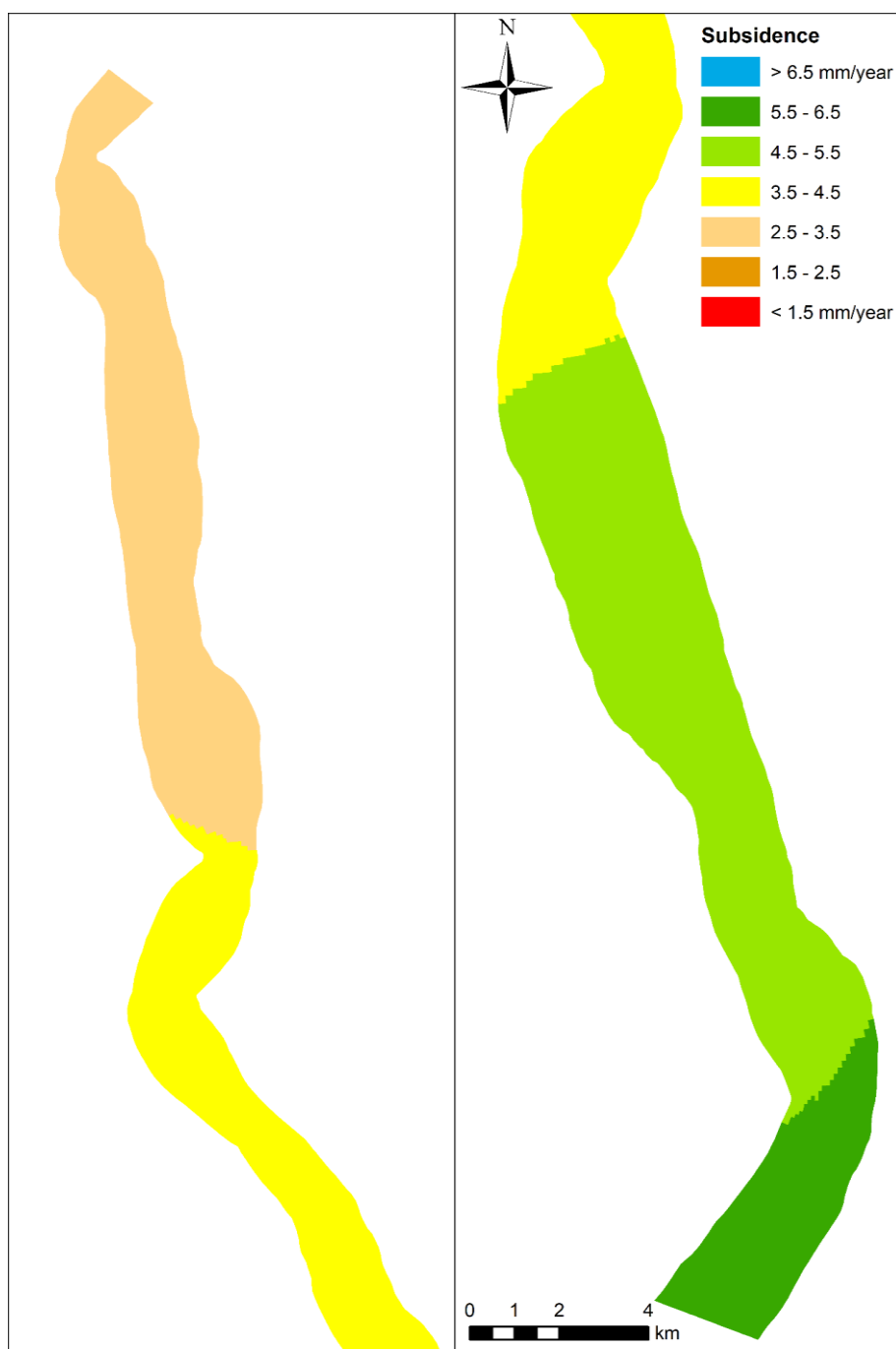


Figure 2-15 Subsidence interpolated to the Sibsa 2019 model grid.

Subsidence for the Sibsa is shown in Figure 2-15. The rates are generally around 5 mm/year, which means that over 30 years the riverbed will be lowered by 150 mm. The bed level changes associated with subsidence are hence small compared to morphological changes.

3 Model development

The model development process involves the following components:

- Curvilinear grid conforming to the bank lines
- Bathymetry contoured to the curvilinear grid
- Boundary conditions (upstream, downstream, side channels)
- Hydrodynamic calibration
- Sediment model formulation
- Sediment boundary conditions
- Sediment model calibration
- Bank erosion model calibration

The components are reported in this chapter.

3.1 Grid and bathymetry

The river system is to a certain degree influenced by floodplain (e.g. mangrove forest and floodplain outside polder areas), which was identified from the available DEM elevations. The MIKE 11 model (SWRM) also shows significant floodplain along Sibs River, which is reflected in the output from the MIKE 11 model.

Initially a full model for 2011 was developed with high resolution (1000x30) in the river channel and with floodplain included (full grid size 1000x68). The full 2011 model including floodplain was used for the hydrodynamic calibration.

Originally it was not the intention to run models over several years. However, the available data (2011 and 2019 bathymetries with similar resolution suited for 2D contours) combined with the systematic and slow planform development made it ideal to run simulations hindcasting 8 years (2011-2019) for morphological calibration.

Including the floodplain in the morphological model is not feasible when running simulations covering several years, and the grid resolution in the river channel was very high in the initial model. Several model runs were conducted to explore the impact of floodplain flow, and it was concluded that although the floodplain adds tidal prism, the impact is relatively small. It is also important to optimise the grid in the river channel to avoid excessive simulation times for the long-term morphological simulations. The model was subjected to stepwise coarsening until it was deemed that further coarsening would impact the result. In this way the coarsest grid that would ensure a grid-independent result was achieved.

The morphological model runs were conducted on a 500x20 curvilinear grid.

3.1.1 2011 model grid and bathymetry

The 2011 model grid and bathymetry were used for morphological model calibration and validation. Figure 3-1 shows the 500x20 curvilinear grid conforming to the 2011 bank lines, while the 2011 curvilinear bathymetry is shown in Figure 3-2.

The longitudinal cell size (Δs) varied in the range 36-256 m (average of 126 m), while the transverse cell size (Δn) varied in the range 18-190 m (average 90 m). For the cell area the range was 656-42,000 m² (average 11,650 m²).

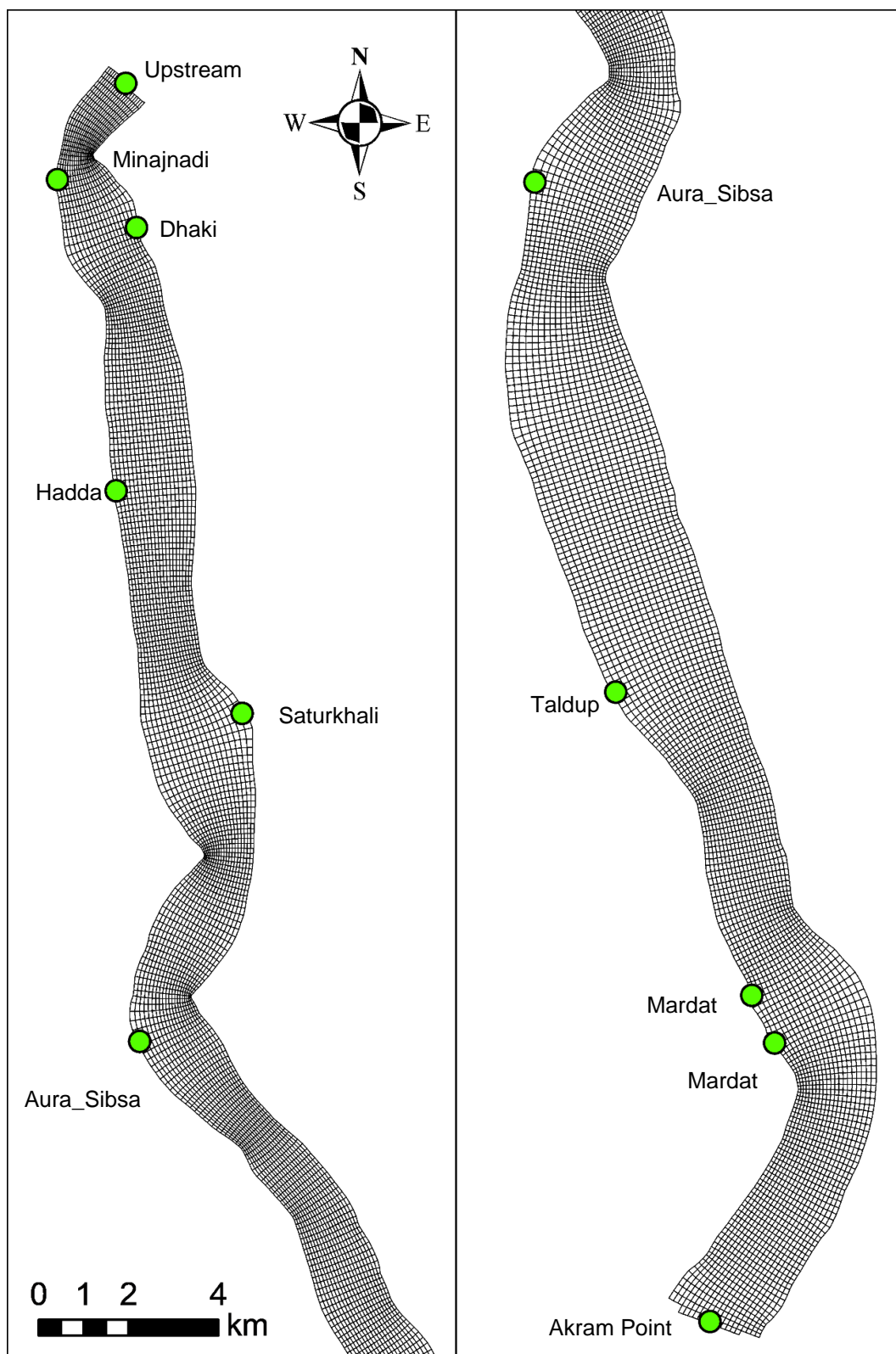


Figure 3-1 Sibs River curvilinear 500x20 grid 2011 with boundary locations shown to avoid too many figures.

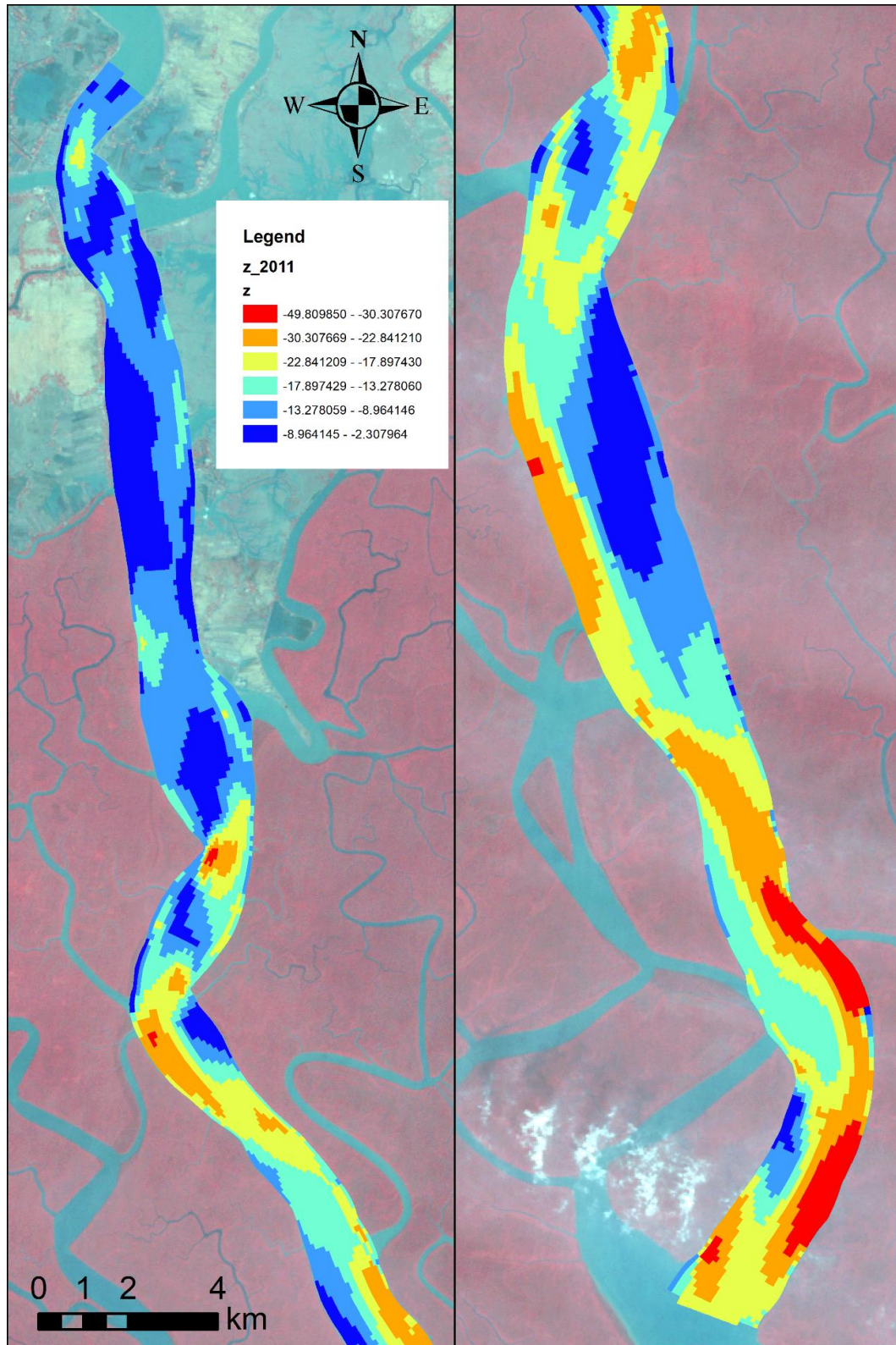


Figure 3-2 Sibs River curvilinear bathymetry 2011 shown with the 2011 Landsat image as background.

Joint Venture of



The expert in **WATER ENVIRONMENTS**

&



in association with



University of Colorado, Boulder, USA
Columbia University, USA

3.1.2 2019 model grid and bathymetry

The 2019 model was developed from the 2019 bathymetry collected for the project and the 2019 bank lines digitized from the 2019 Landsat image.

The 2019 model will be used for scenario simulations, e.g. bank erosion forecasting.

The 2019 bathymetry is shown in Figure 3-4.

It is not possible to tell the difference between the 2011 and 2019 grids without zooming in on local areas. Figure 3-3 shows a comparison of the 2011 and 2019 grids in the large and wide bend in the downstream end of the model.

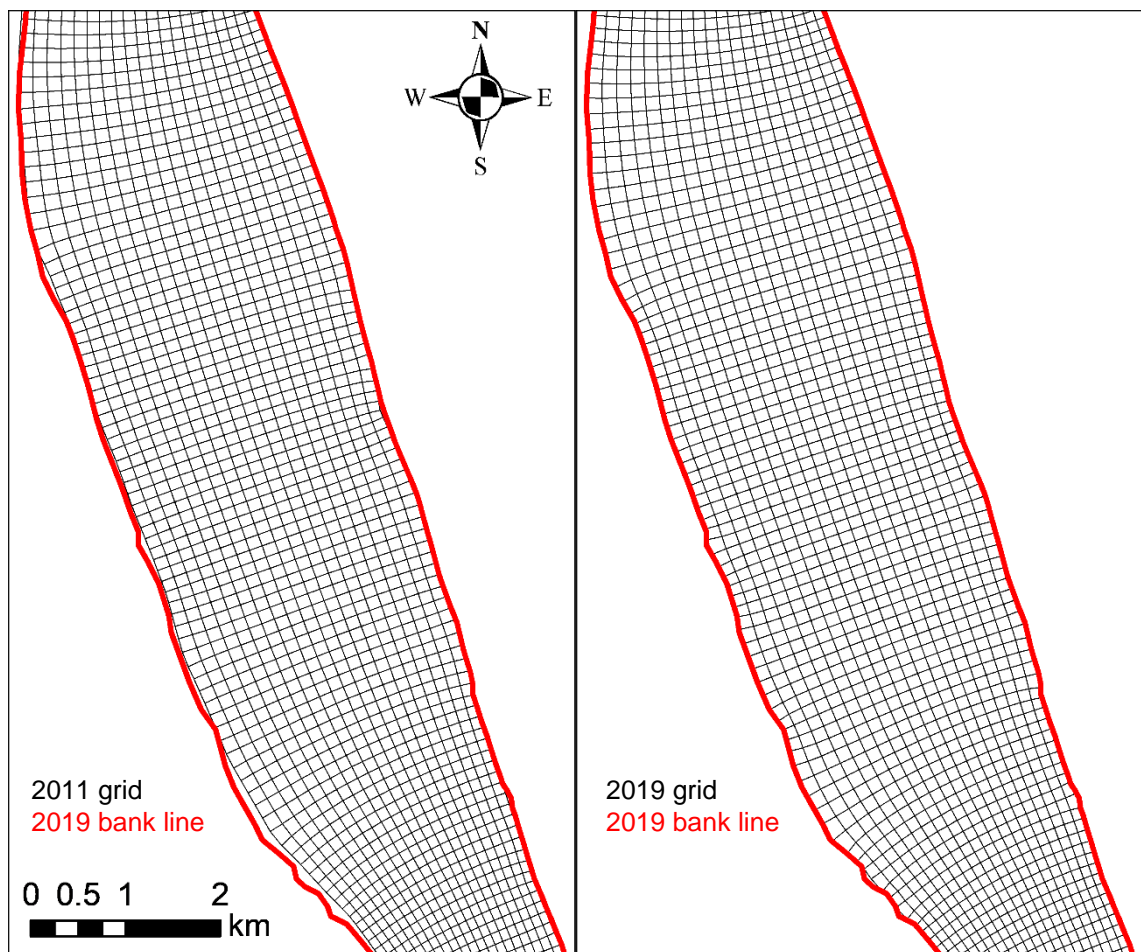


Figure 3-3 Illustration of the differences between the 2011 and 2019 grids, which cannot be identified without looking at the details. This is the large bend in the downstream end with consistent erosion since 1988 along the western bank. The 2019 grid conforms to the 2019 bank line, as seen in the figure. Even at this scale it is necessary to look carefully to see the differences between the grids (hint: western bank in the downstream end).

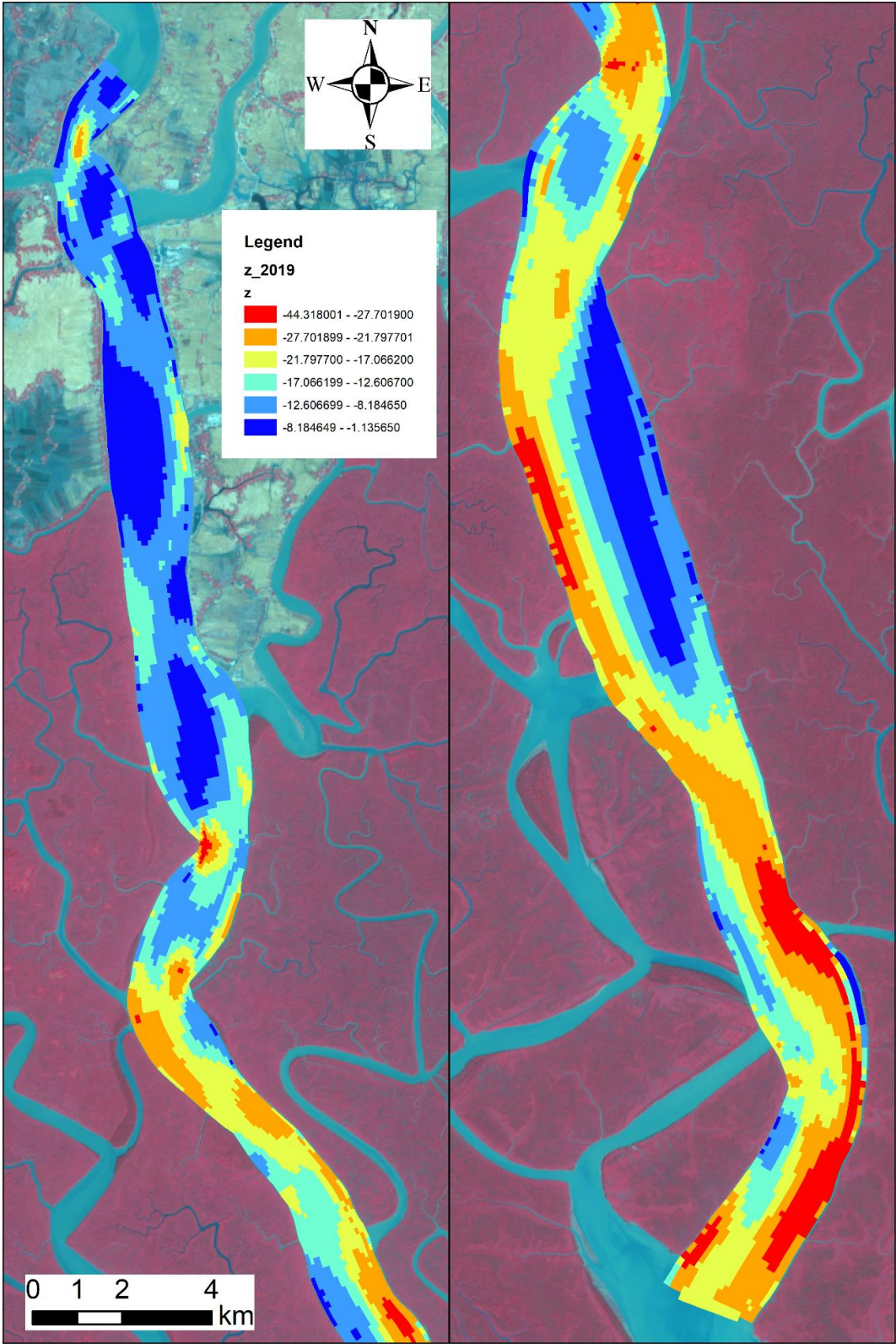


Figure 3-4 2019 bathymetry on 2019 grid with the 2019 Landsat image as background.

3.2 Hydrodynamic boundary conditions

The Sibsa River model has upstream discharge and downstream water level boundary conditions. The upstream boundary discharge was collected from the calibrated and validated South West Regional Model (SWRM). The downstream boundary water level was extracted from the combined river system model which has a water level boundary at Hiron Point.

The side channels discharges were added as source points (adding and removing water to reflect the interaction with the side channels) in the models. It is essential to include the side channels in the hydrodynamic model, as the flow exchanges with these side channels are significant. All the sources were extracted from the South West Regional Model provided by IWM.

For the morphological model runs, IWM provided a continuous time-series for the period 2011-2019 from the SWRM models available for each year. The SWRM is recalibrated each year, hence the time-series for 2011-2019 were merged from 8 individual model runs.

Table 3-1 Boundary conditions for the Sibsa River model.

BTM X [m]	BTM Y [m]	Type	Name	Chainage [m]
440645	492354	Q	Sibsa	10650
448653	434847	H	Sibsa	75000
439126	490221	Q	Minajnadi	15750
440429	483304	Q	Hadda	3000
440951	471068	Q	Aura_Sibsa	500
444761	460159	Q	Aura_Sibsa	19250
446561	448834	Q	Taldup	18700
449586	442092	Q	Mardat	3445
450098	441037	Q	Mardat	5400
440880	489150	Q	Dhaki	13500
443232	478360	Q	Saturkhali	27500

The boundary locations are tabulated in Table 3-1 and shown graphically in Figure 3-1.

Figure 3-5 shows the daily mean flow (flow averaged over two tidal cycles of 24 hours and 50 minutes) at the upstream boundary along with the corresponding minimum and maximum values. The daily mean flow has a clear seasonal signal with no mean flow in the dry season (i.e. purely tidal flow) and small mean flow during the monsoon. The years from 2011 to 2019 even have similar signals, but there are differences between the monsoons.

The Sibsa River has a very low net flow compared to the tidal discharges of the neighbouring Pussur River, which has much more net flow. This aligns with the consensus that the Sibsa River is an estuary with little freshwater flow, while Pussur River has upstream connection to Gorai River.

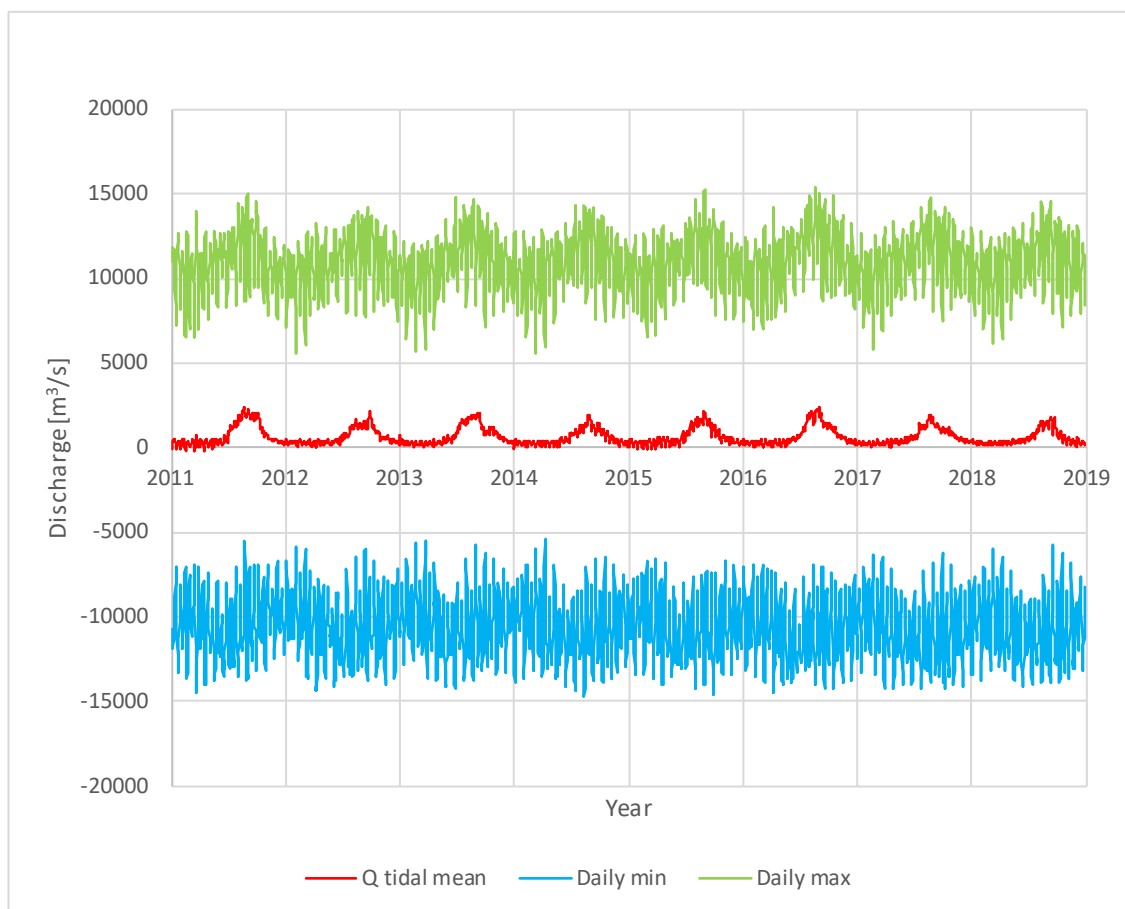


Figure 3-5 Daily minimum, maximum and mean flows 2011-2019 upstream boundary in the Sibsa River model.

3.3 Hydrodynamic boundary conditions for scenario simulations

The SWRM was used for generating boundary conditions for the MIKE 21C models with the inclusion of subsidence in the SWRM cross-sections and sea level rise in the Bay of Bengal tidal water level conditions, both calculated for the year 2050. A gradual calculation of annual variations from 2019 to 2050 is cumbersome because it would require preparation of new cross-sections every year due to subsidence, so instead only the 2019 and 2050 years were used in the MIKE 21C models. Both years were simulated using the 2019 SWRM without (baseline) and with subsidence and climate change.

IWM ran the SWRM for the period:

- 2 November 2018 00:00
- 29 October 2019 16:30

Results were extracted for the Sibsa model for the two scenarios:

- Existing conditions (baseline)
- Climate Change and Subsidence (Sub+CC)

Sibsa has the following open boundaries:

- Upstream discharge
- Downstream water level

There are also several side channels in the Sibsa model for which the same procedure was followed. Refer to Section 3.2 for details about the locations of these boundary conditions.

The full time-series is not meaningful to show due to the detail. Instead, the tidal time-series were post-processed to show the daily mean, minimum and maximum for the discharges upstream and for the water levels downstream.

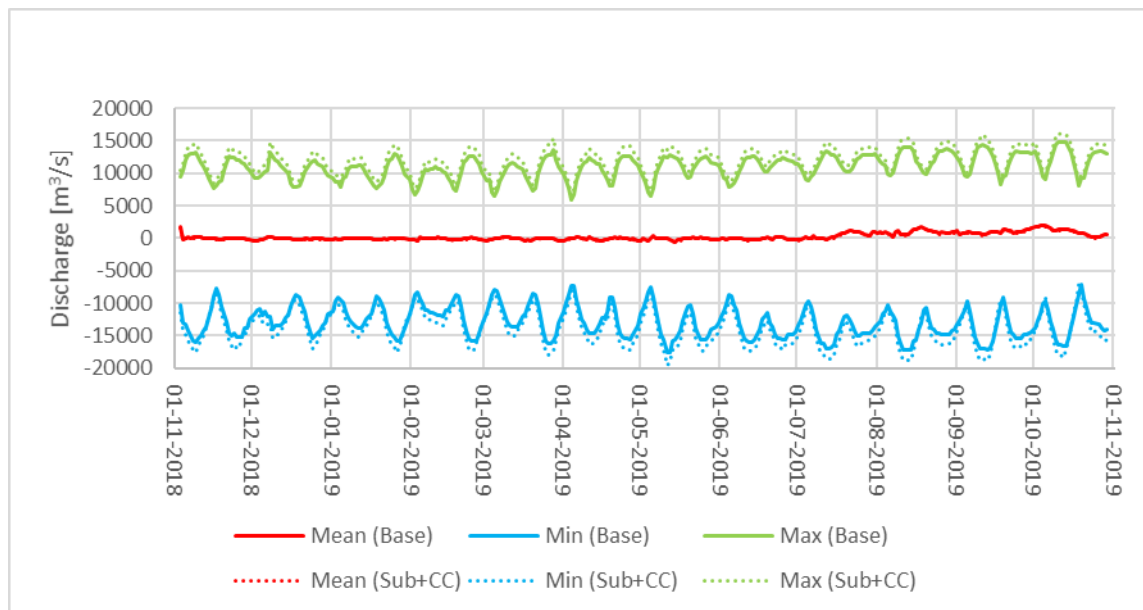


Figure 3-6 Daily minimum, maximum and mean flows 2018-2019 upstream boundary in the Sibsa River model for the two cases Base and Sub+CC.

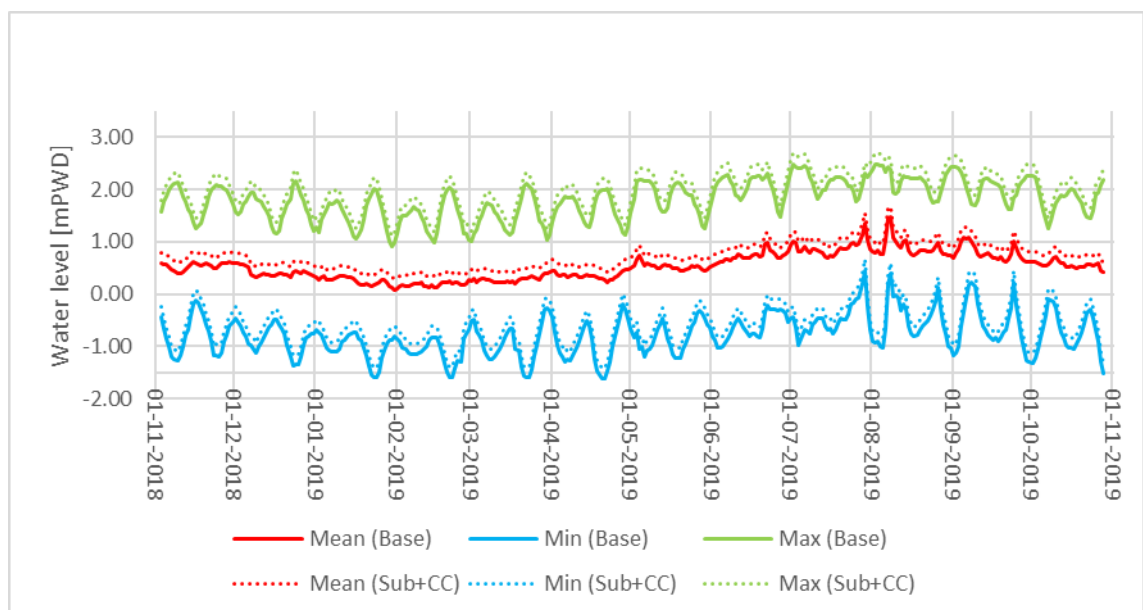


Figure 3-7 Daily minimum, maximum and mean water levels 2018-2019 downstream boundary in the Sibsa River model for the two cases Base and Sub+CC.

Figure 3-6 shows the post-processed daily discharges. The results show that the 2019 SWRM has no dry season net flow and negligible monsoon net flow, which was also the case for the SWRM results delivered for the Interim Report, in line with Sibsa being a dead end. Above all, the post-processed data suggests that the discharges generally increase with subsidence and climate change, which makes sense considering that all tide levels in the Bay of Bengal are increased and the bathymetry is lowered due to subsidence.

The water levels at the downstream boundary daily post-processed values are shown in Figure 3-7. This figure shows the expected rise in the water level due to climate change. The tidal water level increase is 20 cm.

Future sediment concentration boundary conditions were not altered compared to existing concentrations. It should be kept in mind that the model uses sediment concentrations and not sediment fluxes, so while sediment concentrations are considered unchanged in the future, the sediment fluxes can change.

3.4 Hydrodynamic calibration and validation

The data available for calibration and validation of the model are presented in Section 2.2 of this report. The hydrodynamic model was calibrated to field data during 2011 dry as well as monsoon season. The validation was done for 2015 and 2016. The locations of the field data are shown in Figure 2-2.

3.4.1 Hydrodynamic model calibration 2011

The Sibsa River model was calibrated with a constant Manning $M=50 \text{ m}^{1/3}/\text{s}$. The data did not justify a more detailed calibration, although the bed samples suggest that the downstream end is sandy, while the upstream end is cohesive. It is possible to calibrate the model with a resistance map but difficult to carry out with the available water level stations.

The downstream discharge stations are extremely valuable because they give an overall handle on the tidal prism, while there are no observed water levels at the downstream end of the Sibsa River.

Figure 3-8 to Figure 3-10 show the discharge calibration at Akram Point in Sibsa River during 2011 monsoon and dry season. The computed discharge is underpredicted for both flood and ebb flow, especially during spring flood and particularly during the monsoon. The simulated discharges from the SWRM are also shown to make it clear that both the MIKE 21C model and the SWRM underpredict the Akram Point discharge. It is noted that the SWRM has slightly higher Akram Point discharge than MIKE 21C, which is likely caused by floodplain flow in the SWRM. Underprediction in both models is generally worse for ebb flow. Implications are discussed in Section 3.4.3.

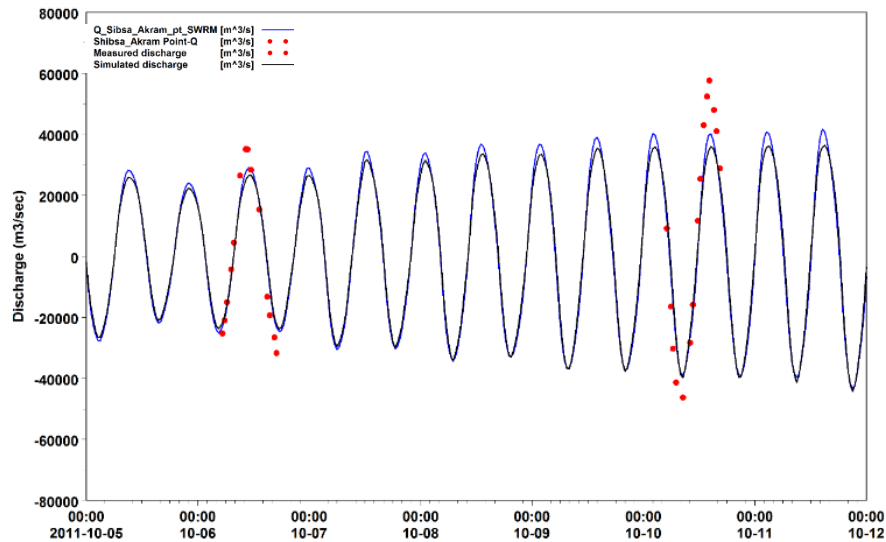


Figure 3-8 Discharge calibration at Akram Point in Sibsa River during the 2011 monsoon (October).

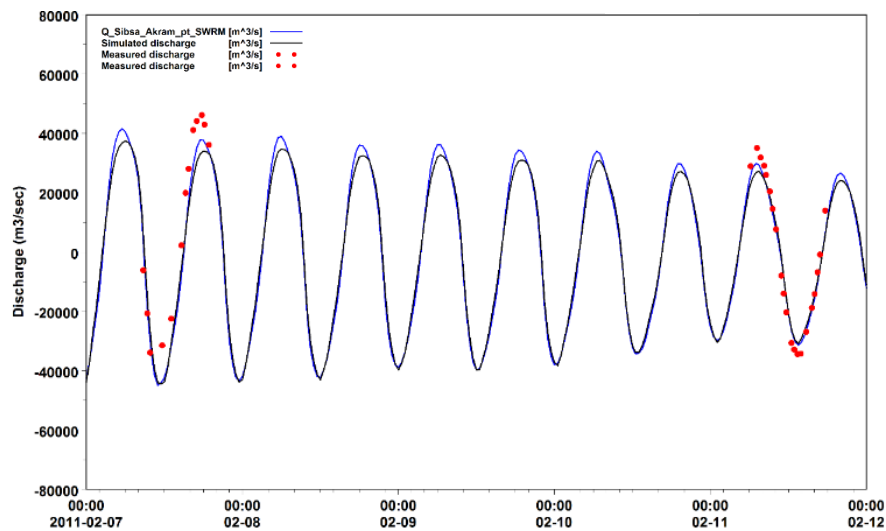


Figure 3-9 Discharge calibration at Akram Point in Sibsa River during the dry season (February).

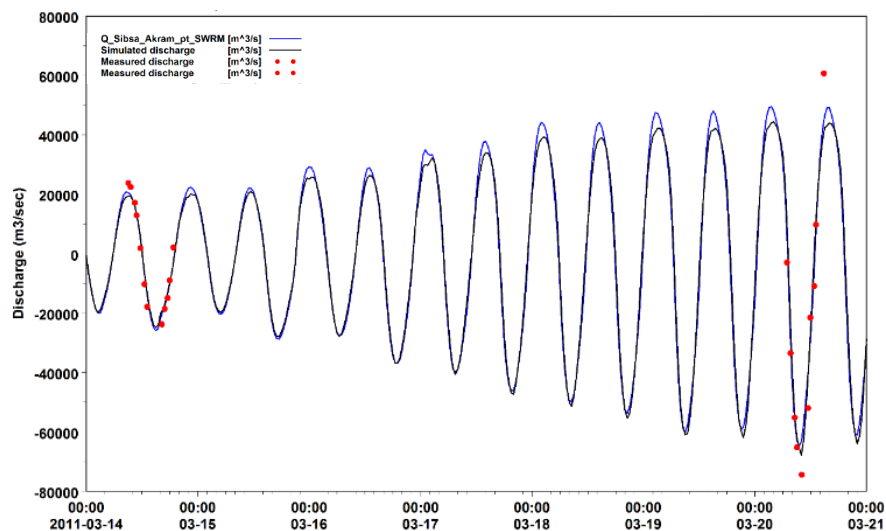


Figure 3-10 Discharge calibration at Akram Point in Sibsa River during the dry season (March).

3.4.2 Hydrodynamic model validation for 2015 and 2016

Water level observations are available for 2015 at Nalian and were used for validation of the hydrodynamic model. Additionally, observed discharges were available for Nalian in 2016.

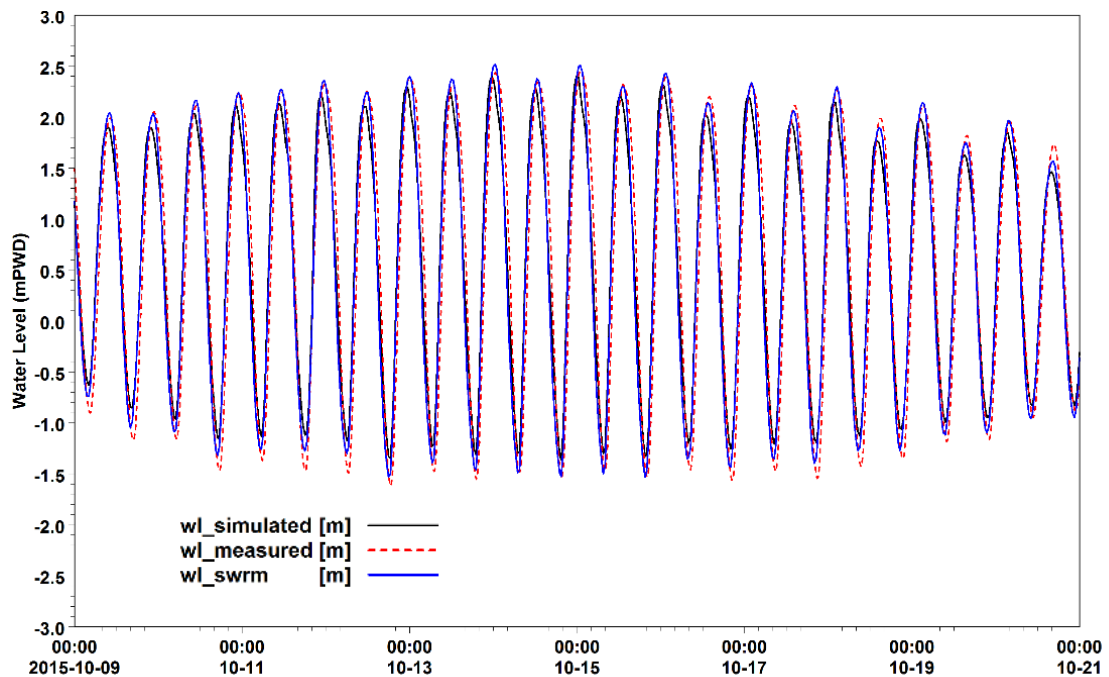


Figure 3-11 Water level validation at Nalian in Sibsa River during 2015. The results include the Sibsa River model and the SWRM, and both validate convincingly against the Nalian water level observations.

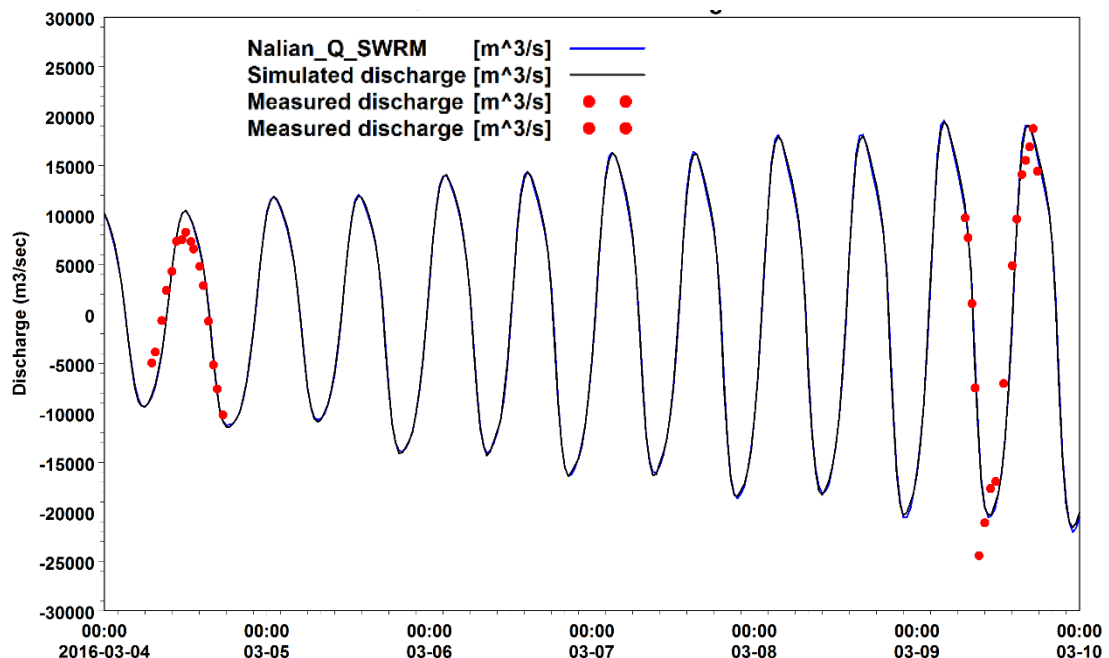


Figure 3-12 Discharge validation at Nalian in Sibsa River during 2016.

Figure 3-11 compares the observed and simulated water levels at Nalian in October 2015. The simulated water levels agree very well with the observations. The discharge validation is shown in Figure 3-12. The discharge agreement is also excellent, even though the discharge is underpredicted further downstream at Akram Point.

3.4.3 Summary of the hydrodynamic calibration and validation

The Sibsa River model has some issues when looking at the calibration and validation of the model. Both the MIKE 21C model and the SWRM underpredict the Akram Point discharges, while both convincingly reproduce the Nalian discharges and water levels.

The problem at Akram Point shows that the Sibsa River in both models does not exchange enough flow with the downstream estuary, while conditions further upstream at Nalian are correctly simulated. The implication is that there is something missing between Akram Point and Nalian, and it is probably the interaction with Pussur River through the many connecting channels, while floodplain between Akram Point and Nalian has only a minor impact (it is included in the SWRM, also underpredicting the Akram Point discharge).

The two rivers, Pussur River and Sibsa River, are known to exhibit complex interaction. In particular, the Sibsa River is distinctly deeper than Pussur River, meaning that the tidal signal propagates faster in Sibsa River, which will impact Pussur River. That does not seem to be correctly reproduced in the SWRM.

The underpredicted discharge at Akram Point is problematic with potential implications for the modelled morphological behaviour. Considering that the boundary conditions for the MIKE 21C model come from the SWRM, it is no surprise that the MIKE 21C model inherits the too low Akram Point discharges from the SWRM.

3.5 Sediment model

The cohesive sediment was modelled using the traditional cohesive sediment erosion (E) and deposition (D) functions, see Mehta et al. (1989).

The erosion rate [g/m²/s] was calculated from:

$$E = E_0 \left(\frac{\tau'}{\tau_{ce}} - 1 \right)^n, \tau' > \tau_{ce}$$

The deposition rate [g/m²/s] was calculated from:

$$D = w_s \gamma_0 C \left(1 - \frac{\tau'}{\tau_{cd}} \right), \tau' < \tau_{cd}$$

Where:

E Erosion rate [g/m²/s]

D Deposition rate [g/m²/s]

E₀ Erosion coefficient [g/m²/s]

τ' Skin friction shear stress

τ_{ce} Erosion shear stress threshold [N/m²]

τ_{cd} Deposition shear stress threshold [N/m²]

C Simulated concentration [g/m³]

w_s Fall velocity [m/s]

n Exponent (non-linearity)

γ_0 Ratio between near-bed and depth-integrated concentration (optional)

The calibrated parameters were:

$$\tau_{ce} = 0.2 \text{ N/m}^2$$

$$\tau_{cd} = 0.1 \text{ N/m}^2$$

$$E_0 = 0.015 \text{ g/m}^2/\text{s}$$

$$w_s = 1 \text{ mm/s}$$

$$n=1$$

$$\gamma_0 = 1$$

Porosity 0.6

3.5.1 Alternative 2-fraction sediment model including sand and silt

The bed samples do not show a consistent picture of the sediment size distribution in the bed in Sibsa River.

Older bed samples suggest that the Sibsa River is sandy downstream and cohesive upstream, the latter confirmed by the new bed samples collected for the present study, while no new bed samples were collected downstream. The most characteristic feature of the Sibsa River compared to the Pussur River is that Sibsa River is essentially a dead river end with very low net flow during the monsoon, while Pussur River has a much higher net flow during the monsoon. It is often seen that an estuary with small net sand transport exhibit strong spatial grain size variations, as is also seen in some of the old Sibsa River bed samples.

The large bar in the downstream end of Sibsa River is not well captured in the model, e.g. the transverse bed slope for the bar is poorly described. If the bar is sandy, the behaviour will be very different from what is simulated. The experience from other models developed during the study is that bars behave very differently when they are sandy compared to muddy and that sand bars can develop much higher curvature due to the potential for dune cover, yielding significant flow deflection from the bars.

The potential use of a 2-fraction model was explored, but it was deemed too subjective due to the lack of data. Especially the lack of bed samples downstream and particle size distribution data for Akram Point are problematic.

3.6 Sediment transport boundary conditions

All boundaries use constant sediment concentrations in the Sibsa River model:

- Upstream concentration: 200 g/m³
- Side channels: 200 g/m³
- Downstream: 200 g/m³

Due to the nature of the advection-dispersion equation, the boundary conditions are only enforced when water flows into the model, e.g., at the upstream end the boundary condition was only enforced for ebb flow.

3.7 Calibration against observed bed level changes 2011-2019

The best way to calibrate a morphological model is always to hindcast the observed morphological development. In the present project, bathymetries for 2011 and 2019 were available. Both datasets were collected by IWM using similar resolution and survey methodology. The time span between these two datasets as well as their quality offer an excellent basis for an accurate determination of the morphological changes and thereby the opportunity for calibrating the morphological model.

Figure 3-13 shows the observed and simulated bathymetry developments in the hindcast period 2011-2019. The agreement between simulated and observed bed level changes was very good in the upstream end and less satisfactory in the downstream end. Many attempts were made to improve the downstream end, but without success.

The shortcomings in the model calibration are discussed further in the next section where they are more easily seen in the longitudinal variations.

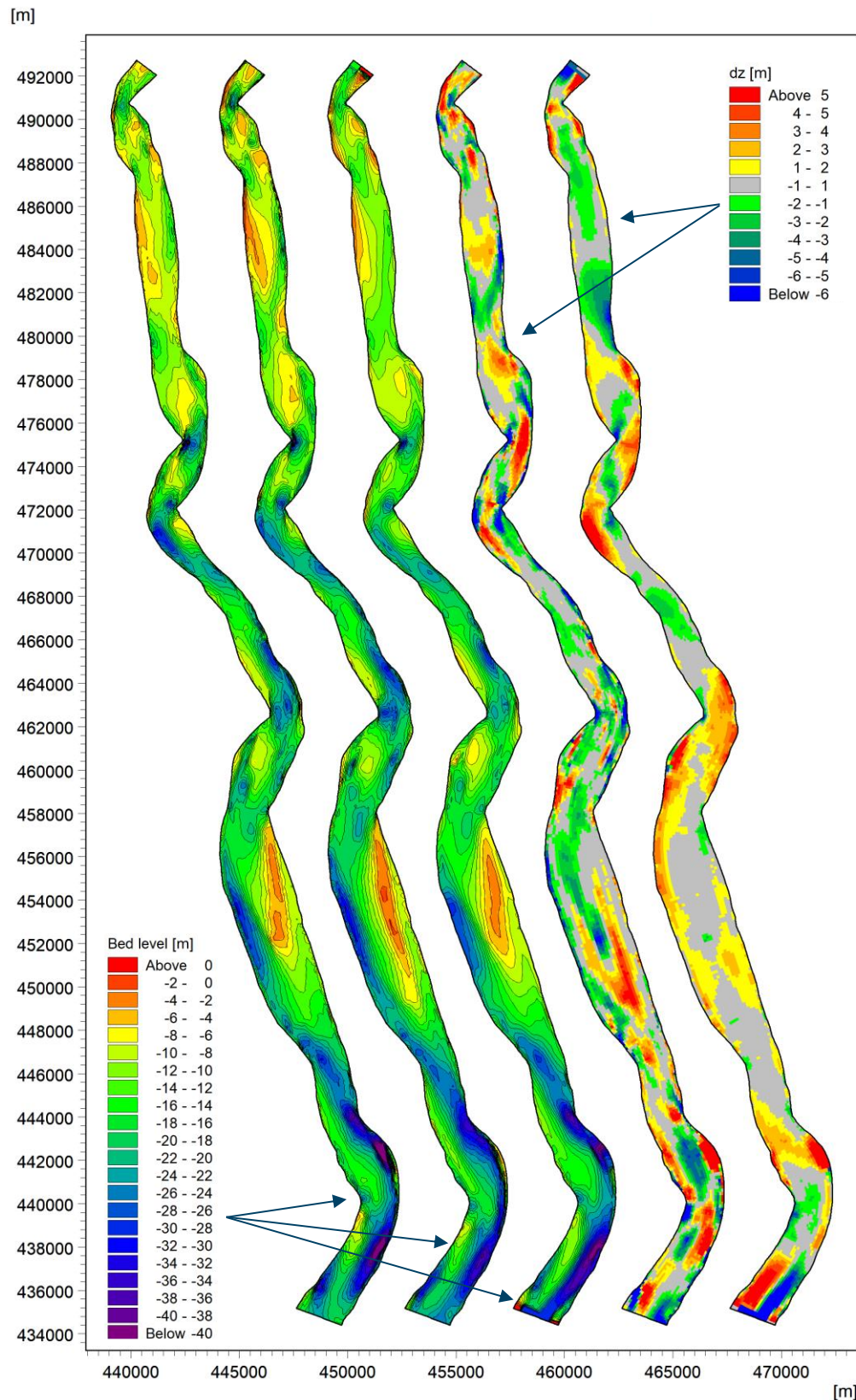


Figure 3-13 Comparison of observed and simulated bathymetry development 2011-2019. From left: Observed bathymetry 2011, Observed bathymetry 2019, Simulated bathymetry 2019, Observed bed level changes 2011-2019, Simulated bed level changes 2011-2019.

Joint Venture of



The expert in **WATER ENVIRONMENTS**

&



in association with



University of Colorado, Boulder, USA
Columbia University, USA

3.8 Longitudinal validations

The spatial bed levels and bed level changes are very useful for showing the model calibration. Another way to compare is to use volume curves, which are calculated by width-integrating the bed level changes to obtain:

- Width-averaged bed level change as a function of chainage
- Accumulated bulk volume curve showing the deposition upstream of the considered chainage

The volumes are calculated from bed level changes and are hence bulk volumes.

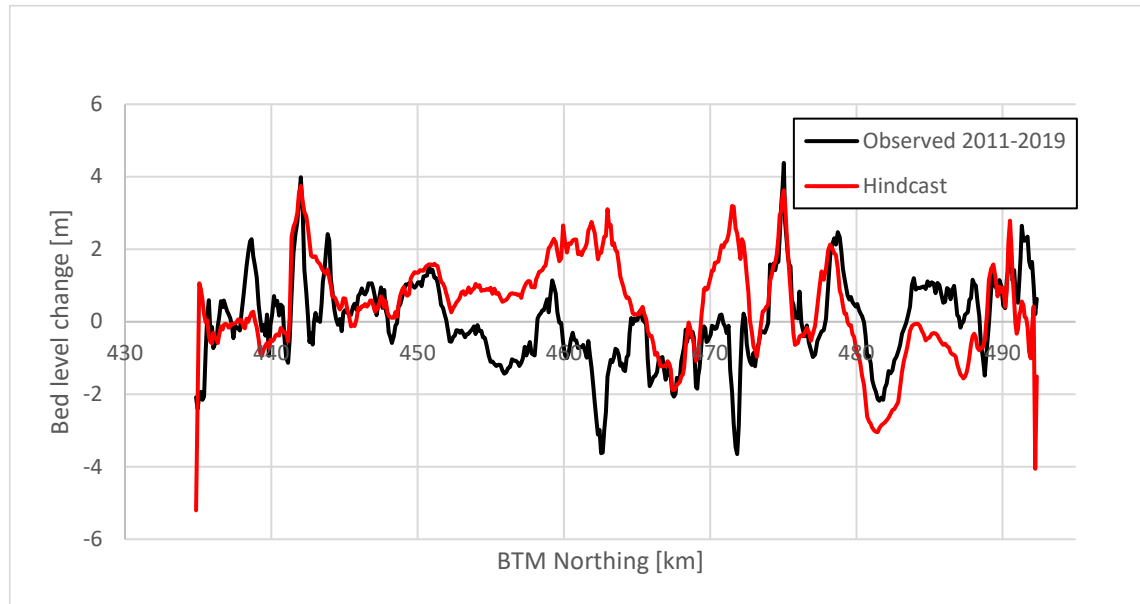


Figure 3-14 Comparison of observed and simulated width-integrated bed level changes 2011-2019.

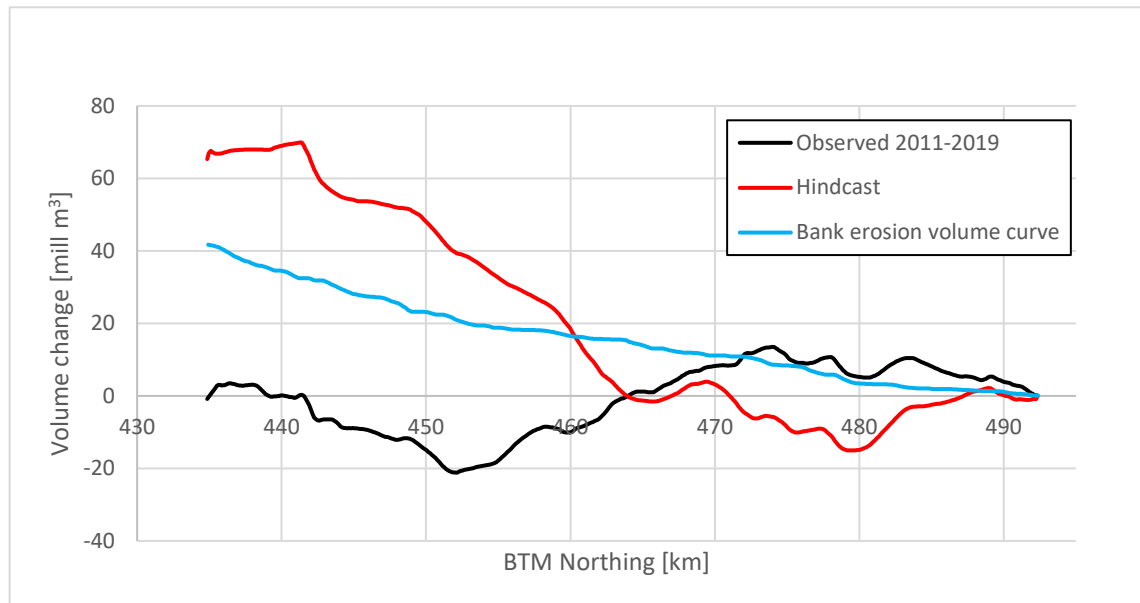


Figure 3-15 Comparison of observed and simulated bulk volume curves for 2011-2019.

The curves for the calibrated model are shown in Figure 3-14 and Figure 3-15.

The local bed level changes look convincing, except in the middle of the model reach. In the upstream and downstream parts, the longitudinal pattern is clearly correct in the model, while there

is a major error in the middle of the model. The adopted sediment model is probably a better representation of the Sibsa River in the upstream end where the sediment model is consistent with the available bed samples, and the Nalain discharges are correctly simulated. Further downstream some old bed samples suggest that the river is at least partly sandy. If the downstream end is sandy, the behaviour will obviously be very different in a simulation.

It can also be noted that bank erosion contributes significantly to the sediment budget.

It is known from the hydrodynamic model calibration that the Akram Point discharge is underpredicted by the model. If the Akram Point discharge stems flow exchange with the Pussur River and floodplain, this can explain, at least on paper, why deposition is observed around BTM northing 460 km, while the observations show erosion (returning flow). The returning flow can also explain why the deposition seems to want to move downstream compared to the central part of the model.

It is also instructive to observe that the overall volume change in the river in 2011-2019 was neutral. The integrated bulk volume curves show that the downstream end exhibited erosion, while deposition took place further upstream.

3.9 Bank erosion model

Several bank erosion formulas were tested during the developments of the models. A formula based on Hasegawa (1989) was selected as the most optimal formula:

$$E = E_h |V| \left(1 - \left(\frac{h_c}{h} \right)^{2/3} \right)$$

Where E is the erosion rate [m/s], E_h a non-dimensional calibration parameter, V is the near-bank flow velocity [m/s], h the near-bank water depth [m], and h_c the critical water depth [m] below which no erosion takes place. Calibration simulations resulted in the following parameters in the derived Hasegawa (1989) bank erosion formula:

$$E_h = 10^{-6}$$

$$h_c = 10 \text{ m}$$

The calibration result is presented and discussed in the following.

The observed and simulated bank erosion in 2011-2019 along the east and west banks are compared in Figure 3-16 and Figure 3-17. The agreement between simulated and observed bank erosion rates is reasonable.

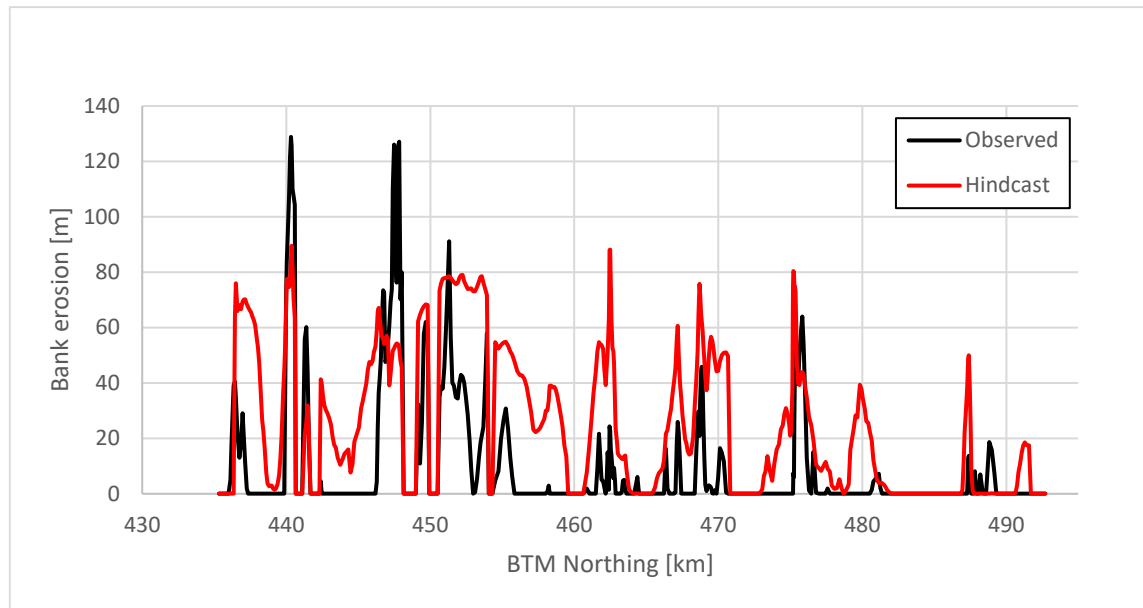


Figure 3-16 Observed and simulated west bank erosion for the Sibsa River model 2011-2019.

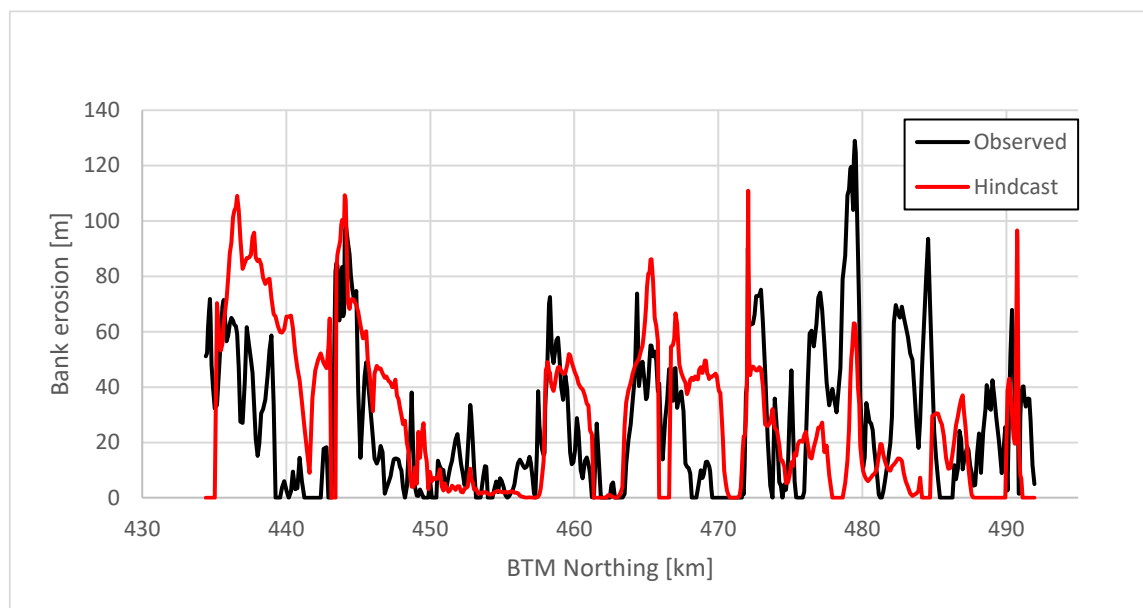


Figure 3-17 Observed and simulated east bank erosion for the Sibsa River model 2011-2019.

3.10 Comparison of observed and simulated bank lines 2011-2019

The bank erosion hindcast simulation was conducted without updating the bank lines. This is easier for calibration purposes because updating of the bank lines will change the grid, leading to many complications when post-processing the results. The error associated with not updating the bank lines is small for cases where the bank erosion is much smaller than the width, which is the case for 2011-2019. However, for longer model runs, the feedback between planform and bathymetry must be accounted for. Considering that the application model should run much longer timescales compared to 2011-2019, the application model was prepared for using dynamic grid updating.

Bank line changes are small compared to the width of the river. It is therefore necessary to zoom in to specific reaches of the river to detect the detailed developments. In the following the simulated and observed bank lines changes at selected reaches are presented.

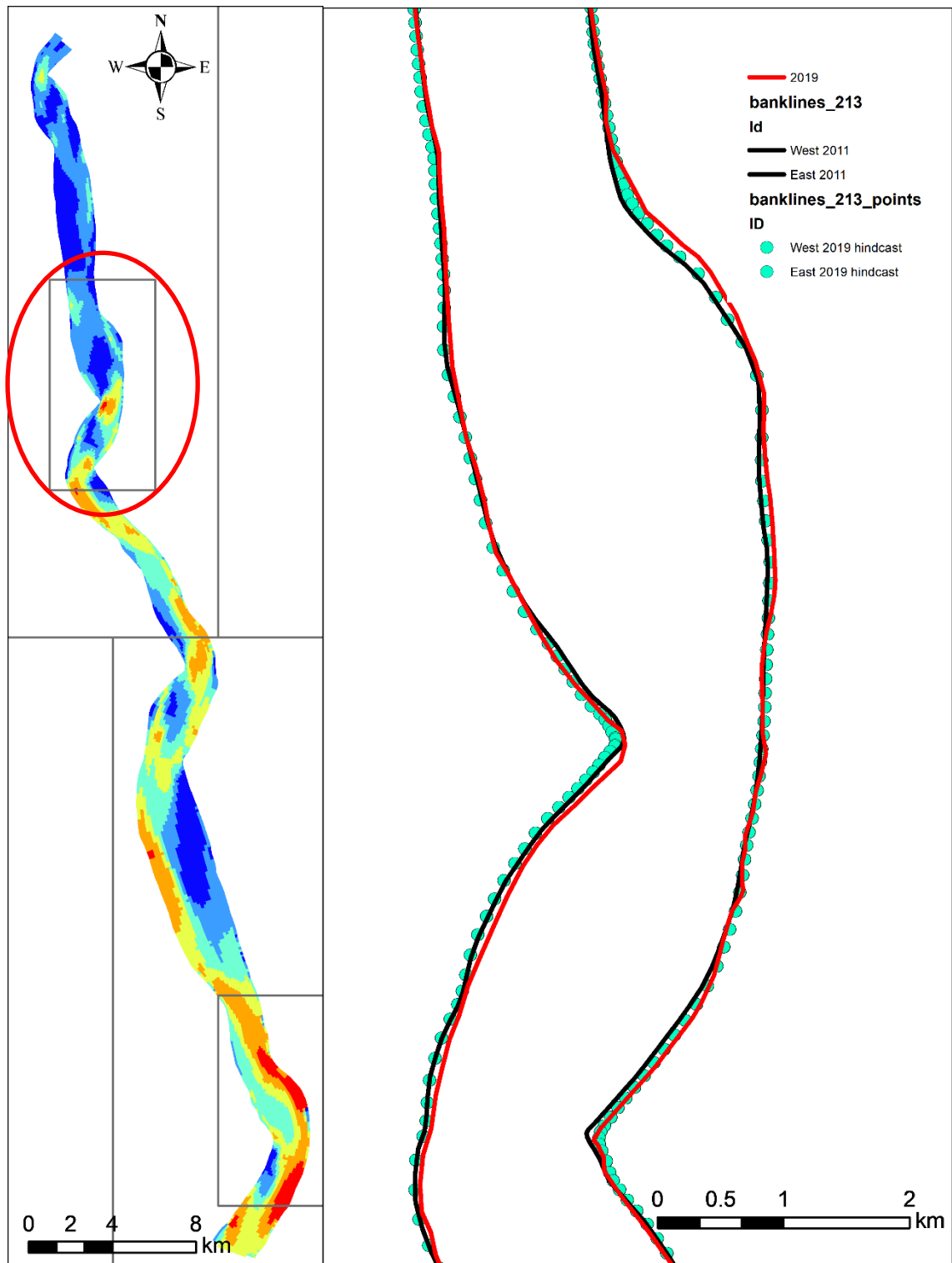


Figure 3-18 Comparison of observed and simulated bank lines in a local area in the upstream end.

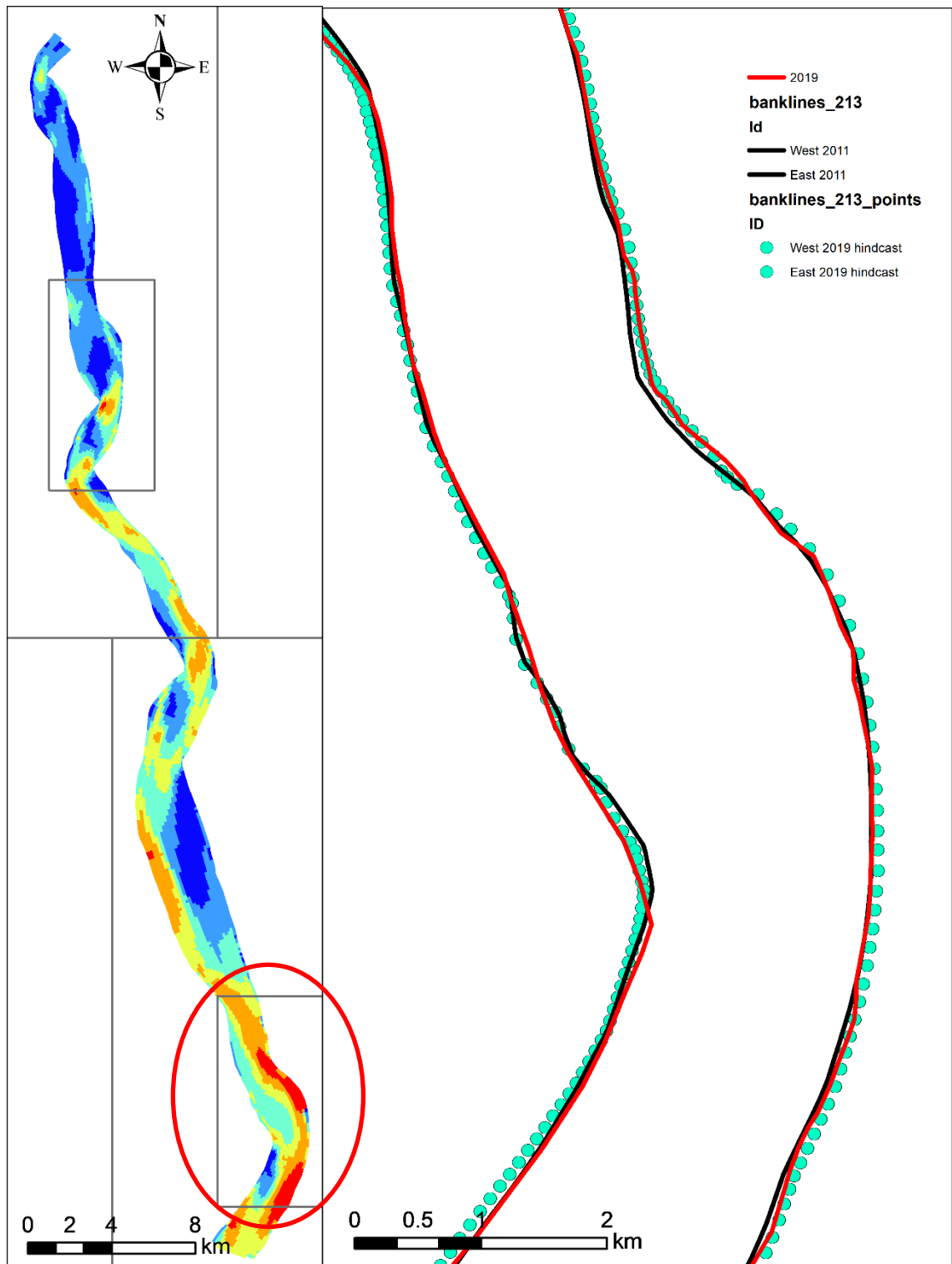


Figure 3-19 Comparison of observed and simulated bank lines in a local area in the downstream end.

Local bank line details are shown in Figure 3-18 and Figure 3-19. These represent the actual bank line movements corresponding to the bank erosion as a function of northing coordinate.

4 Model applications

The model applications are reported in this section.

4.1 Bank erosion forecast 30 years into the future

The existing and 30 years into the future boundary conditions were applied in conjunction to represent a reasonable time-series representing the next 30 years. The existing and 30 years into the future boundary conditions were applied in conjunction to represent a reasonable time-series representing the next 30 years. Ideally, a continuous time-series should be available for the whole period to reflect the gradual increase in sea level and gradual lowering of the bathymetry due to subsidence. Ideally, a continuous time-series should be available for the whole period to reflect the gradual increase in sea level and gradual lowering of the bathymetry due to subsidence. However, this is very cumbersome to do in the SWRM that provides boundary conditions for the Sibsa model. Instead, the 30 years are covered by two simulations. The first simulation covers 15 years starting from the 2019 conditions (grid and bathymetry) using the existing 2019 boundary conditions generated by the SWRM. When this simulation is done, the results are processed into conditions representing 15 years into the future with subsidence representing 30 years into the future subtracted from the bathymetry. The second simulation uses that bathymetry and the associated grid as initial condition and runs 15 years using the future using boundary conditions from the SWRM.

This is hence a stepwise approach in which the first 15 years represent existing conditions and the next 15 years represent conditions 30 years into the future.

Figure 4-1 shows observed bathymetries from 2011 and 2019 along with simulated future bathymetries from 2034 and 2049.

The overall pattern does not change, but there are some clear shortcomings in the model behaviour, which are seen more clearly on the longer timescale. When inspecting the bathymetries, some of the short outer bends experience sedimentation, leading to erosion of the sharp inner bends, which will also be clear when the bank lines are inspected. The shortcoming was also experienced in the Pussur River model when that model was formulated as a single fraction sediment model with a fixed Manning number, as is the case for the Sibsa River model. Due to lack of data, the Sibsa River model was not subjected to the same scrutiny that applied to the Pussur River model. It is known from data that there is sand in the Sibsa River, but there was only one old data point showing sandy d_{50} in the downstream end of Sibsa River.

Despite the shortcomings in the bends, the Sibsa River model shows that the bathymetry changes are relatively small over the long period 2011-2049.

The width-integrated bed levels are shown in Figure 4-2. The results show the same trend that was observed during the model calibration, namely that the Sibsa has a relatively stable total sediment volume. For the period 2011-2019 the total observed sediment volume in the river was almost unchanged, while some shifting upstream was observed. For the simulations into the future the opposite is observed, but the effect is not significant. Obviously, the total sediment volume in the Sibsa is sensitive to the uncertain sediment concentration boundary conditions.

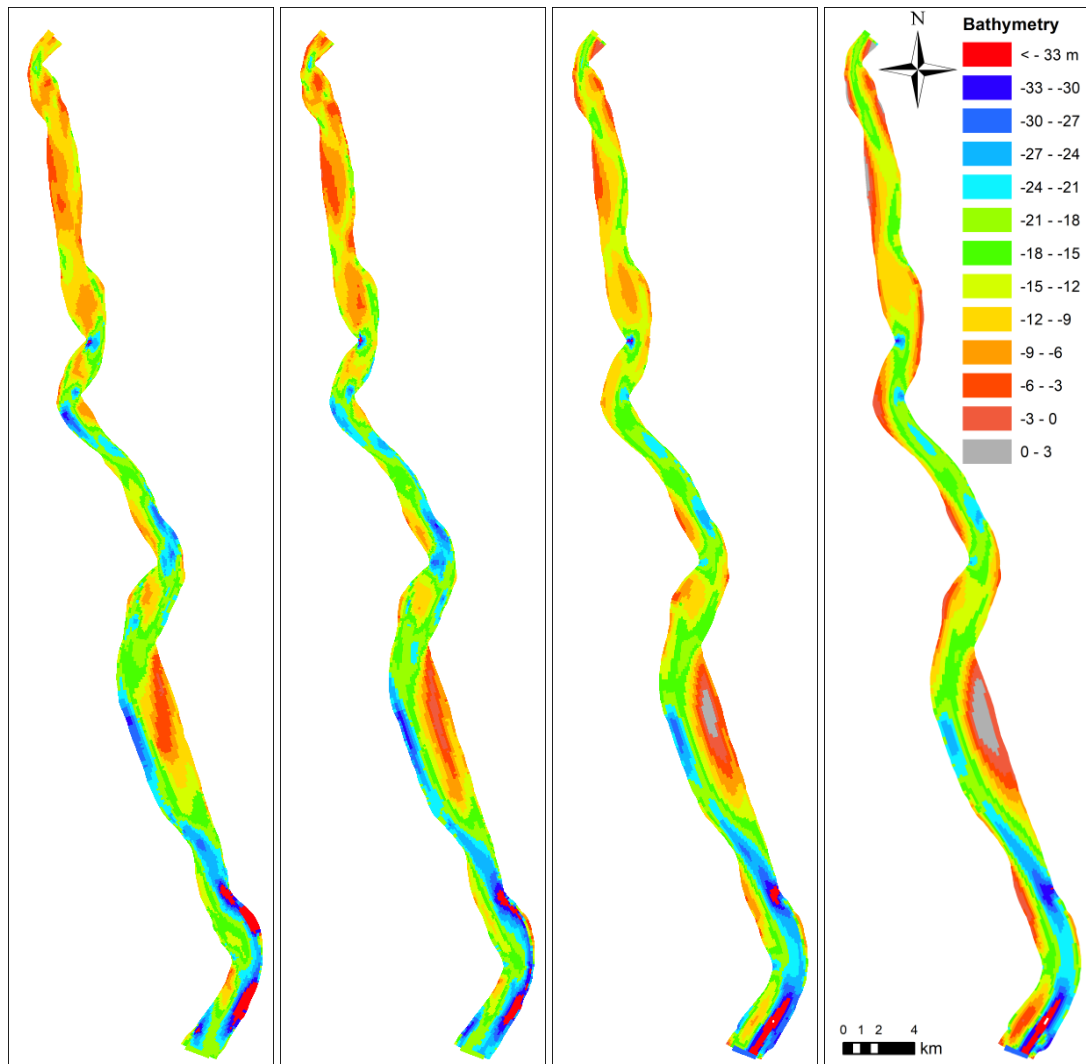


Figure 4-1 Bathymetries from various years. From left: 2011 (observed), 2019 (observed), 2034 (simulated), 2049 (simulated).

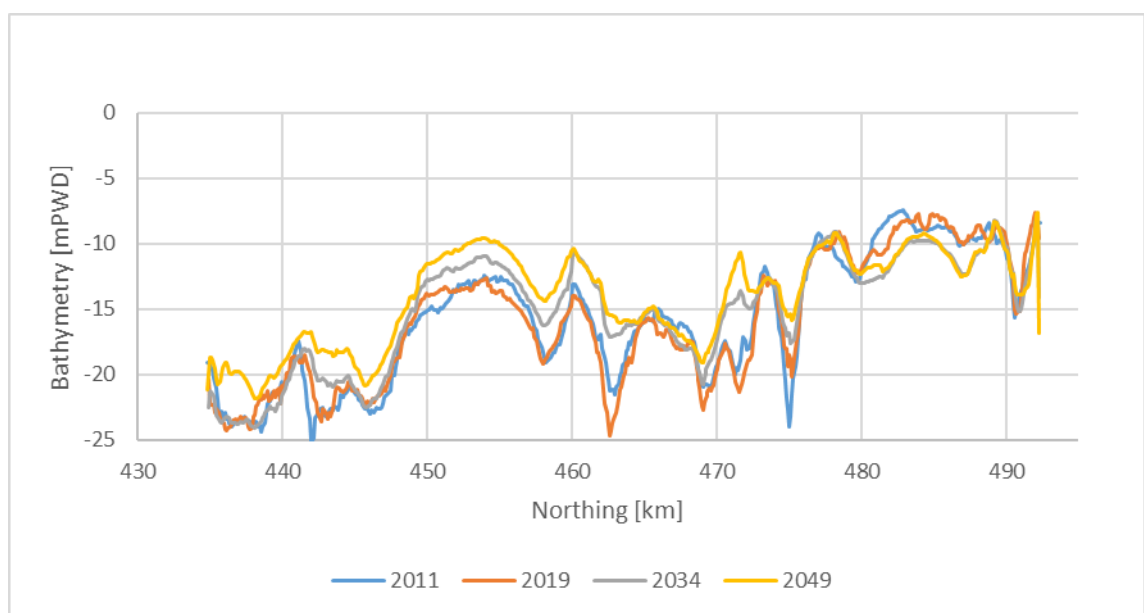


Figure 4-2 Width-integrated bed levels as a function of northing in the Siba River for 2011 (observed), 2019 (observed), 2034 (simulated) and 2049 (simulated).

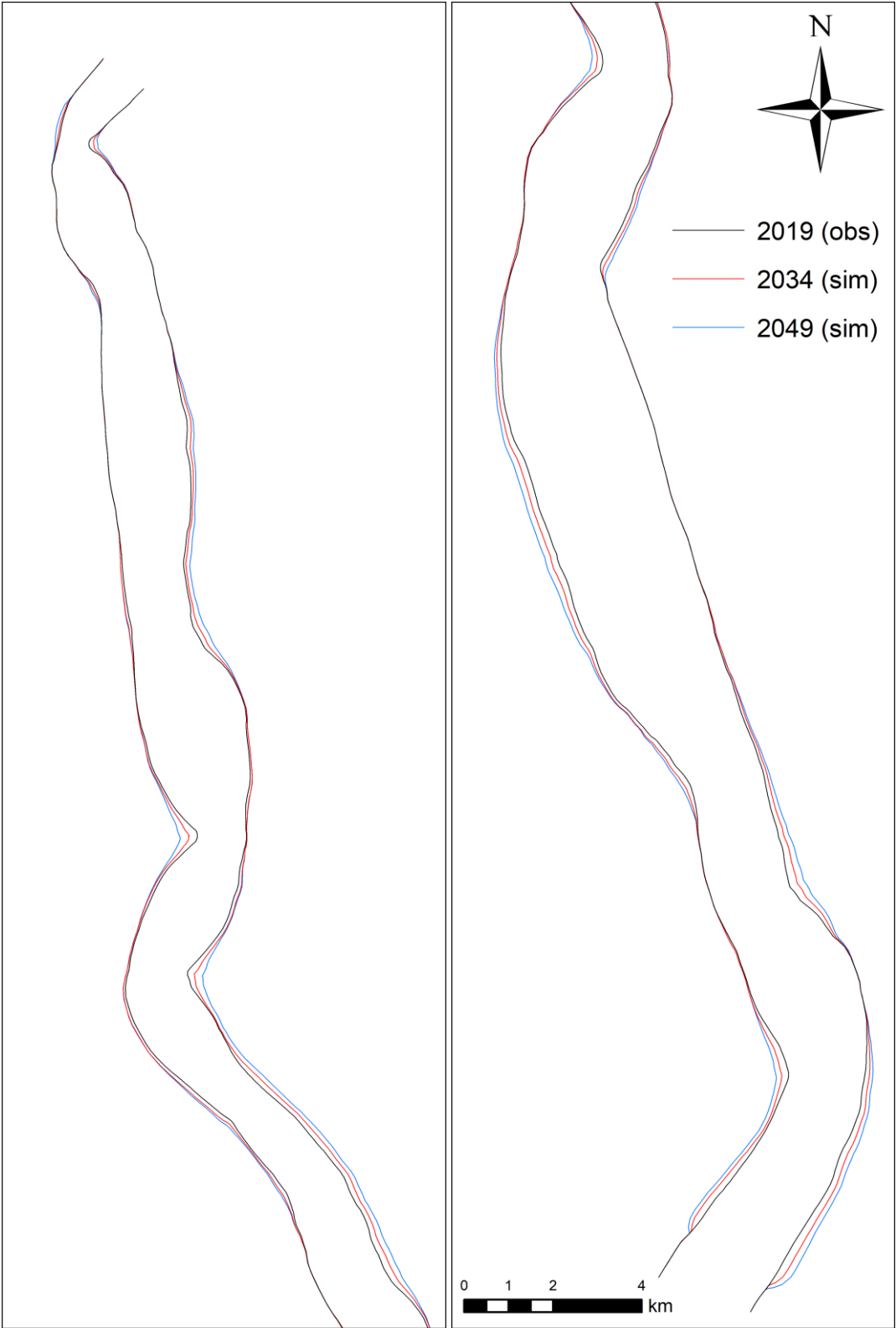


Figure 4-3 Bank lines 2019 (observed), 2034 (simulated), 2049 (simulated).

Simulated bank lines 30 years into the future are shown in Figure 4-3. The bank erosion pattern does not change significantly in the future, but there are shortcomings in the simulated bed levels, which clearly also impact bank erosion.

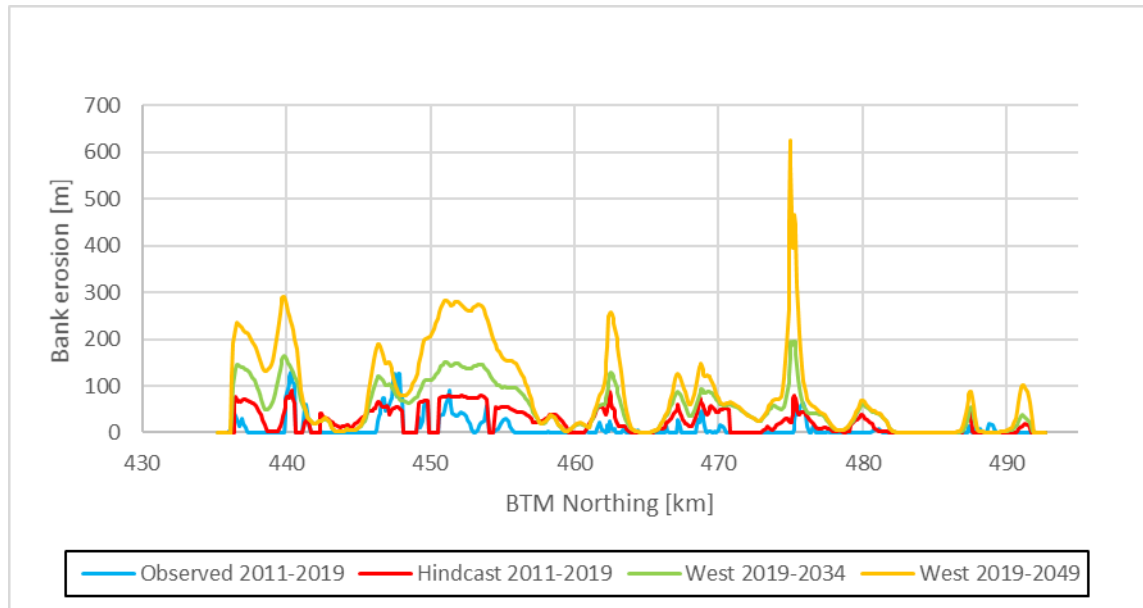


Figure 4-4 Bank erosion along the Sibsa River west bank for 2011-2019, 2019-2034 and 2019-2049.

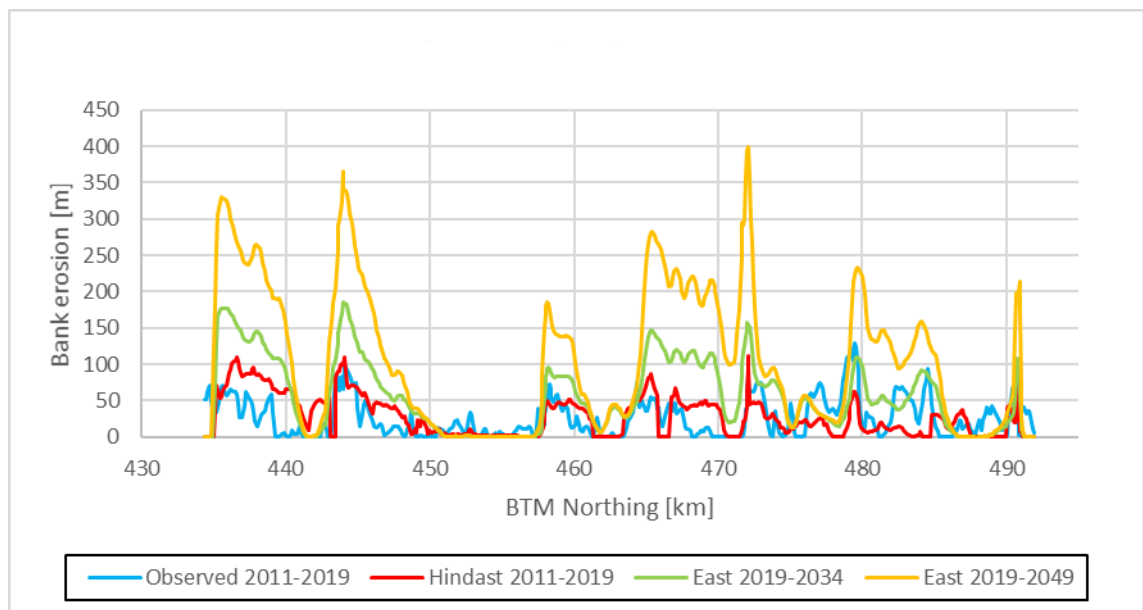


Figure 4-5 Bank erosion along the Sibsa River east bank for 2011-2019, 2019-2034 and 2019-2049.

Figure 4-4 and Figure 4-5 show the simulated bank erosion as a function of the northing coordinate, for reference compared to the 2011-2019 simulations and observations. The results show that the eroding banks are generally the same, despite the shortcomings identified in the simulated future bathymetries.

4.2 Impact of climate change on future bank erosion

With the application model it is quite easy to quantify the impact of climate change on bank erosion over the next 30 years. Due to the way the model was set up for the 30 years, it is merely a matter of running an alternative 2034-2049 without climate change (but with subsidence included).

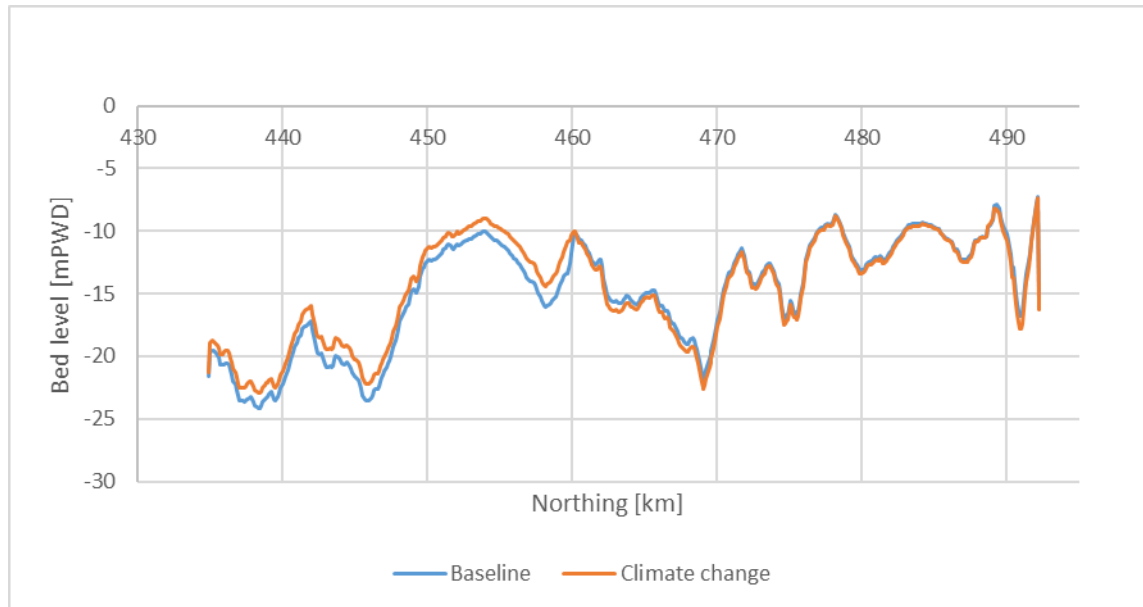


Figure 4-6 Simulated effect of climate change in 2049 in the shape of width-integrated bed levels along the Sibsa River.

Figure 4-6 shows the width-integrated bed levels along the Sibsa. The results show that climate change causes the bed levels to generally increase in the downstream end, while the impact upstream is very small.

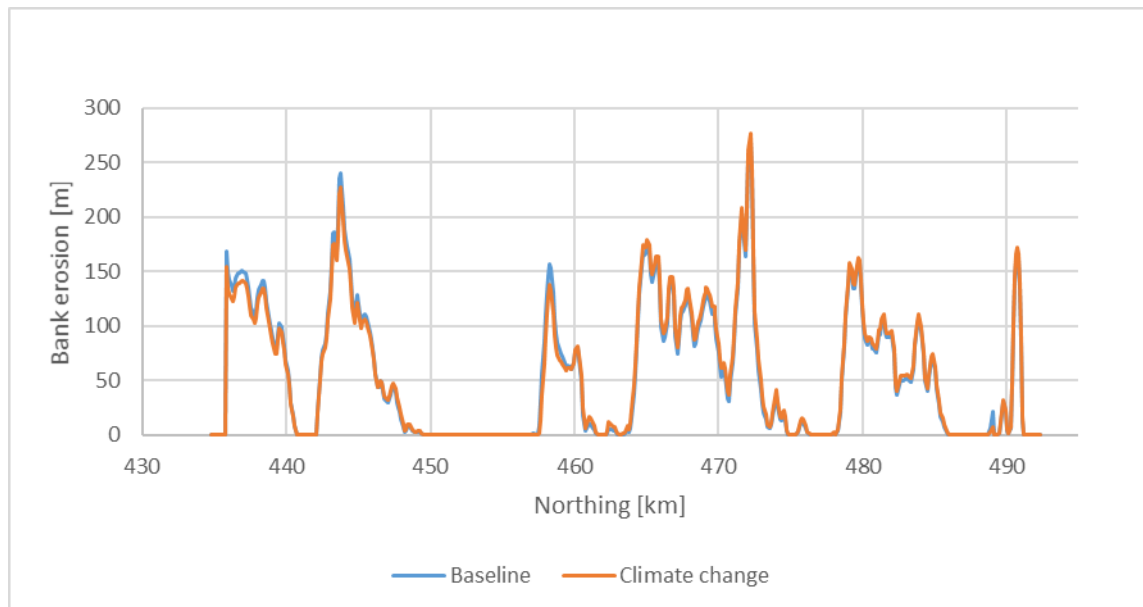


Figure 4-7 Simulated bank erosion along the east bank 2034-2049 with and without climate change.

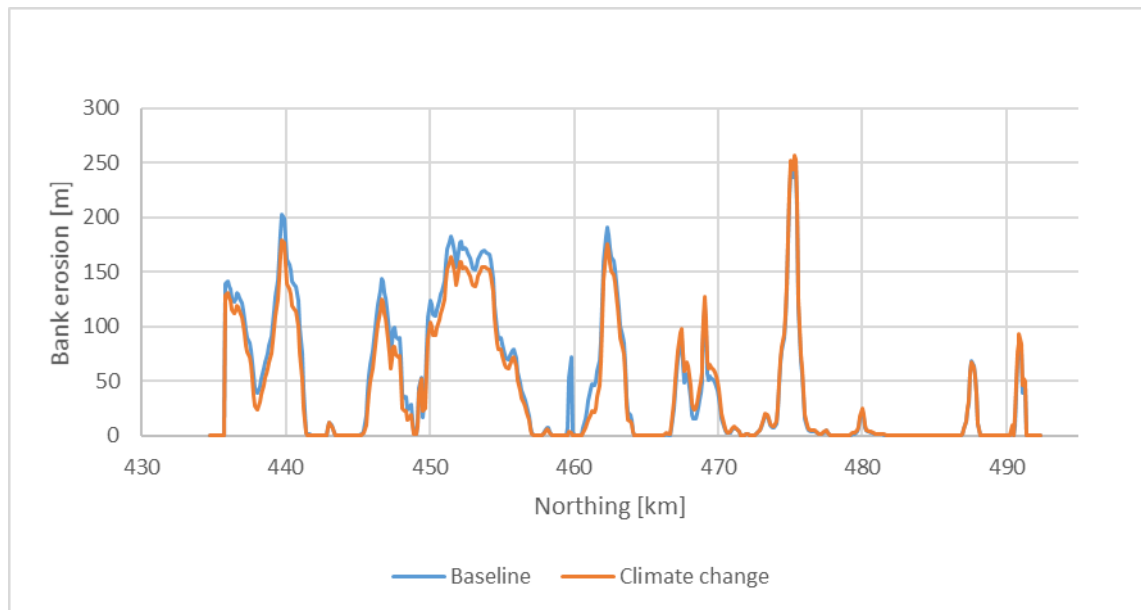


Figure 4-8 Simulated bank erosion along the west bank 2034-2049 with and without climate change.

Bank erosion rates are identical in the two scenarios for the period 2019-2034, while they are different in the period 2034-2049. Figure 4-7 and Figure 4-8 show the simulated bank erosion for the period 2034-2049 with and without climate change. The results show that climate change reduces bank erosion in Sibsa River. This is a surprising result, as the increased water level at the downstream end should increase the tidal discharges. However, when inspecting the width-integrated bed levels in Figure 4-6 it is seen that the bed levels with climate change increase a lot more than the downstream water level, which will reduce the tidal discharges.

4.3 Protection of the long eroding western bank

The impact of bank protection on bed levels and bank erosion was quantified by running additional simulations covering 2019-2034 with existing boundary conditions. The existing conditions (baseline) simulation was done without updating the grid, while a parallel simulation was conducted with the very characteristic long western bank protected.

The grid was not updated to allow for easier calculation of induced bed level changes, which are difficult to calculate based on results on different grids. This introduces a small error because in reality, the simulation with the eroding bank would gain a slightly wider channel along the bank, and hence the simulation with bank protection should in reality cause a bit more scour compared to allowing erosion.

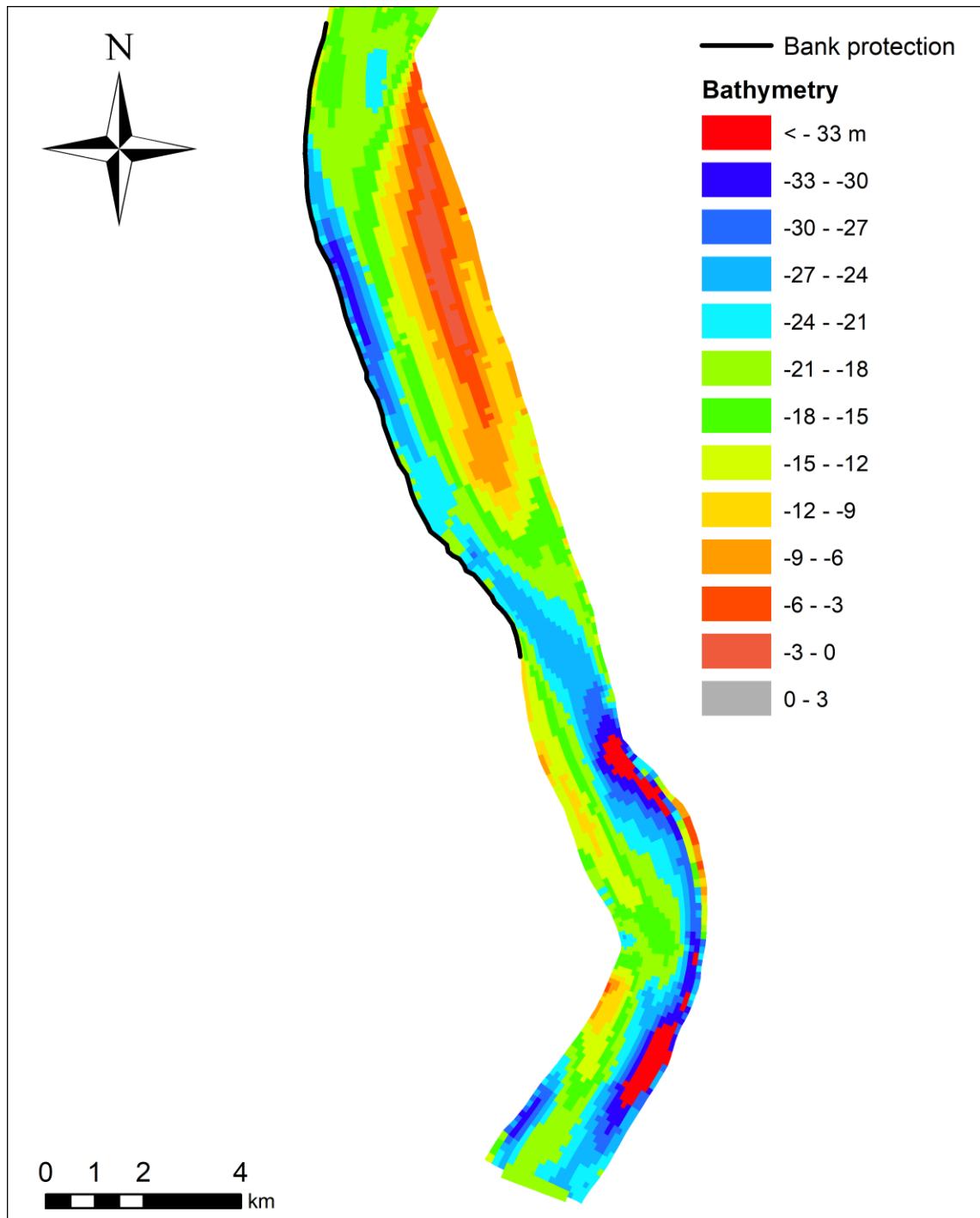


Figure 4-9 Bank protection was considered along this bank to quantify the impact on local bed levels from bank protection. It is noted that there is no polder along the western bank in this area, so the case is purely hypothetical.

The protected bank is shown in Figure 4-9. The bank was selected because it is the most consistently eroding bank in Sibsa River, although it should also be said that there is no polder at this location. Hence, the case is hypothetical.

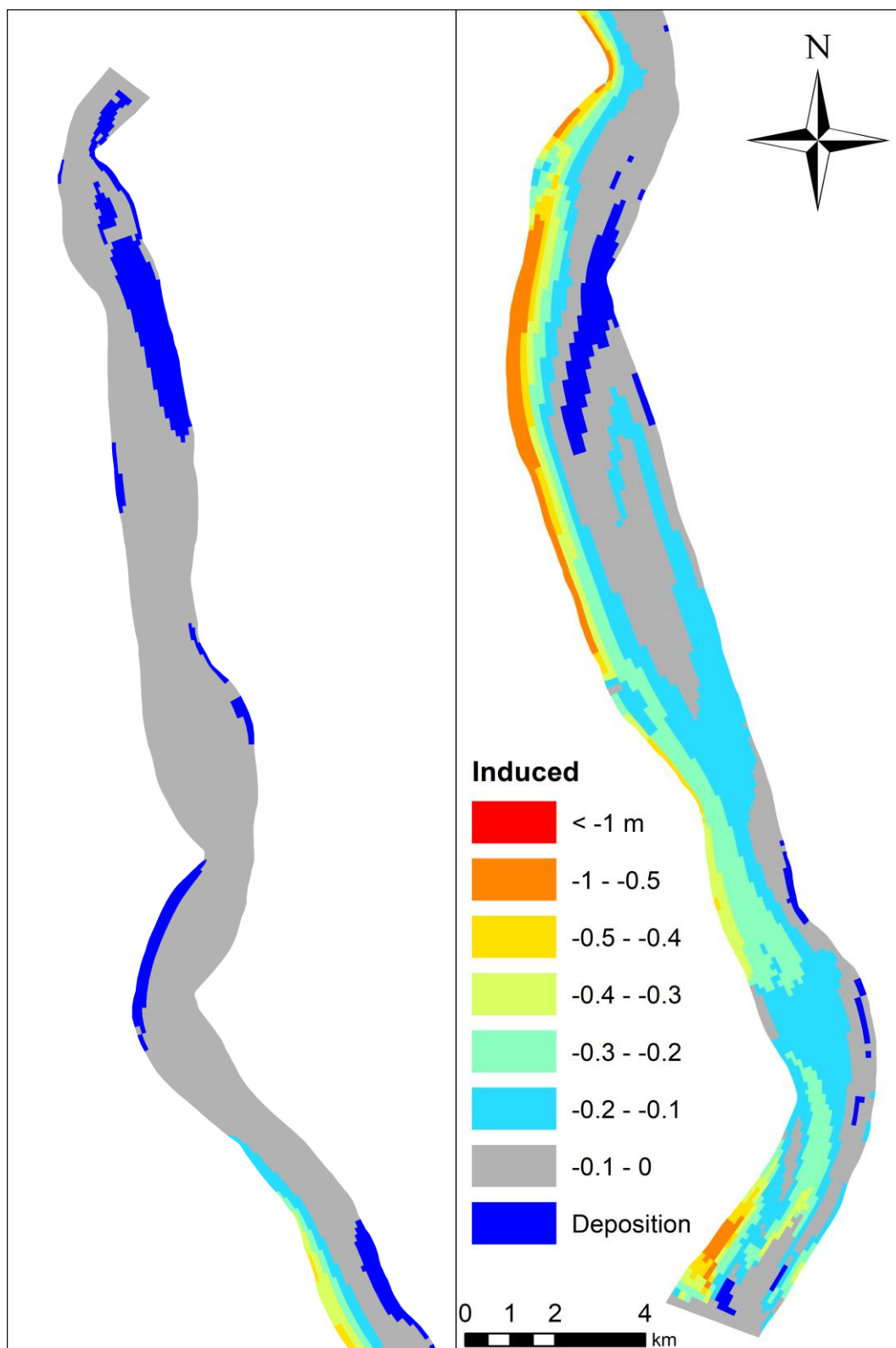


Figure 4-10 Induced bed level changes 2019-2034 associated with protecting one bank from erosion.

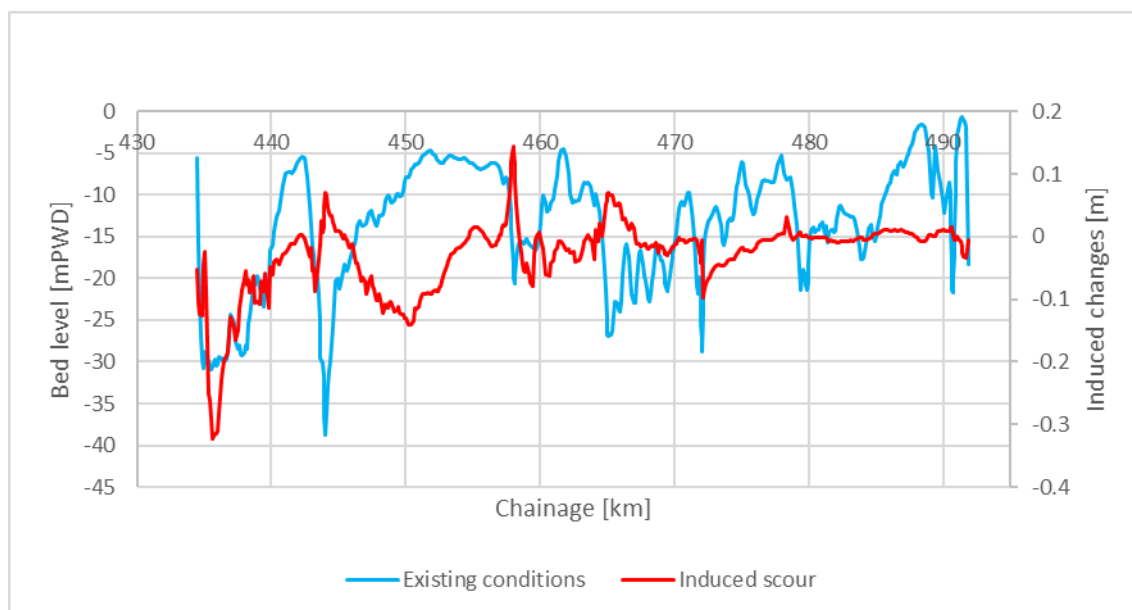


Figure 4-11 Simulated bed levels for existing conditions along the east bank along with differences induced by protecting the bank.

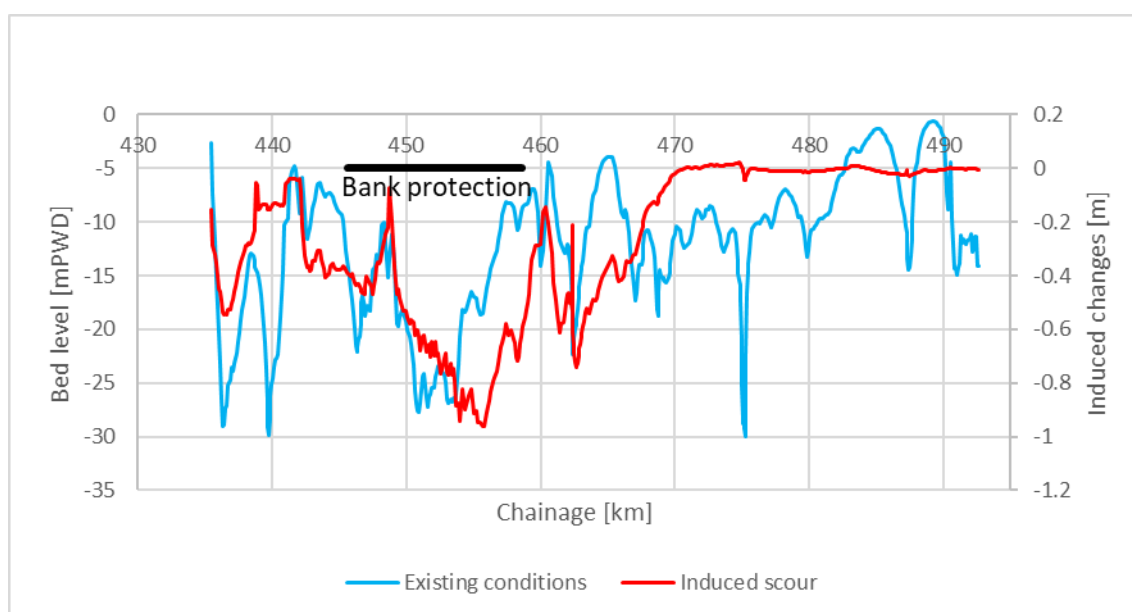


Figure 4-12 Simulated bed levels for existing conditions along the west bank along with differences induced by protecting the bank.

Figure 4-10 shows the induced bed level changes caused by bank protection, and the usual reduction of bed levels along the bank can be seen clearly.

The bed levels along the banks are illustrated in Figure 4-11 and Figure 4-12. It is seen that bank protection will lead to bed levels lowered up to 1 m along the protected bank, but there are also impacts upstream and downstream of the bank protection. Along the opposite (east) bank the bed levels can also be reduced, especially in the downstream direction, but the main impact is clearly at the protected bank and extending a bit upstream and downstream.

The differences in bank erosion are very small and difficult to illustrate graphically. The simulated bank erosion rates are not shown.

5 Conclusions

The present report documents the development of the MIKE 21C model of the Sibsa River.

Several historical bathymetry datasets were available for the Sibsa River. However, only the two most recent datasets were considered in the 2D model, as the older datasets did not have enough detail for 2D contouring. The two most recent datasets were from 2011 and 2019, and they even have almost identical resolution, offering an excellent basis for calibrating the model by hindcasting 2011-2019.

Hydrometric data in the shape of water levels and discharges was used for calibrating the hydrodynamic model.

Several bed samples processed into particle size distribution were available. However, some old bed samples were only available as location and d_{50} -values. Those bed samples are very important because they show sand in the downstream end, but without the actual size distribution it is difficult to use these in the model. Even with the old bed samples available, the data coverage is still insufficient for the development of a 2-fraction sediment model. There is no doubt that the Sibsa River has a sediment regime locally characterized by a mix of sand and silt, but the available data does offer a clear picture of how this works.

Suspended sediment samples have only been collected at the Nalian station in the Sibsa River, while there is no suspended sediment data available at Akram Point. Sibsa River also has particle size distribution data for the suspended sediment, which is unusual. The particle size distribution data was only available for ebb/flood slack conditions but shows that the suspended sediment has generally much lower fall velocities (stronger effect for slack conditions) compared to the bed samples. The lack of concentration data and associated particle size distribution data at Akram Point is a shortcoming in a river that could be morphologically influenced by sand in the downstream end. Without the Akram Point suspended sediment data, including particle size distribution, the sediment transport in the downstream end could not be determined, which is important for the morphological behaviour, especially for the sand import to the river from the downstream estuary.

Bank erosion was processed from Landsat images 1988-2019. The historical bank lines show very consistent and systematic bank erosion for the whole period. For most banks along the Sibsa River it was observed that bank eroding in 1988 was also eroding in 2019, and the annual bank erosion rates were similar for the banks, both spatially and temporally. The bank lines were processed into erosion as a function of northing along the west and east banks, and it was demonstrated that bank erosion correlated extremely well with bed levels in the way that essentially all eroding banks have deep water and are in outer bends. The sediment volumes associated with bank erosion are significant compared to volumes associated with bed levels. The period 2011-2019 showed almost neutral sediment behaviour, i.e. only internal movement, while the bank erosion contribution was significant compared to these transported volumes.

A curvilinear grid was generated for the Sibsa River with 500x20 grid points. The 2011 bathymetry data was contoured on this grid. A separate 2019 grid was developed from the 2019 bank lines with the 2019 bathymetry interpolated.

Hydrodynamic boundary conditions were provided by IWM from the SWRM for the period 2011-2019 (30 min time-step). The boundary conditions consisted of upstream discharge, several side channels and downstream water level time-series. Of particular interest for the Sibsa River is that the upstream end has a very low net flow during the monsoon (zero net flow during the dry season), which means the Sibsa River is almost a dead end. This suggests that the Sibsa River should be a longitudinal sediment sorter with cohesive sediment upstream and sand downstream (imported from downstream), which is consistent with the bed samples.

The hydrodynamic model calibration and validation show that the Sibsa River model consistently underpredicts discharges at the downstream Akram Point. No attempt was made to solve this problem, as it is inherited with the boundary conditions from the SWRM. The problem was analysed, and it was concluded that the upstream Nalian discharges appear to be correct, so either the local floodplain exchange is underpredicted or the SWRM does not correctly capture the known complex interaction between the Sibsa River and the Pussur River. This shortcoming could also influence the simulated morphological behaviour in the downstream end.

The sediment model was formulated as a silt model with a representative fall velocity of 1 mm/s. This was based on the bed samples, while the fall velocities for the suspended sediments based on the suspended samples are an order of magnitude lower. Due to this it is difficult to calibrate the silt model to both bed levels and sediment concentrations, and emphasis was therefore on the bed levels, which are far more important than the sediment concentrations.

The alternative use of a 2-fraction sand and silt model implied by some bed samples and the hydraulics (upstream dead end) was explored. However, this was very problematic due to the lack of bed samples and suspended sediment concentrations at Akram Point.

The cornerstone of the morphological calibration is a morphological hindcast 2011-2019. For the Sibsa River this can be conducted with reasonable reproduction of bed level changes in the period, even when suffering from uncertainties in the data and model inputs. The model also calibrates well to observed sediment concentrations at Nalian, although this was de-emphasized in the model development because it was deemed that bed level changes were more important than sediment concentrations.

The Sibsa River model calibrates extremely well in the upstream end, while in the downstream end the model calibration is not satisfactory. This discrepancy can be tied to the probably sandy bed in the downstream end, lack of Akram Point concentration data and the consistent underprediction of discharges at Akram Point.

Of particular interest in the downstream end is what looks like a large sand bar poorly described in the silt model. If the downstream sediment is sandy, the bar behaviour would be very different. In the silt model description, the bar does not exhibit a behaviour suggesting significant transverse sediment transport, which would be expected in a sand formulation.

Bank erosion was simulated using almost the same formula used for other rivers in the project. Bank erosion hindcasting 2011-2019 showed good agreement with the observations, with the correct banks eroding and the magnitude correctly reproduced. However, bank erosion in the Sibsa River does not correlate as strongly with the bed levels as seen in other rivers. Bank erosion in Sibsa River appears to be a messier signal than e.g. in the Pussur River.

5.1 Recommended future data collection

The available data suggests that the riverbed consists of mixed sand and mud, but there were too few bed samples and suspended sediment samples available to make a reliable 2-fraction model. In addition, the underprediction of the flow exchange at Akram Point is problematic in both hydraulic and morphological models.

The following future data collection will improve the understanding of Sibsa River:

- Data collection aimed at improving the Akram Point discharge is essential for improved understanding of the river hydraulics. The Akram Point discharge improvement needs to start in the SWRM, which provides the boundary conditions to MIKE 21C.
- There are too few bed samples available in the Sibsa River to describe the spatial distribution of sand and silt. Many more samples should be collected, both longitudinal and transverse and on various morphological features (bars, channels, islands etc).

- ADCP data should be measured in riverbends to improve understanding of the velocity distributions. Traditionally IWM do not collect ADCP data in bends, but this should be done, and the data should be processed into velocity profiles and not just discharges.
- Suspended sediment concentrations and particle size distribution data should be collected at Akram point. At present no observations are available.
- Bank material samples (particle size distributions) should be collected for the Sibsa River. At present no observations are available.
- Identification of dunes from e.g. multibeam bathymetry data on the sand bars.

It is noted that IWM regularly collect ADCP data in the rivers. However, for convenience, the ADCP profiles are usually collected in straight reaches and processed into discharges. Hence the capability and expertise within ADCP data collection is already available, while the suggestion made in this report is to use the capability in a slightly different way by collecting the ADCP data in specific sharp bends with dune cover and post-process the ADCP data into discharges (as usual) and depth-integrated velocity fields.

It is also noted that traditional single beam echo-sounder is normally adopted in the rivers, and single beam is sufficient for the full bathymetries. However, local multibeam echo-sounder data is very valuable (especially for identifying dune fields, which cannot be done from single beam data perpendicular to the flow direction), and the capability is readily available at IWM.

5.2 Recommended model improvements

The largest shortcoming in the model lies in the lack of ability to correctly predict bed level changes in the downstream end. Improvements in this area require more data. The model performance can be significantly improved with a 2-fraction sediment description provided there is sufficient data to construct such a model.

If the downstream end can be shown to be partly sandy, and requiring a 2-fraction model, then it is very likely that a dune model will be required as well to get the correct description of flow deflection from bars.

5.3 Conclusions from the scenario simulations

The developed model was applied for the following scenario simulations:

- Bank erosion projection 30 years into the future
- Impact of climate change 30 years into the future
- Impact of bank protection on bed levels

Bank projection 30 years into the future showed no qualitative changes to the river bathymetry. The results showed the same trend that was observed during the model calibration, namely that the Sibsa has a relatively stable total sediment volume, while some shifting upstream was projected. Some shortcomings were identified in the model. When inspecting the bathymetries, some of the short outer bends experience sedimentation, which should probably not occur. It was speculated that the main reason lies in the simple 1-fraction silt model, while it is known anecdotally that the Sibsa River also contains sand in the riverbed.

Simulated bank lines 30 years into the future showed that the bank erosion pattern does not change significantly in the future, i.e. the same banks will erode with the similar rates, but shortcomings in the simulated bed levels clearly also impact bank erosion.

Climate change does not lead to increased tidal discharges in the Sibsa River, while the downstream water level obviously increases due to sea level rise. The model showed that due to climate change, the Sibsa River experiences sedimentation in the downstream end, while the upstream impact is very small. Results show that climate change reduces bank erosion in Sibsa River. The model also shows that climate change reduces bank erosion in Sibsa River.

The impact of bank protection was conceptually tested along the characteristic long eroding western bank in the downstream end of the Sibsa River. The model showed that bank protection will lead to bed levels lowered up to 1 m along the protected bank, but there are also impacts upstream and downstream of the bank protection. The differences in bank erosion are very small and difficult to illustrate graphically and are concluded to be negligible.

6 References

Hasegawa, K. (1989). *Universal bank erosion coefficient for meandering rivers*. Journal of Hydraulic Engineering, 115(6), 744-765.

Krumbein, W. C. (1934). *Size frequency distributions of sediments*. Journal of Sedimentary Petrology. 2 (4).

Mehta, A. J., Hayter, E. J., Parker, W. R., Krone, R. B., & Teeter, A. M. (1989). *Cohesive sediment transport*. I: Process description. Journal of Hydraulic Engineering, 115(8), 1076-1093.

Mosselman, E. (1995). *A review of mathematical models of river planform changes*. Earth Surface Processes and Landforms, 20(7), 661-670.

